THE UNDERSCOUR OF RUBBLE MOUND BREAKWATERS BY WAVE ACTION

by

K. ALLARDICE, B.Sc.(Eng.) (Cape Town)

A thesis submitted in partial fulfilment
of the requirements for the degree
Master of Science in Engineering.

Department of Civil Engineering
UNIVERSITY OF CAPE TOWN.

November, 1977.

L I S T   O F   C O N T E N T S

Page

PART III

DECLARATION OF CANDIDATE

I, Keith Allardice, hereby declare that this thesis is my own work and that it has not been submitted for a degree at another university.

Signed by candidate Signature Removed
November, 1977

ABSTRACT

Rubble mound seawalls, groins and breakwaters are still the most common type of shore-protection structures currently in use. Major reasons include: easiness to construct and repair, flexible with respect to settlement, favourable wave energy dissipation, fitness for any water depth and foundation, and because of their economical nature if rubble-stones are readily available.

A complete failure of the rubble mound structure can be expected if the stone gradation is improper or if filters are not provided, or are improperly constructed to specification. Many failures have been attributed to internal erosion whereby beach materials are removed by percolating water, such as that due to water waves and surface run-off. Washing-out of the backfills, settlement of the main structure and overtopping of the subsequent waves will follow eventually.

Two-dimensional model experiments have been conducted in order to clarify the basic characteristics of sand scour under dolos-protected rubble mound breakwaters, and to investigate some preventive measures against the scouring process. The inter-relationships of parameters associated with the scouring process have been investigated.

Sand scour in a three-dimensional model has been discussed, and design procedures associated with Rubble Mound Breakwater and Dolos concrete armour units have also been included.

This thesis is also intended to call the attention of researchers to consider foundation erosion, and protection by filter systems, in their future experimental studies on stability of rubble mound structures.

A C K N O W L E D G E M E N T S

The writer wishes to thank Professor F.A. Kilner for his guidance throughout the thesis, and in particular for his help and constructive critism on the manuscript.

The writer is indebted to the CSIR and the University of Cape Town for financial assistance during this project.

Thanks are also due to Bridget Spalding for typing the manuscript, to Harold Cable for printing the thesis and to the laboratory staff, especially Alton Siko for his assistance and support throughout the experimental programm.

LIST OF SYMBOLS

LOWER CASE:

a	wave amplitude	m
c	wave celerity	m/s
d_b	depth of water at point of breaking	m
d_s	depth of water at structure	m
f	wave frequency	Hz
g	acceleration due to gravity	m/s^2
h	dolos height (see Figure 13)	m
k_f	bottom friction coefficient (see Equation 4.10))	–
k_s	shoaling coefficient (see Equation (4.10))	–
k_r	refraction coefficient (see Equation (4.10))	–
k_Δ	layer coefficient (see Equation (11.5))	–
m	nearshore beach slope (y/x)	–
n	number of dolos layers (1 or 2)	–
r	dolos waist ratio (see Figure 13)	–
t	time elapsed	s
u_*	horizontal velocity within the boundary layer (see Equation (18.4))	m/s
x	horizontal axis direction	–
x_p	distance travelled by wave during breaking (see Figure 3)	m
y	vertical axis direction	–
z	cover layer thickness	m

UPPER CASE:

A	$H_i + H_r$	m
B	$H_i - H_r$	m
C	shape factor of armour unit (see Table 10.2)	–

C_D	drag coefficient	–
C_L	lift coefficient	–
C_r	reflection coefficient = H_r/H_i	%
C_W	crest width of breakwater	m
D	particle diameter	μm
D_{50}	effective sand diameter 50 % finer	μm
F_D	drag force (see Equation (18.2))	N
F_G	force due to gravity (see Equation (18.3))	N
F_L	force due to lift (see Equation (18.2))	N
F_n	normal force on the rubble mound	N
F_T	total hydrodynamic force (see Figure 15)	N
H	design wave height	mm or m
H_b	breaker height	m
H_i	incident wave height	m
H_o	deep water wave height	m
H'_o	deep water wave height in recording area	m
Hm_o	characteristic wave height (see Equation (4.2))	m
H_r	reflected wave height	m
H_s	significant wave height	m
H_{10}	average of highest 10 % of all waves	m
H_1	average of highest 1 % of all waves	m
K_D	stability coefficient	–
L	wavelength	m
L_o	deep water wavelength	m
N	number of armour units per unit area	–
N_{RP}	pier Reynolds number (see Equation (17.1))	–
N_s	sediment number (see Equation (17.2))	–
P	average porosity (see Equation (10.1))	%
R	wave run-up	m

S	sand scour depth	m
S_L	sand scour wavelength	m
S_m	sand bar height	m
S_r	relative density of armour unit (ρ_r/ρ_w)	-
T	wave period	s
T_s	significant wave period	s
T_z	zero crossing wave period	s
U	horizontal free stream velocity	m/s
V	volume of dolos	m^3
W	armour unit mass	kg

GREEK:

α	seaward slope angle of the breakwater	degrees
β	ratio of breaking depth to breaker height, i.e. d_b/H_b	-
ρ_r	density of armour unit	kg/m^3
ρ_s	density of sediment	kg/m^3
ρ_w	density of water	kg/m^3
ρ	density of fresh water	kg/m^3
δ	approach beach slope angle	degrees
θ	angle of wave incidence	degrees
τ_p	dimensionless plunge distance of a breaker	-
Ω	reference wind speed velocity at 19,5 m above sea surface	m/s

SUBSCRIPTS:

max	maximum
min	minimum

PART I

RUBBLE MOUND BREAKWATERS

CHAPTER 1

INTRODUCTION:

As this thesis centres on the use of rubble mound breakwaters, an explanation of definitions and design procedures is necessary.

Zwamborn (1976) [39] defines a breakwater as a structure which protects the entrance to a harbour against wave and sediment intrusion, or which encloses an artificial harbour area. Where the structure is built parallel to the shore and in very shallow water, it is called shore protection. Both structures can be of the same cross-section although design conditions are different because the shore protection is invariably in or near the breaker zone.

CHAPTER 2

BREAKWATER TYPES:

There are two main breakwater types, viz. the vertical wall and the mound types, with the following variations:

vertical wall - natural rock, gravity wall, dowelled natural rock wall, concrete block gravity wall, caisson gravity wall, rock-filled sheet pile cells, rock filled timber or steel cribs and perforated concrete wall.

mound type - natural rock, including armouring, natural rock with concrete block armouring, randomly placed concrete blocks and stone-asphalt mixtures.

Combinations of these two types are called composite breakwaters.

Rubble mound breakwaters are at present no doubt the most commonly used type of breakwater. The Shore Protection Manual (1973) [32] describes a rubble structure as being composed of several layers of random-shaped and random-placed stones, protected with a cover layer of selected armour units of either quarry stones or specially shaped concrete units. Armour units in the cover layer may be placed in an orderly manner to obtain good wedging or interlocking action between the individual units, or they may be placed at random. Present technology does not provide guidance to determine the forces required to displace individual armour units from the cover layer. Armour units may be displaced by a large area of the cover layer sliding down the slope *en masse*, or individual armour units may be lifted and rolled either up or down the slope. Empirical methods have been developed that, if used with care, will give a satisfactory determination of the stability characteristics of these structures when under wave attack by storm waves.

Rubble mound breakwaters have distinct advantages over the other types, *inter alia:*

- flexibility - damage and settlement may be easily rectified;

- no concentrated foundation pressures - thus suitable for questionable foundation conditions;
- easy to construct both from land and from sea platforms;
- absorbs rather than reflects wave energy thus reducing the chances of resonances;
- even with wave conditions in excess of the design conditions, the structure will normally sustain only local damage; total failure seldom or never occurs.

The breakwaters however, also have the following disadvantages:

- they require large amounts of stone due to their large cross-section and a suitable quarry must be nearby;
- the inside of the breakwater cannot be used directly as a quay (this is overcome by the use of a composite breakwater);
- normally a rubble mound structure is not water-tight which may cause problems with cooling outlet harbours.

CHAPTER 3

THE HISTORIC DEVELOPMENT OF RUBBLE MOUND BREAKWATERS:

Probably the first breakwater built as a rubble mound topped by a superstructure consisting of heavy blocks dowelled together (i.e. a composite breakwater) was that built at Piraeus in 500 B.C. [31,39]. The Dutch started the construction of a rubble mound breakwater at Mouille Point, Cape Town, in 1743, and the first completed rubble mound breakwaters were built in France, at Cherbourg (1788 - 1826) in England, at Plymouth (1811 - 1848) and in the U.S.A., at Delaware (1828 - 1869) [39].

These older rubble mound breakwaters consisted of a core of mixed stone sizes, e.g. quarry run, covered by an armour of heavy stones. The stability of the armour stone is dependent mainly on the mass and the shape of the individual pieces or armour rock, the slope on which they are placed and the wave height attacking the slope.

Although all the formulae show improved stability for flatter slopes, a slope of 1:3 is considered to be a practical limit, otherwise the structure is too large and thus uneconomic. Also, armour stone in excess of 20 tonne (1 tonne = 1000 kg) cannot be economically quarried which puts a limit to the use of this type of breakwater armouring for conditions where waves do not exceed about 7 metres. Thus, concrete blocks were introduced as breakwater armouring where wave heights were greater than 7 m or where large blocks of rock could not be obtained at an economic price. Initially, smooth rectangular blocks were used, either packed in a pattern or dumped at random (40 tonne blocks were used at most South African ports). These blocks could be made at any required size as dictated by the wave conditions (100 tonne cubes were used at Humboldt Bay, California). Since 1952, when the first special shape concrete block, the Tetrapod, was used at Sousse Harbour in Tunisia (4 tonne units with 1 per cent reinforcing) at least 30 other special shaped blocks were developed [32,39]; some are shown in Figure 1. Depending on the design, these special shaped blocks tend to link together to form a more stable cover layer while the unit weight can be smaller than for the rectangular blocks.

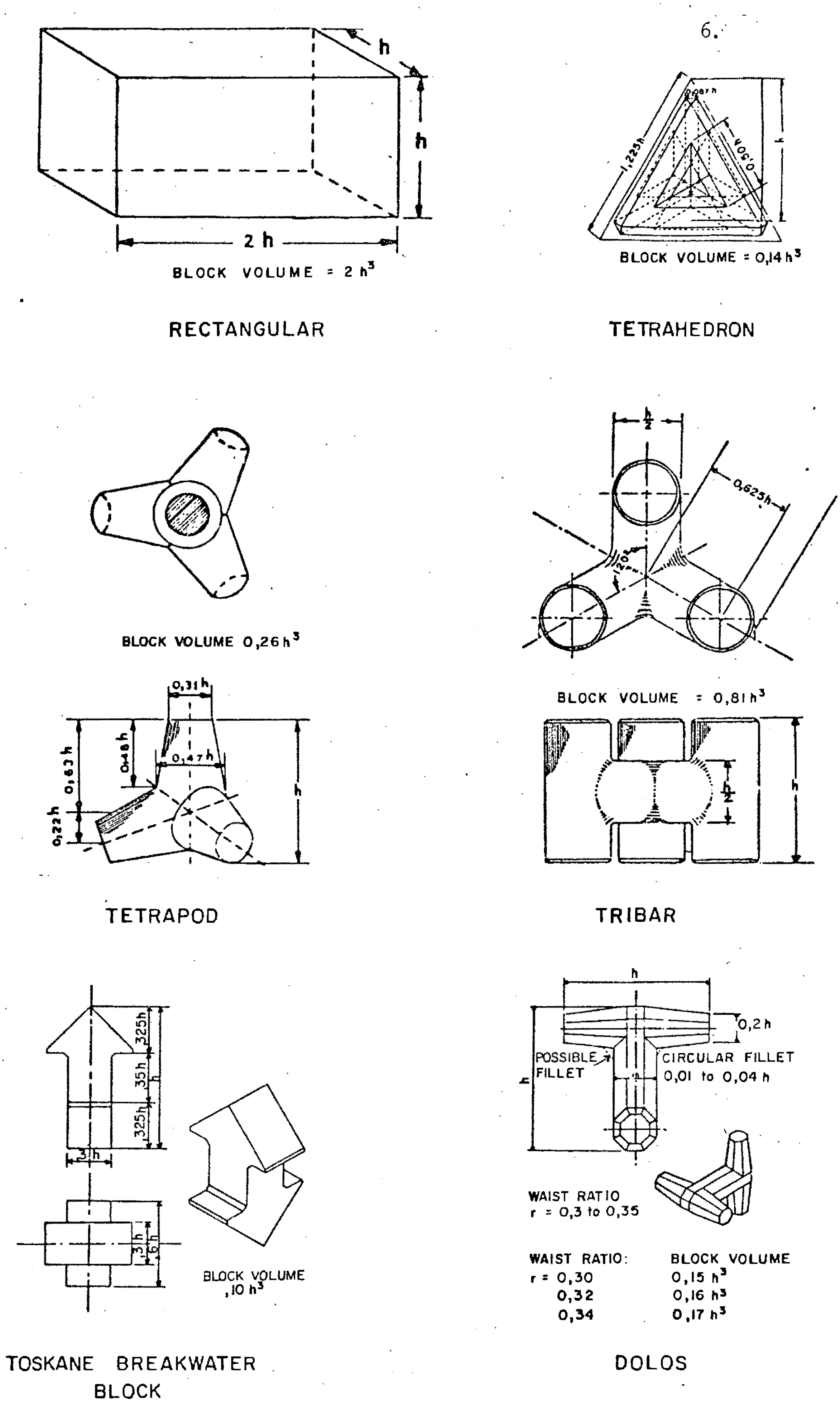

FIGURE 1 Concrete Armour Units

ZWAMBORN (1976)

CHAPTER 4

DESIGN CRITERIA FOR RUBBLE MOUND BREAKWATERS:

To design a rubble mound breakwater, the following data on the marine environment must be available [32].

- Wave heights, periods and directions. This is the most important data necessary to determine a stable breakwater cross-section.
- Tide and storm surge levels. These levels determine the height of the structure and also affect its stability.
- Ocean and nearshore current directions and strengths as affected by the harbour structure. These data are required to determine possible scour and deposition patterns, also during construction, which may affect the breakwater design.
- Bottom contours and type of material in the area concerned. Water depths determine the height of the structure and bottom slope affects the breaker heights. Water depths also partly determine whether a structure is subjected to breaking, non-breaking, or broken waves for a particular design wave condition.

4.1 Determination of Wave Conditions:

Breakwater design should preferably be based on wave data recorded in the area concerned over a sufficiently long period (minimum 2 to 3 years) to provide statistically meaningful data. The recording area should normally be in deep water or at least so far offshore that the data can be used for the various parts of the harbour structure. On the other hand, the recording area must not be too far so that it is possible to convert the data, using normal refraction theory, to the breakwater site.

All the wave data applicable to the project site should be evaluated for possible use as design criteria. Visual observations of storm waves may provide an indication of the wave height, period, direction, storm duration, and frequency of occurrence. Instrumentation for recording wave height and period at a point has been developed, while wave direction must be obtained from visual observations as instrumentation for this purpose is presently being developed. (Retief and Vonk presented a paper at the Fourteenth Coastal Engineering Conference at Copenhagen on a "low-cost inshore wave direction finder"). Where reliable, statistical deep water-wave data are available, these can provide the necessary shallow-water wave data. If wave data are not directly available at the site, the best available procedure must be employed, with sound engineering judgement, to transform available deep water and extreme offshore wave data to the structure site.

Wave characteristics are normally determined for deep water, and then propagated shoreward to the structure. Deep water significant wave height H_o, and significant wave period T_s may be determined if wind speed, wind duration and fetch are known. This information, with water-level data, is used with refraction analyses to determine wave conditions at the site.

Wave conditions at a structure site at any time depend critically on the water level. Consequently, a design still water level (SWL) or range of water levels, must be established in determining wave forces on a structure. Structures may be subjected to radically different types of wave action as the water level at the site varies. A given structure might be subjected to non-breaking, breaking and broken waves during different stages of the tidal cycle. The wave action a structure is subjected to may also vary along its length at a given time. This is true for structures oriented perpendicular to the shoreline such as groins and jetties. The critical section of these structures may be shoreward of the seaward end of the structure depending on the structure crest elevation, tidal range, and bottom profile.

The wave height usually obtained from statistical analysis of synoptic weather charts is the <u>significant height</u>, H_s. Assuming a Rayleigh wave-height distribution, H_s may be further defined in approximate relation to other height parameters of the statistical wave-height distribution:

$H_{\frac{1}{3}}$ or H_s = average of highest $\frac{1}{3}$ of all waves recorded,

$H_{10} \approx 1{,}27H_s$ = average of highest 10 per cent of all waves, (4.1)

and $H_1 \approx 1{,}67H_s$ = average of highest 1 per cent of all waves.

The probability of occurrence of this wave height, H_s, is then based on the occurrence of storms containing this parameter.

Alternatively, the characteristic wave height, Hm_o, can be used,

$$\text{where} \quad Hm_o = 4\sigma = 4\sqrt{\int_0^\infty S(f)df}\,, \tag{4.2}$$

where $m_o = \int_0^\infty S(f)df$ is the area of the energy density spectrum, i.e. the total energy of the wave system, and the r.m.s. value is the most basic parameter explaining the wave amplitude, a.

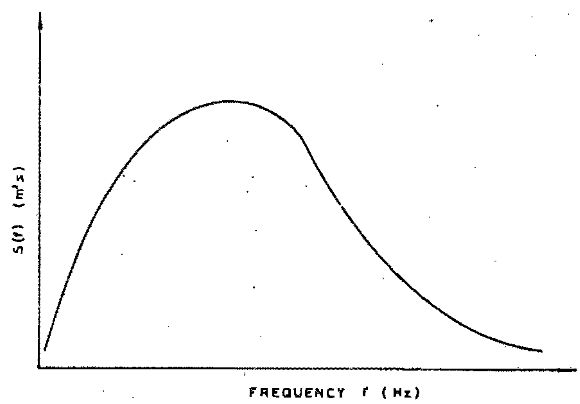

FIGURE 2 Wave Energy Spectrum

An example of an equation fitting the graph of Figure 2 is the expression for the Pierson-Moskowitz spectrum which is of the form*

$$S(f) = 0{,}0005/f^5 \ \exp\left(-4{,}4/(f\Omega)^4\right) m^2 s \text{ units} \tag{4.3}$$

where f = frequency in Hz = $1/T$

Ω = reference wind velocity at 19,5 m above the sea surface

T = Wave period (seconds)

If the record has only a narrow band of frequencies, the distribution

*Theoretical Spectra such as the P.M. Spectrum do not seem to be applicable to South African nearshore conditions. However, from wave data obtained for the Koeberg Power Station project and Richards Bay, it was found that the JONSWAP spectrum represents the local conditions reasonably well [39].

of wave heights - 2a - is in the form of a Rayleigh Distribution, where the probability of occurrence of a wave of amplitude, a, occurring is given by:

$$p(a) = \frac{a}{m_o} \exp\left[-\tfrac{1}{2}\frac{a^2}{m_o}\right] \tag{4.4}$$

Adopting this narrow distribution of wave heights, i.e. the Rayleigh Distribution, the ratio of the upper $\frac{1}{n}$ th average waves to the energy $m_o^{\frac{1}{2}}$ can be obtained,

$$\text{e.g. } \bar{H}_{\frac{1}{3}} = 4{,}004\, m_o^{\frac{1}{2}} = Hm_o$$

Normally, $Hm_o \approx H_s$

Regarding wave period data, the zero crossing period, $\bar{T}_z$, is the easiest to determine from a record. However, T_p, the peak period is more representative, where

$$T_p = 1/f_p \text{ and } f_p \text{ is the frequency of the peak of the wave energy spectrum} \tag{4.5}$$

$$\text{Also } Tm_{0,1} = \frac{m_o}{m_1}, \text{ where } m_n = \int_0^\infty f^n S(f)df, \tag{4.6}$$

which is the mean period, could also be used but again it is more logical to use T_p, also because $T_p > \bar{T}_z$ and $Tm_{0,1}$, and damage is usually worse for the longer periods. The choice of a representative wave period requires experience, and some ocean structures may have to be designed for their most critical excitation frequency, without reference to recorded wave periods.

4.2 Selection of Design Wave:

The choice of a design wave height depends on whether the structure is subjected to the attack of non-breaking, breaking, or broken waves and on the geometrical and porosity characteristics of the structure.

If breaking in shallow water does not limit the wave height, a non-breaking wave condition exists and for this condition, the design height is selected from a statistical height distribution.

For rubble mound structures, the design height is usually the significant wave height, H_s. Waves higher than H_s impinging on these structures seldom create serious damage for short durations of extreme wave action. When an individual stone or armour unit is displaced by a high wave, smaller waves of the train may move it to a more stable position on the slope.

Damage to rubble mound structures is usually progressive, and an extended period of destructive wave action is required before a structure ceases to provide protection. It is therefore necessary in selecting a design wave to consider both frequency of occurrence of damaging waves and economics of construction, protection and maintenance. In some tropical areas, hurricanes may provide the design criteria, where frequency of occurrence of the design hurricane at any site may range from once in 20 to once in 100 years. However, it may be uneconomical to build a structure that would withstand the hurricane conditions without damage, hence H_s may be a more reasonable design wave height. In areas where the weather pattern is more uniform, severe storms may occur each year, and the use of H_s as a design wave height under these conditions could result in extensive annual damage and frequent maintenance because of the higher frequency and duration of waves greater than H_s in the spectrum. Here, a higher design wave H_{10}, may be advisable.

Selection of the design height between H_s and H_{10} is based on the following factors: [32]

(a) degree of structure damage allowable and associated maintenance costs,
(b) availability of armour materials, and
(c) comparative alternate size or type of armour unit and their costs.

Selection of a design wave height also depends on whether the structure is subject to attack by <u>breaking waves</u>, and when designing for this condition it is desirable to determine the maximum breaker height to which the structure might reasonably be subjected. This design breaker height, H_b, depends on critical design depth at the toe, d_s, slope on which the structure is built, m(ratio of vertical to horizontal distance), incident wave steepness, and distance travelled by the wave during breaking, x_p [32], where

$$x_p = \tau_p H_b \tag{4.7}$$

and

τ_p = (4,0 - 9,25 m), the dimensionless plunge distance of the breaker.

See Figure 3. [32]

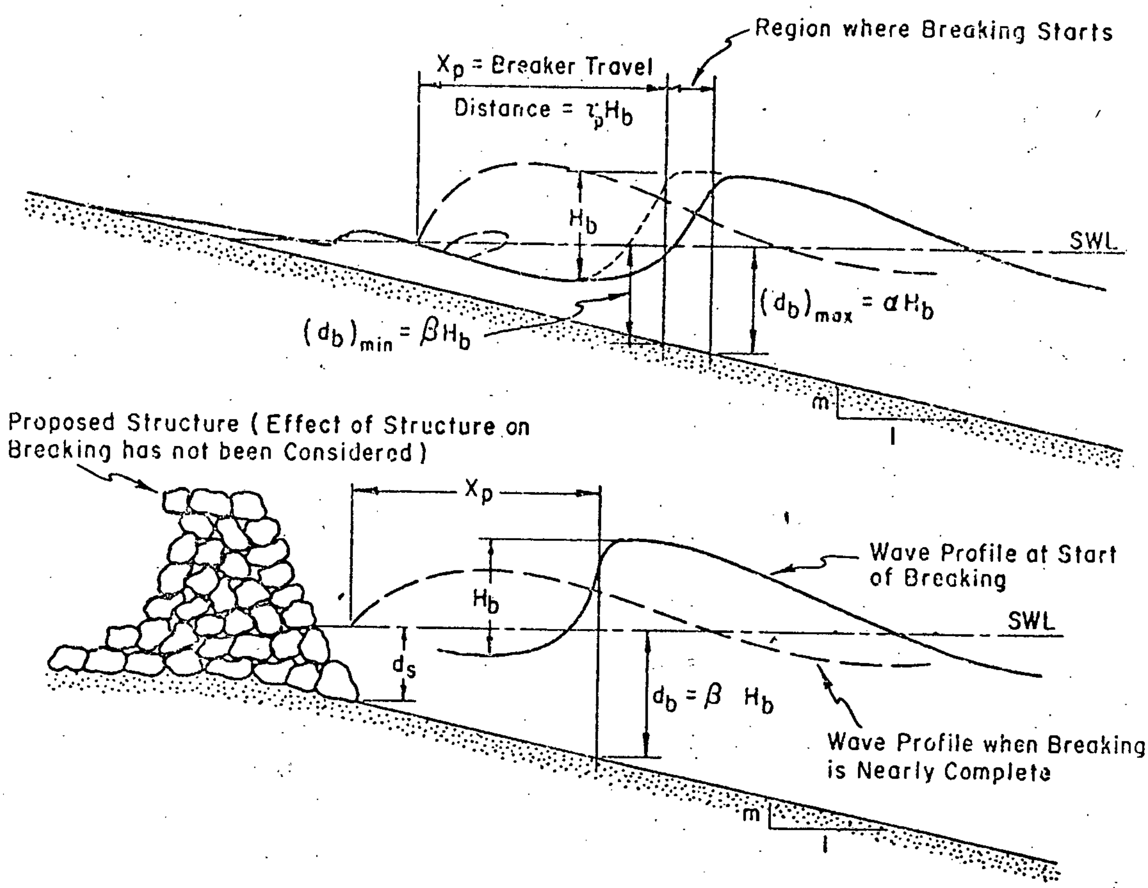

FIGURE 3 Definition of Breaker Geometry

Assuming that the design wave is one that plunges on the structure, design breaker height may be determined from:

$$H_b = \frac{d_s}{\beta - m\tau_p} \tag{4.8}$$

where β = ratio of breaking depth to breaker height

= d_b/H_b

τ_p = the dimensionless plunge distance x_b/H_b from Equation (4.7)

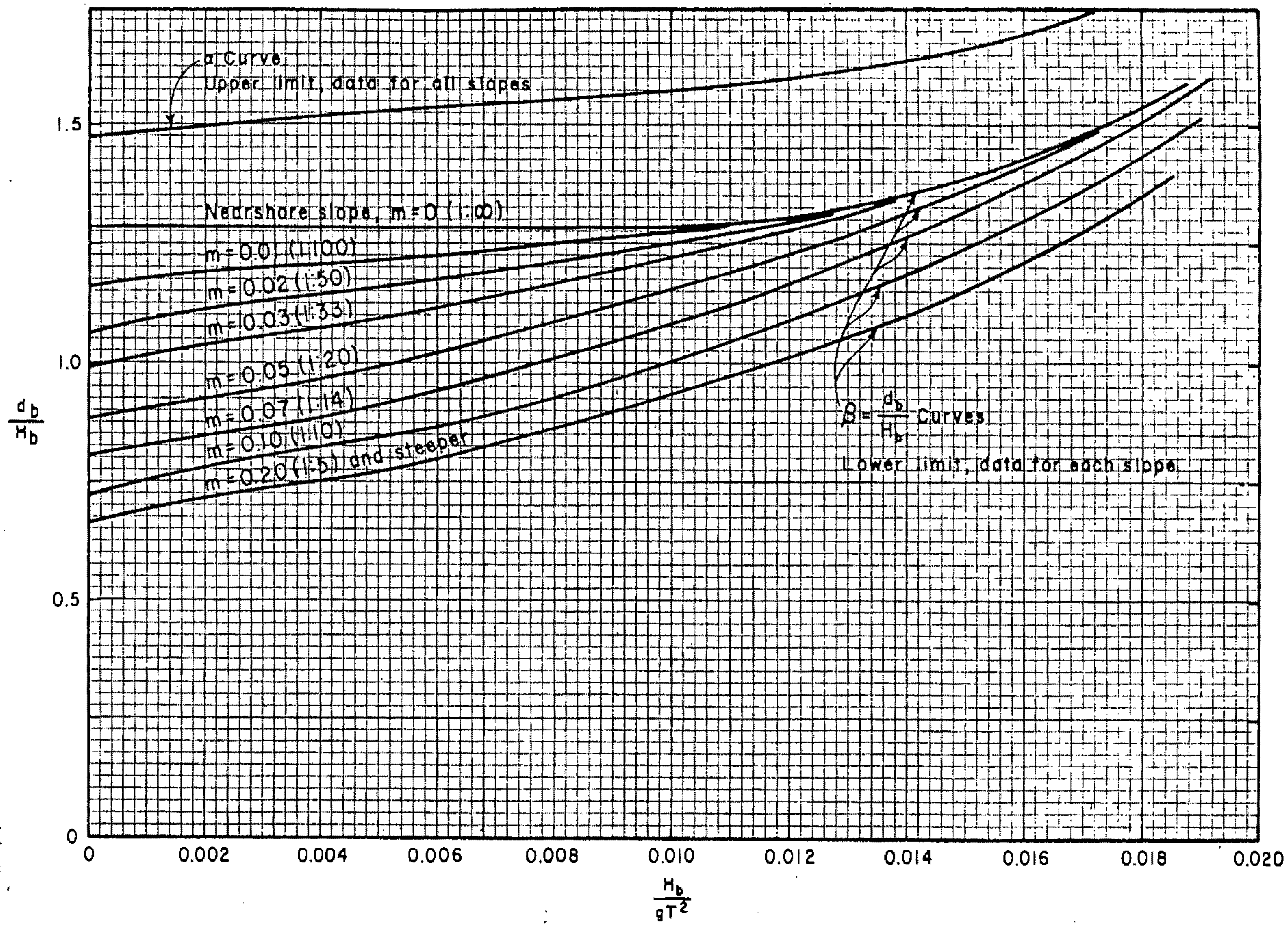

FIGURE 4 α and β versus H_b/gT^2

CERC (1973)

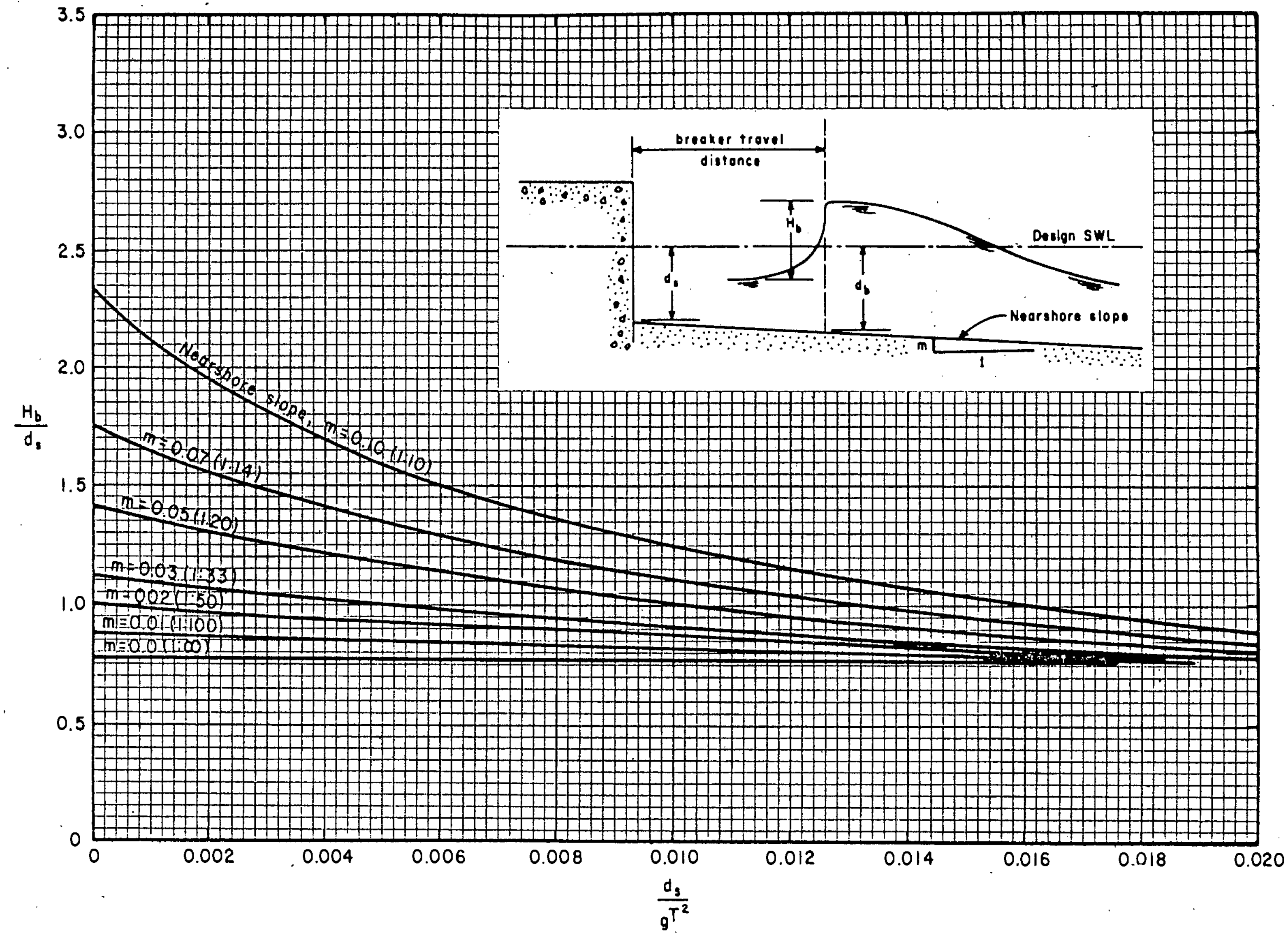

FIGURE 5 Dimensionless Design Breaker Height vs Relative Depth at Structure

CERC (1973)

The value of β, as seen from Figure 4, cannot be obtained until H_b is evaluated, and to aid in finding H_b, Figure 5 has been derived from Equations (4.7) and (4.8) using β values from Figure 4. [32]

If maximum design depth at the structure and incident wave period is known, design breaker height can be obtained from Figure 5.

With the aid of Figure 6 [32], the value of H_b can be evaluated directly from H_0', the deep water wave height in the recording area (or the deep water wave height equivalent to observed shallow water wave if unaffected by refraction and friction).

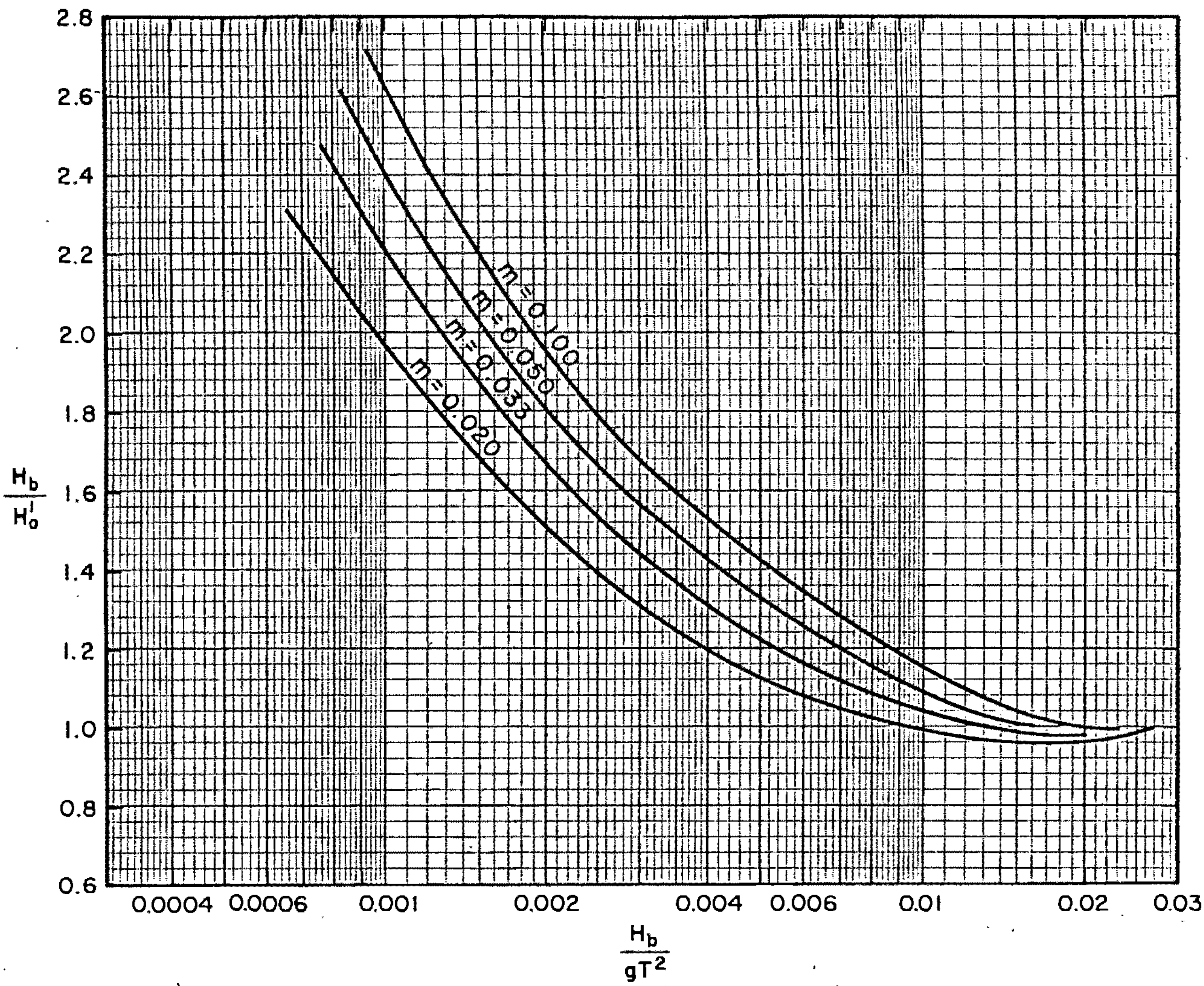

FIGURE 6 Breaker Height Index, H_b/H_o' vs Deep Water Wave Steepness, H_o'/gT^2

CERC (1973)

4.3 Limiting Wave Heights:

According to solitary wave theory, a wave starts to break when:

$$H_b = 0,78\ d_b \qquad (4.9)$$

where d_b is water depth at breakpoint.

Thus, the limiting wave height (or maximum) which can occur at a structure in a water depth d is 0,78d, provided no scour takes place which would increase the water depth and thus the limiting wave height.

Wave reflection from the structure would seem to cause earlier breakage of the incoming wave, but tests by Jackson [14] showed little influence of wave reflection on the limiting wave height.

However, the solitary theory only applies for flat beach profiles, i.e. slopes $\leq$ 1:150. For steeper slopes, the limiting wave height can be considerably higher and H_b for this case is evaluated by the methods discussed in sub-section 4.2. Again assuming no scour, the maximum wave height reaching the structure follows from d_s using Figure 5. If it is found that the design wave height, H, reaching the structure is equal to or greater than the limiting value, i.e. $H \geq H_b$, H_b is used as the design wave height [39]. If H_b is significantly smaller than H, its occurrence will be much more frequent and a comparison of the design associated deep-water wave height, H_b determined from Figure 5, with actual deep-water wave statistics characteristics at the site will give some indication of how often the structure could be subjected to breakers as high as the design breaker. Deep water height can be obtained from Figure 7 [32] and information obtained from refraction analysis (see sub-section 4.4). Figure 7 is a modified form of Figure 6.

4.4 Wave Transformation:

To determine the actual wave height at the breakwater, the wave transformation from the recording site to the breakwater site must be taken into account. Denoting the wave height in deep sea H_o and in the recording area H_o', the wave height at the breakwater site H is obtained from:

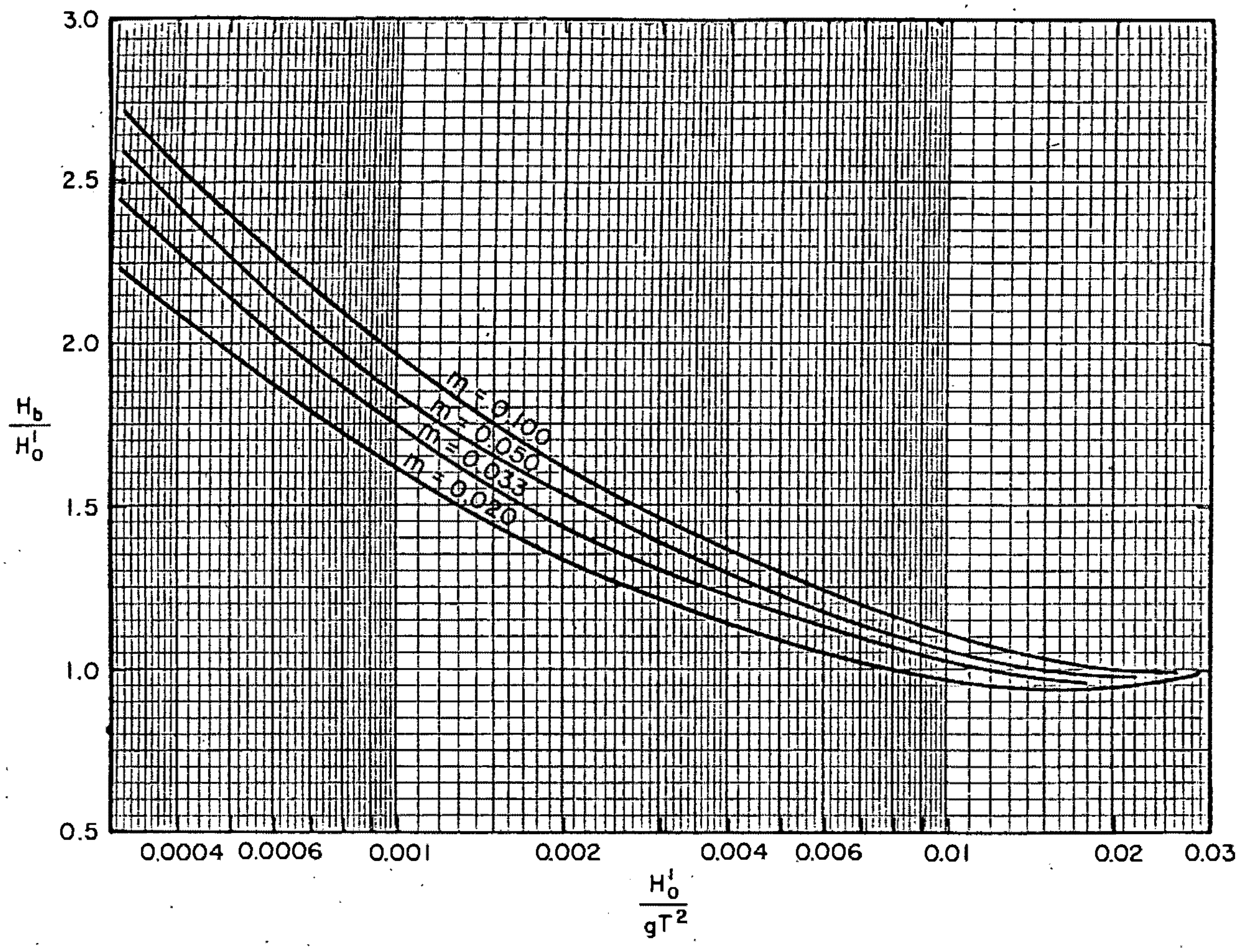

FIGURE 7 Breaker Height Index, H_b/H_o'

vs H_b/gT^2 CERC (1973)

$$H = k_s \, k_r \, k_f \, H_o \tag{4.10}$$

where k_s = shoaling coefficient, being the root of the group velocity ratio, deep water to local value.

k_r = refraction coefficient, being the root of the width between wave orthogonals, deep water to local value.

k_f = the bottom friction coefficient, which can be taken as unity, except where waves travel a long distance in relatively shallow water [39].

The deep water wave characteristics needed in Equation (4.10) follow from:

$$H_o = H'_o / k'_s \, k'_r \, k'_f \tag{4.11}$$

where k'_s, k'_r and k'_f apply to the transformation from deep sea to the recording point (which is usually in fairly deep water in which case $k'_s = k'_f = 1$), and

$$l_o = 1{,}56 \, T^2 \tag{4.12}$$

where T = wave period.

The above formulae give the wave height at the breakwater site provided the waves do not break prior to reaching the site.

CHAPTER 5

DESIGN OF THE STRUCTURE CROSS-SECTION:

Because storm-wave trains contain waves higher than the significant height, it is important that rubble mound breakwaters be designed so that they will not fail when subjected to waves with heights moderately larger than the selected design wave height.

A rubble structure is normally comprised of a bedding layer and a core of quarry run stone covered by one or more layers of larger stone and an exterior layer(s) of large quarry stones or concrete armour units. Typical rubble mound cross-sections for non-breaking and breaking waves are shown in Figures 8 and 9.

A logic diagram for the preliminary design of a rubble mound structure can be seen in the CERC Shore Protection Manual [32] and it is considered beyond the scope of this thesis to be included here.

The following structure geometry should also be investigated in the design:

(a) crest elevation and width,
(b) concrete cap for rubble structures,
(c) thickness of armour layer and underlayers, and number of armour units,
(d) bottom elevation of primary cover layer,
(e) structure head and lee side cover layer,
(f) secondary cover layer,
(g) underlayers, and
(h) bedding layer or filter blanket layer.

The above points are considered in PART II on the Dolus armour unit and when the rubble mound cross-section is designed for use in the model tests in the laboratory.

Some authors [3, 15] advocate the S-Geometry profile for rubble mound structures, particularly for conditions with relatively low tidal

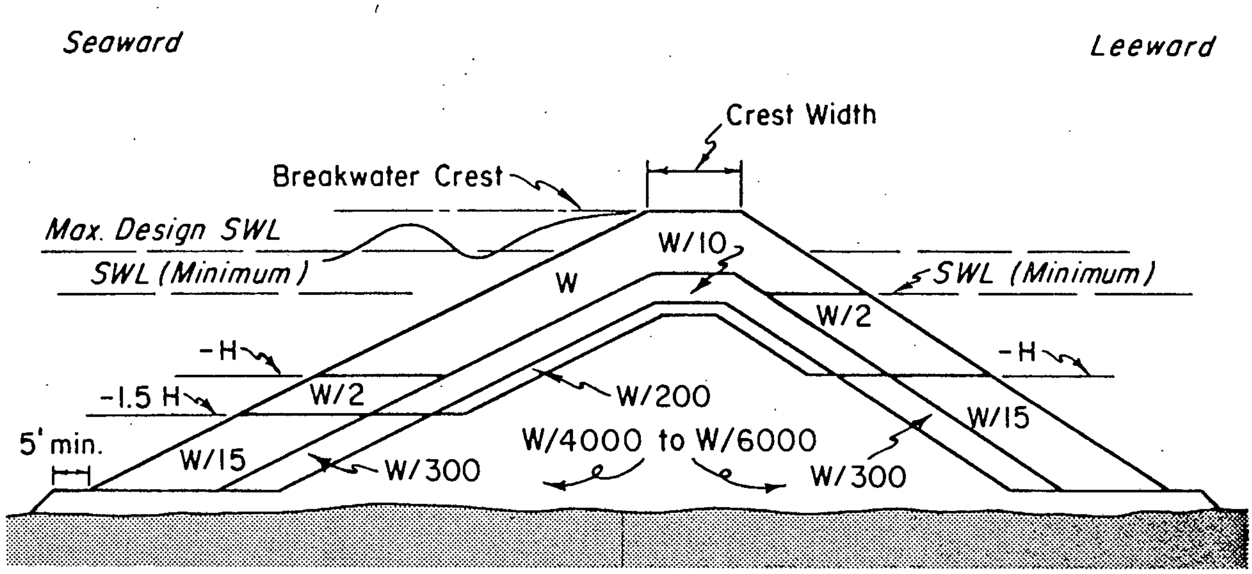

Idealized Multilayer Section

Rock Size	Layer	Rock Size Gradation (%)
W	Primary Cover Layer	125 to 75
W/2 and W/15	Secondary Cover Layer	125 to 75
W/10 and W/300	First Underlayer	130 to 70
W/200	Second Underlayer	150 to 50
W/4000–W/6000	Core and Bedding and Filter Layer	170 to 30

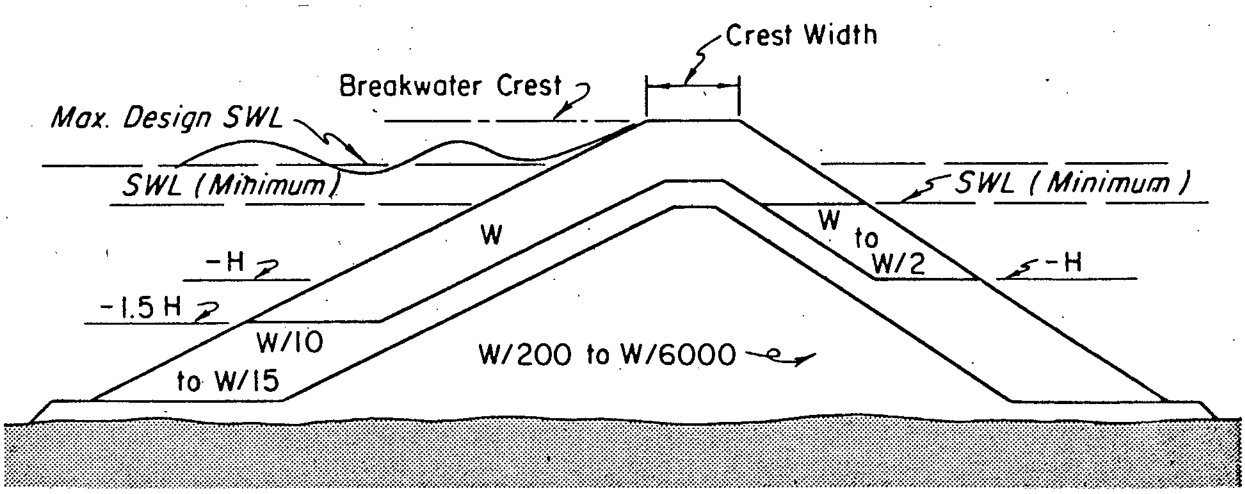

Recommended Three-layer Section

FIGURE 8 Rubble Mound Sections for Non-Breaking Wave Conditions

CERC (1973)

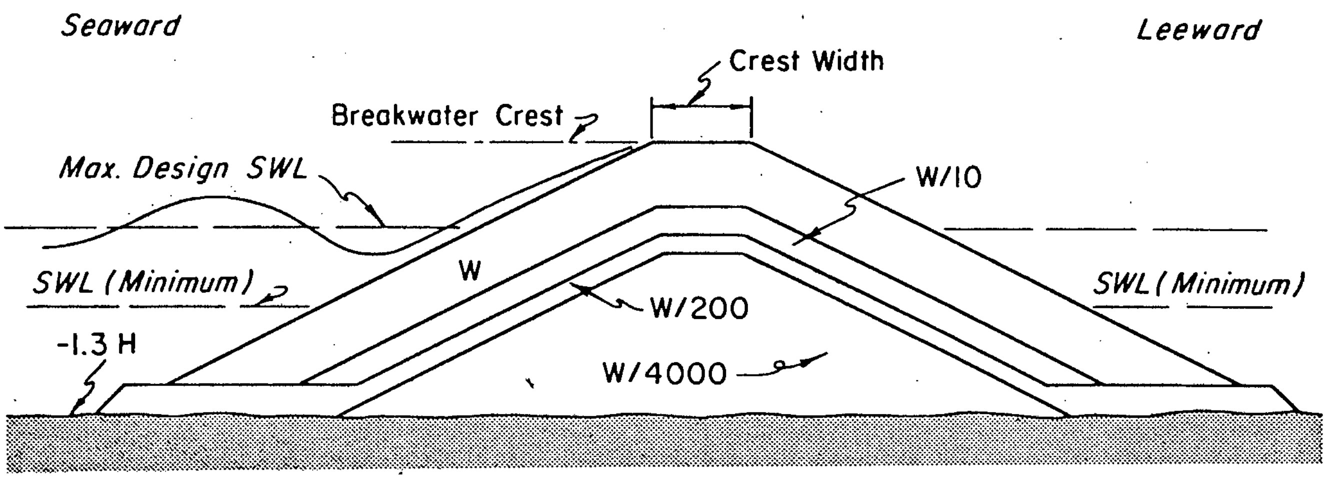

Idealized Multilayer Section

Rock Size	Layer	Rock Size Gradation (%)
W	Primary Cover Layer	125 to 75
W/10	First Underlayer	130 to 70
W/200	Second Underlayer	150 to 50
W/4000	Core and Bedding and Filter Layer	170 to 30

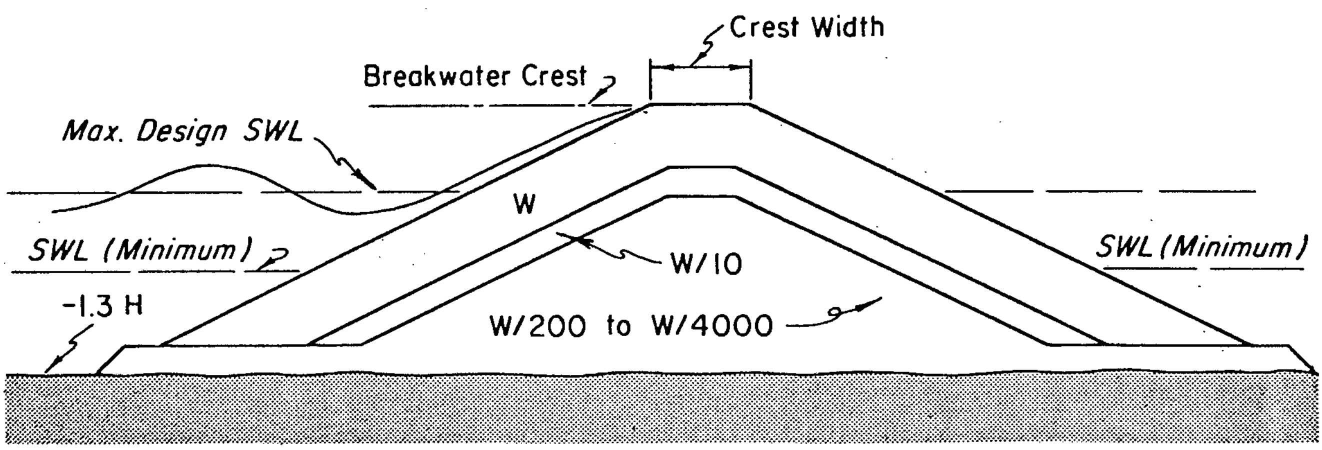

Recommended Three-layer Section

FIGURE 9 Rubble Mound Sections for Breaking Wave Conditions

CERC (1973)

ranges. Due to local failures on a straightlined breakwater profile and basing analyses on self-adjusted 'beaches', it is deemed possible to divide the rubble mound slope for design and construction, into 3 zones, each with its characteristic block properties (Figure 10).

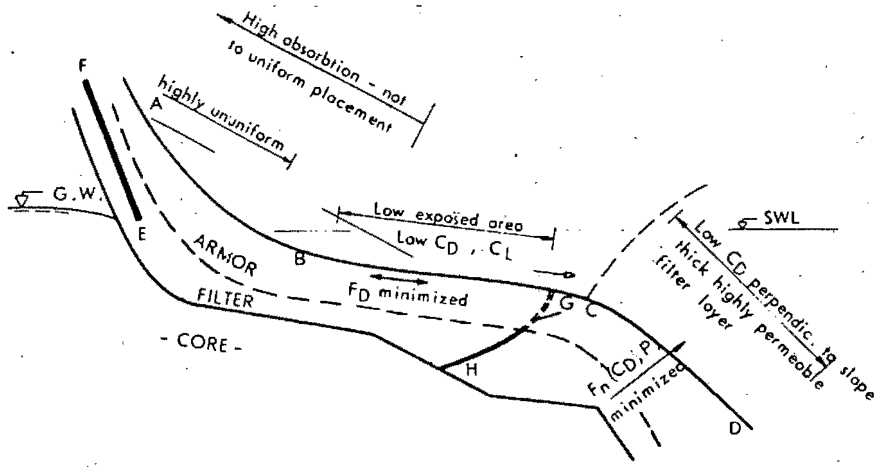

The 'false' beach, BC, evolves a new breaking point at C, which reduces run up (plunging waves and out of phase damping ($t_o/T/2$)).

The impervious layer, FE, prevents inflow above point E which reduces the build up of hydrostatic pressure in the mound. The impermeable layer, GH, prevents backwach-outflow to be concentrated at the breaking point, where the external forces are maximized.

The steep slope, CD, makes the backwash-incipient breaker interaction less violent and further separates backwash from the retreating velocity field in the toe of the breaking wave.

The breakwater slope is divided into three zones, each with its characteristic block-properties. This results in more evenly exposed structure which increases safety against failure. In all cases, however, some flexible interlocking effects is very significant.

FIGURE 10 Optimization of Breakwater Properties BRUUN (1976)

The 'platform', B C , has a relatively gentle slope (e.g. 1 in 3), and waves plunge at C . Run-up is reduced by turbulence and energy absorption in the 'stilling basin', BC. The steep slope C D , separates the toe of the breaking waves, and therefore makes the interaction between these destructive forces less violent and reduces the maximum normal (F_n) and parallel drag (F_D) forces at the lowest level of wave retreat where these forces are usually most critical for stability. A layer HG, with low permeability, prevents outflow from being concentrated at the breaking point where the external forces, primarily suction at the toe of the breaking wave, are maximized. Another layer, FE, with lower permeability, prevents inflow above point E, reducing the build up of hydrostatic pressure in the mound during wave retreat. In zone BC, the drag coefficient

(C_D) of the blocks parallel to the slope and the exposed area of armour blocks should be minimized. In zone CD, the drag coefficient of the armour blocks perpendicular to the slope should be minimized due to high normal forces and concentrated outflow. The upper slope, AB, may be relatively rough as it is not exposed to high velocities. Roughness decreases uprush and results in lower downrush velocities.

CHAPTER 6

OPTIMIZATION OF DESIGN:

Once the basic design of a rubble mound breakwater has been established, the design can be optimized to arrive at the most economical solution. The various aspects which can be looked into include:

- the choice of main armouring which should be checked on a comparative cost basis;
- choice of design wave and accepted damage to give minimal overall cost;
- crest level and degree of overtopping;
- detailed crest design including splash walls.

Although a basic design can be based on available data at the site, model tests are considered essential for the final design in all but the most straightforward cases. Aspects which can be checked from model tests include [39]:

- effect of shoaling water;
- effect of local wave concentration due to irregular bottom topography;
- effect of irregular waves, particularly for deep water breakwater;
- effect of different wave directions;
- damage as a function of wave height;
- effect of storm duration;
- effect of different crest levels;
- inside slope design;
- design of splash wall;
- breakwater head design.

Normally, tests have been limited to two-dimensional flume tests, but in many cases three-dimensional effects are significant and cannot be neglected, e.g. Richards Bay, Gansbaai and Koeberg breakwaters [39]. Where indicated, three-dimensional model tests should therefore be carried out at a sufficiently large scale to avoid scale effects (a scale of 1 in 50 suffices while a scale of 1 in 100 may in some cases give conservative results).

PART II

THE DOLOS CONCRETE ARMOUR UNIT

CHAPTER 7

INTRODUCTION:

The Laboratory investigations were conducted using model Dolosse in preference to other armour units or natural rock because they have proved to be the most effective armour unit for the protection of breakwaters against wave action. As this thesis does not incorporate the destruction of the rubble mound breakwater via the displacement of the armour units, but rather the subsidence of the armour covering due to underscour, the armour unit most resistant to intensified wave action has been utilized.

CHAPTER 8

THE DEVELOPMENT OF THE DOLOS:

After a serious breach occurred in the East London breakwater in 1944, its 1 km seaward face was protected with 37 tonne rectangular concrete blocks. By 1963 it was estimated .... "that the outer half of the breakwater had lost at least 50 per cent of its seaward random block protection, while a few sections were almost stripped bare to the original mound core. It was, therefore, evident that the existing 37 tonne armour blocks did not provide a stable protection and, if the high costs of replacement were to be brought down to a reasonable figure, some other type of armour block would have to be used" [19]. Numerous armour units, which to a large extent had replaced the original concept of natural rock blocks (whose weight was in the excess of 30 tonnes), were considered. However, these special shaped blocks such as tetrapods, hexapods, stabits, etc. were not utilized due to patent rights and the high cost involved. Consequently, Mr. E.M. Merrifield, Harbour Engineer, East London, decided to investigate a new type of armour unit. After testing numerous shaped wooden models he concluded that the Dolos anchor-shaped block best satisfied the requirements of a successful armour unit. These requirements were:

(a) a high void to solid ratio to facilitate the dissipation of wave energy,
(b) each block should be linked with others to form a knitted composite structure,
(c) the block should have sufficient mechanical strength to facilitate rouch handling when being placed,
(d) a block shape which could be economically manufactured.

Tests were carried out by the CSIR in Pretoria with model breakwater blocks placed at random in a double layer on a 1 in $1\frac{1}{2}$ slope. Results of these tests compared favourably with tests done by numerous other research teams, and the advantages of the Dolos over the other concrete armour blocks were recorded. These results appear at a later stage of this section.

CHAPTER 9

THE STABILITY ANALYSIS:

The phenomenon of waves exerting forces on breakwaters is very complex. It is very difficult to determine exactly the magnitude and distribution of forces but there are many available theoretical and empirical design methods for rubble mound breakwaters. The most important quantity to be determined in the design is the weight of the armour units in the breakwater cover layer.

Comprehensive investigations by Hudson [12,13] at the U.S. Army Engineer Waterways Experiment Station (WES) resulted in a formula being developed and modified from the one previously used by Iribarren, to determine the stability of armour units on rubble structures. The stability formula, based on the results of extensive small-scale model testing and some preliminary verification by large-scale model testing is:

$$W = \frac{\rho_r H^3}{K_D (S_r - 1)^3 \cot \alpha} \quad \text{(kg)} \tag{9.1}$$

where W = armour unit mass in kg,

ρ_r = density of the armour unit,
= 2245 kg/m^3 for concrete

H = design wave height in metres*

S_r = relative density of the armour unit = ρ_r/ρ_w
and ρ_w = 1025 kg/m^3 for salt water,
and = 1000 kg/m^3 for fresh water,

α = angle of the structure slope measured in degrees from the horizontal,

and K_D = stability coefficient which varies primarily with the shape of the armour units, roughness of the armour unit surface, sharpness of edges and the degree of interlocking obtained in placement. (See Table 9.1)

---

*(See note at the end of this section on page 46)

No-Damage Criteria and Minor Overtopping							
Armor Units	n *	Placement	Structure Trunk		Structure Head		
			K_D §		K_D		Slope
			Breaking wave	Nonbreaking wave	Breaking wave	Nonbreaking wave	cot θ
Quarrystone							
Smooth rounded	2	random	2.1	2.4	1.7	1.9	1.5 to 3.0
Smooth rounded	>3	random	2.8	3.2	2.1	2.3	‖
Rough angular	1	random †	†	2.9	†	2.3	‖
Rough angular	2	random	3.5	4.0	2.9	3.2	1.5
					2.5	2.8	2.0
					2.0	2.3	3.0
Rough angular	>3	random	3.9	4.5	3.7	4.2	‖
Rough angular	2	special ‡	4.8	5.5	3.5	4.5	‖
Tetrapod and Quadripod	2	random	7.2	8.3	5.9	6.6	1.5
					5.5	6.1	2.0
					4.0	4.4	3.0
Tribar	2	random	9.0	10.4	8.3	9.0	1.5
					7.8	8.5	2.0
					7.0	7.7	3.0
Dolos	2	random	22.0 ¶	25.0 ¶	15.0	16.5	2.0 £
					13.5	15.0	3.0
Modified Cube	2	random	6.8	7.8	—	5.0	‖
Hexapod	2	random	8.2	9.5	5.0	7.0	‖
Tribar	1	uniform	12.0	15.0	7.5	9.5	‖
Quarrystone (K_{RR}) Graded angular	–	random	2.2	2.5			

* n is the number of units comprising the thickness of the armor layer.

† The use of single layer of quarrystone armor units subject to breaking waves is not recommended, and only under special conditions for nonbreaking waves. When it is used, the stone should be carefully placed.

‡ Special placement with long axis of stone placed perpendicular to structure face.

§ Applicable to slopes ranging from 1 on 1.5 to 1 on 5.

‖ Until more information is available on the variation of K_D value with slope, the use of K_D should be limited to slopes ranging from 1 on 1.5 to 1 on 3. Some armor units tested on a structure head indicate a K_D-slope dependence.

¶ Data only available for 1 on 2 slope.

£ Slopes steeper than 1 on 2 not recommended at the present time.

TABLE 9-1 Suggested K_D Values for Use in Determining Armour Unit Weight

CERC (1973)

Equation (9.1) is intended for conditions when the crest of the structure is high enough to prevent major overtopping.

The dimensionless stability coefficient K_D in Equation (9.1) accounts for all variables other than the structure slope, wave height, unit mass of armour units (ρ_r), and the relative density of water at the site (i.e. fresh or salt water). These variables include:

- shape of armour units,
- number of layers of armour units,
- manner of placing of armour units,
- degree of interlocking of armour units,
- type of wave attacking structure (breaking or non-breaking),
- part of structure (trunk or head),
- angle of incidence of wave attack,
- model scale (Reynolds Number),
- distance below still-water level that the armour units extend down the face slope,
- size and porosity of the underlayer material,
- core height relative to still-water level,
- crown type (concrete cap or armour units over the crown and extending down the back slope),
- crown elevation above still-water level relative to wave height,

and - crest width.

Results of tests conducted by Merrifield *et al* [19] on the stability of various concrete armour units under wave attack (shown in Figure 11), compared favourably with the results of Hudson [13], and it can be seen from this figure and Table 9.2 (extracted from Figure 11), that the Dolos is more stable than any other type of block. (This also becomes evident by the comparison of values in Table 9.1).

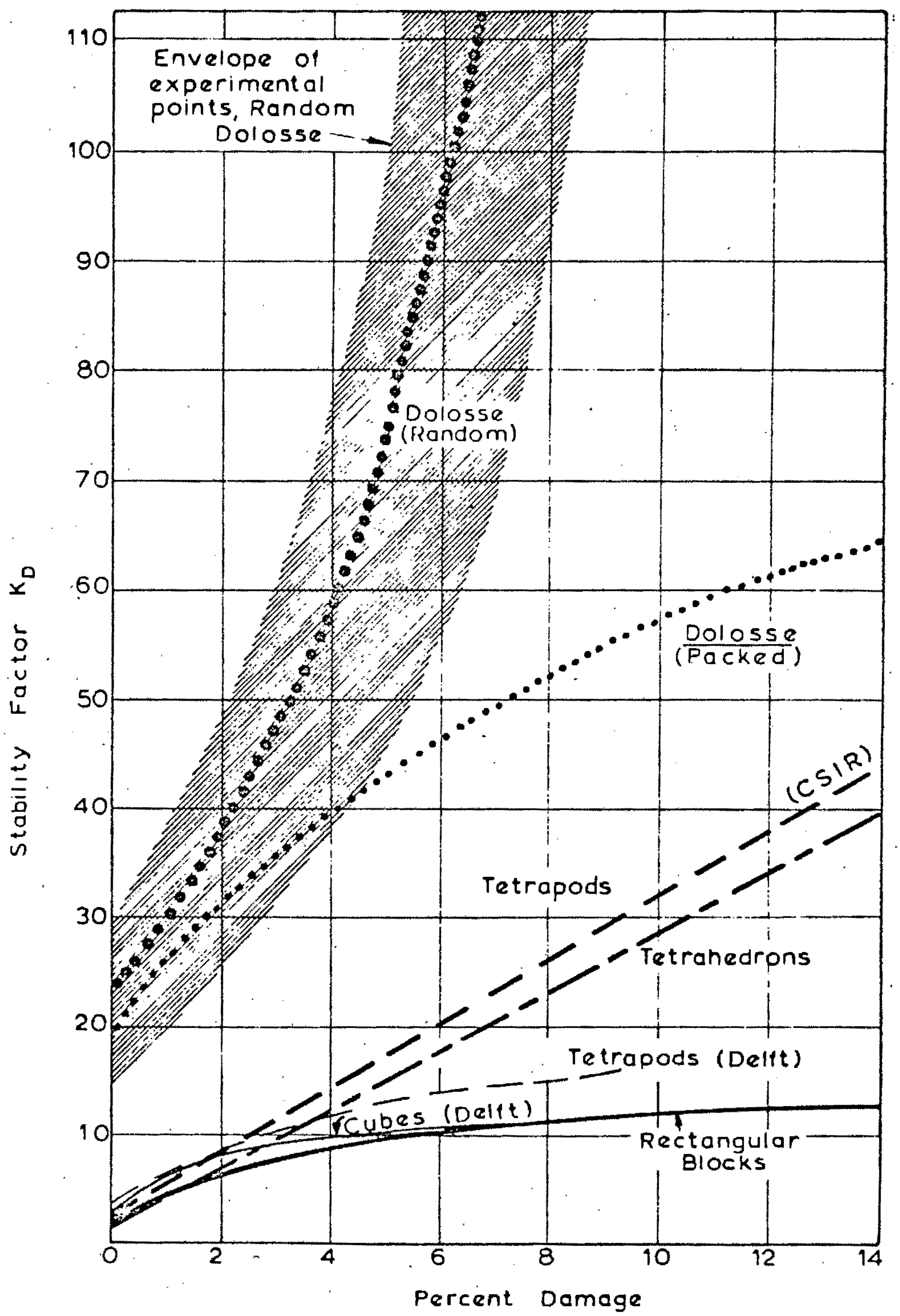

FIGURE 11 Stability factors vs total damage

MERRIFIELD (1966)

TABLE 9.2: CSIR'S STABILITY FACTORS (K_D) FOR THE 0%-DAMAGE CASE

Armour Unit	Method of Placing	K_D	
		Damage	Total damage
Rectangular blocks	random, double layer	2,5	2,3
Tetrahedrons	" " "	1,5	1,2
Tetrapods	" " "	6,5	2,5
Dolosse	" " "	40	24
Dolosse	uniform, single layer	25	20

The values of K_D in Table 9.2 were obtained for the 0 per cent damage case where the value of H was taken to be the wave height at which damage started. The term 'damage' was accessed in terms of the movement of a block over a distance greater than 50 mm. For those blocks which rocked to and fro so that structural damage would probably have occurred due to the loss of the block to wave absorption, a term 'total damage' was used. This was a conservative assumption .... "as practical experience has shown that the conical design of the Dolos limbs enables it to rock with the first storm and move into a far firmer interlocking position" [20].

Since the required armour block weight is inversely proportional to the stability coefficient, the high values of K_D for Dolosse imply smaller individual units and therefore, less concrete volume, when designing for a particular wave height. For example, a wave height of 7,5 m yields the following approximate block sizes and concrete volumes for equal stability:

Type of Block	Rectangular	Tetrahedron	Tetrapod	Dolos
Block Mass (tonne)	46	39	34	11
Concrete Vol (m^3/m^2)	2,7	2,5	2,4	1,7

Other recent tests have been undertaken on Dolos stability [37] and the initial CSIR results have been substantially confirmed so that the Dolos is now widely considered as the most stable breakwater concrete armour unit available.

CHAPTER 10

POROSITY, SHAPE FACTOR AND RELATIVE WAVE RUN-UP:

Breakwater design requires, in addition to quantative data to insure stability of armour units and prevent excessive overtopping, accurate information concerning the porosity of the cover layer as a function of shape, mass and density of the individual armour units.

The Porosity (P) is defined as the percentage voids of the total volume of the cover layer. The porosity of a given number of layers of armour units of mass W, and density ρ_r, can be determined from [12]:

$$P = (1 - \frac{N_r \cdot W}{A \cdot \rho_r \cdot Z}) \, 100 \qquad (10.1)$$

where P = average porosity in per cent, of the cover layer,

N_r = experimentally determined number of armour units for a given surface area A,

and Z = cover layer thickness (see Equation (11.3)).

A high porosity of the armour layer is beneficial since wave run-up as well as the total concrete volume required in the cover layer are reduced.

Porosity values for cover layers of different type armour blocks were obtained in the tests conducted by Merrifield and these are shown in Table 10.1.

TABLE 10.1: POROSITIES OF COVER LAYERS IN PER CENT

Type of block	Hudson	Paape et al	CSIR	Accepted
Cubes	47	47	-	
Rectangular blocks	-	-	50	50
Tetrapods	50	53	55	53
Tetrahedrons	-	-	60	60
Dolosse (random)	-	-	60	60
Dolosse (packed, single layer)	-	-	41	41

The porosity of randomly dumped dolosse is high and consequently, this results in a significant reduction in wave run-up.

The required number of blocks for a given block weight is proportional to the Shape Factor, C, of the armour unit, and thus a low value of C is desirable. A comparison of Shape Factors for various units is shown in Table 10.2 [19], C being determined from Equation (11.2).

TABLE 10.2: SHAPE FACTORS (C) OF ARMOUR UNITS

Type of block	Hudson	Paape et al	CSIR	Accepted
Cubes	1,1	-	-	
Rectangular blocks	-	-	1,0	1,0
Tetrapods	1,0	1,0	1,0	1,0
Tetrahedrons	-	-	1,2	1,2
Dolosse (random)	-	-	1,3	1,3
Dolosse (packed)	-	-	1,2	1,2

The high values reflected for Dolosse in the above table mean that for a given block size the cover layer is relatively thick (see Equation (11.3), which could be an explanation for the high stability of the Dolos.

The Wave Run-up, that is the vertical height above still water level that the rush of water reaches, determines the top elevation to which the structure must be built to prevent overtopping. The actual run-up depends on the characteristics of the structure, i.e. the shape and roughness of the armour units, the water depth, and the incident wave characteristics [23]:

$$\frac{R}{H} = f\left(\frac{H}{T^2}, \frac{d_s}{H}, \cot\alpha, \text{roughness of facing}\right) \qquad (10.2)$$

where T = the wave period,

d_s = water depth at the structure

and $\frac{R}{H}$ = relative run-up (see Figure 12).

As can be expected from the high porosity values, the Dolos, dumped at random, showed smaller run-up figures than all the other blocks considered in the tests by Merrifield *et al.* These maximum relative wave run-up values are shown in Table 10.3.

TABLE 10.3: MAXIMUM RELATIVE WAVE RUN-UP

Type of block	Rectangular block	Tetrapods	Tetrahedrons	Dolosse (random)	Dolosse (packed)
R/H	1,00	0,90	0,98	0,83	0,90

The positions of R and H are explained below in Figure 12 for a recommended rubble mound breakwater.

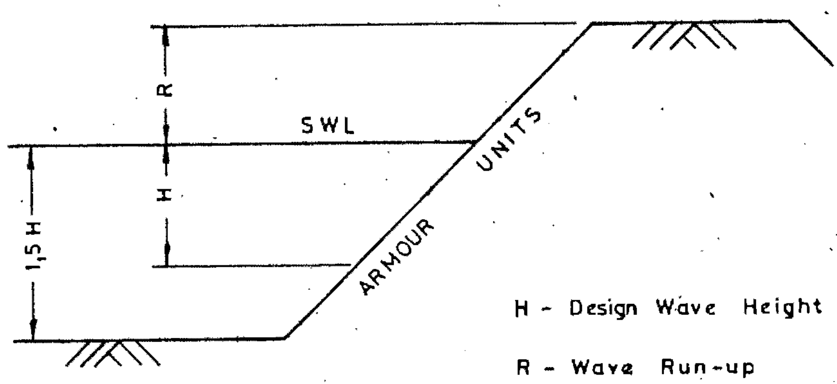

FIGURE 12 Relative Wave Run-up

CHAPTER 11

DESIGN CRITERIA FOR DOLOS ARMOURING: [19, 21, 38]

The required mass, W, of an individual armour unit is defined by the Hudson formula (Equation (9.1)), the value of K_D being obtained from Table 9.1, for the local wave conditions.

$$\text{i.e.} \quad W = \frac{\rho_r H^3}{K_D (S_r - 1)^3 \cot \alpha} \quad \text{(kg)}$$

Having obtained W from the above equation, the height of the Dolos may be reduced from:

$$V = K h^3 \tag{11.1}$$

where h = Dolos height (see Figure 13) (m)
V = W/ρ_r, the Volume of the Dolos (m^3)
and K = 0,15 for waist ratio r = 0,30
= 0,16 for waist ratio r = 0,32
= 0,17 for waist ratio r = 0,34

and, r = waist to height ratio as defined in Figure 13 and Equation (11.8).

i.e. width of the waist of the Dolos will be given by 0,30h, 0,32h and 0,34h for the cases considered.

Harshkumar [9] states that for $r = 0{,}32$, $K = 0{,}1549$ as compared to 0,16 and this difference results in large savings in concrete volume for projects involving large sized dolosse (20 - 40 tonne) in great numbers. This, however, is of mere academic importance as regards this thesis.

The number of armour units, N, required to cover a unit area (m^2) is given by:

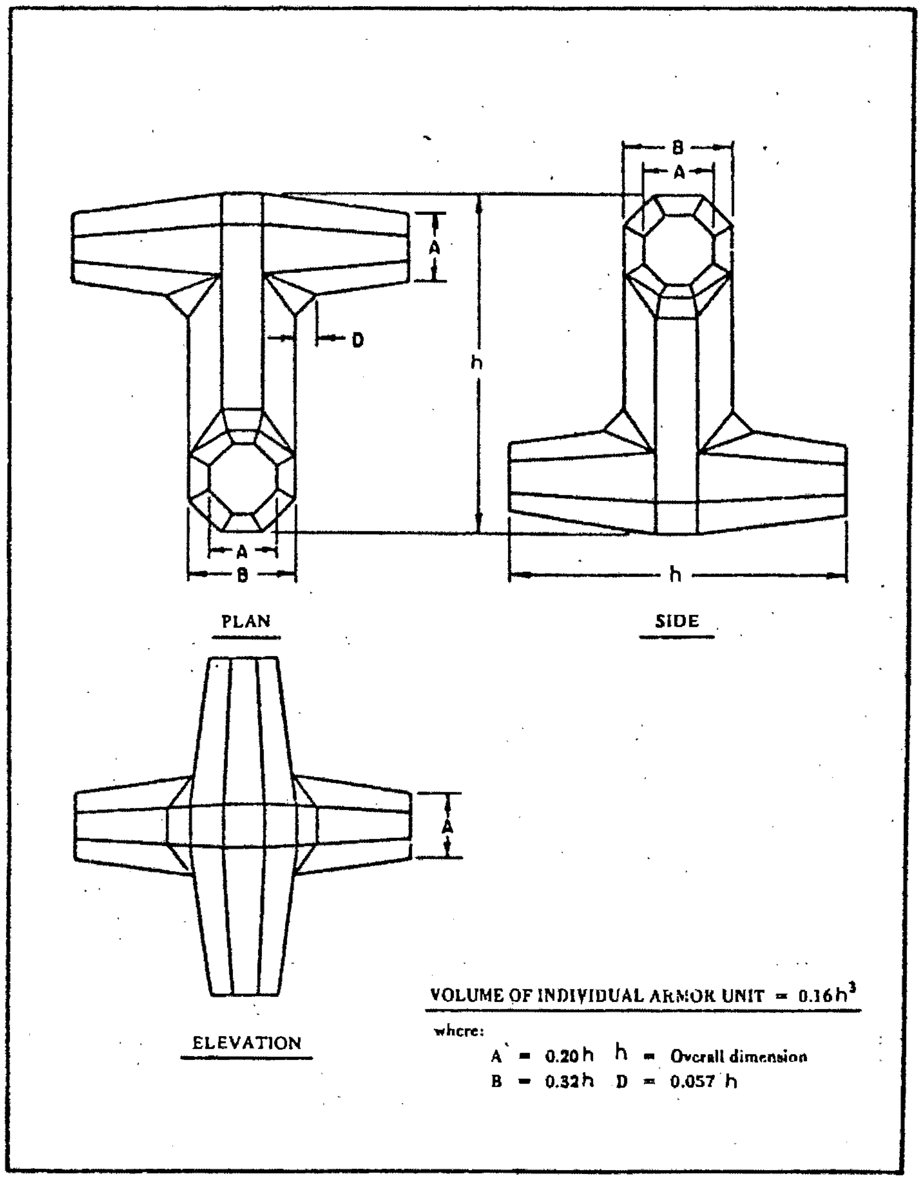

FIGURE 13 The Dolos

$$N = nC(1 - \frac{P}{100}) V^{-\frac{2}{3}} \qquad (11.2)$$

and the cover layer <u>thickness</u>, Z, will be

$$Z = nC(V)^{\frac{1}{3}} \qquad (11.3)$$

where, n = number of Dolos layers (single or double),
C = shape factor,
P = percentage porosity,
and V = armour block volume (m^3)

Recent experiments [38] give values for C between 1,3 and 0,9 and P between 50 and 60 per cent, so that Equations (11.2) and (11.3) may be reduced.

Overtopping of a rubble structure usually can be tolerated if it does not cause damaging waves behind the structure. Whether overtopping occurs depends on the height of the crest of the structure relative to the height of <u>wave run-up</u>, R.

The height of the protective Dolos armour layer above still water level depends on this wave run-up, and is given by:

$$R = 0{,}83\ H \text{ (see Table 10.3)} \qquad (11.4)$$

The <u>width of the crest</u> of the breakwater depends greatly on the degree of overtopping. Where there will be no overtopping, crest width is not critical. As a general guide, crest width may be obtained from the following equation: " length " of armour

$$C_w = n\, k_\Delta \left(\frac{W}{\rho_r}\right)^{\frac{1}{3}} \qquad (11.5)$$

where, C_w = crest width (m),
n = number of armour units in width across the crest (3 is minimum),
k_Δ = layer coefficient (equals 1 for random placed Dolosse),
W = mass of the armour unit in the primary cover layer (kg)
ρ_r = density of the armour unit (kg/m^3).

Practically, the crest width must be wide enough to accommodate construction and maintenance equipment from the structure.

There is also a limit to the size of the core material of the Dolos armoured rubble mound breakwater, and to insure that this material does not wash out between the dolosse, an underlayer of large stone must be provided. The recommended stone weight is:

$$W_u = \frac{W}{5} \tag{11.6}$$

and the thickness of this underlayer follows from:

$$Z_u = n_u C_u (V_u)^{\frac{1}{3}} \tag{11.7}$$

where, n_u = 2(double layer),
C_u = 1,15(quarry stone),
and V_u = $W_u/2640$ (m^3), where 2,64 is the relative density of quarry stone.

The strength of an individual Dolos unit has been reduced by the investigation of various waist ratios. The waist ratio, r, is defined as:

$$r = 0,34 \sqrt[6]{W/20} \tag{11.8}$$
$$\geq 0,30, \quad \text{where } W \text{ is in tonnes.}$$

Extensive studies of the stress distribution in Dolosse for different loading conditions using photo-elastic stress analysis, and much practical experience in the use of this unit, has led to the conclusion that unreinforced Dolosse with waist ratios in the range 0,3 to 0,5 are sufficiently strong to withstand all the forces they are subjected to during handling, placing and in service.

In some cases [5], unreinforced Dolosse were considered inefficient as in Humboldt Bay Harbour, San Francisco where 42 tonne (42000 kg) and 43 tonne (43000 kg) Dolosse have had to withstand an assault by winter waves, 12 m in height. Here, a conclusion was reached that ... "reinforcing is essential in maintaining the integrity of the

Dolosse during the dynamic loading created by large waves during a storm and that reinforced Dolosse will assure the necessary stability for the interlocking structure at Humboldt Bay."

In practice, Equations (9.1) to (11.7) yield a "first estimate" of the main dimensions of Dolos armouring. Criteria graphs were presented by Merrifield [20] for general use in selecting the size of the Dolos to be used, and for the preparation of estimate quantities.

However, the final design depends on local conditions, and more detailed calculations, suplemented by hydraulic model tests, are necessary to arrive at the optimum design.

CHAPTER 12

THE ECONOMICS OF THE DOLOS:

When using Dolos armouring, a saving in concrete volume in the cover layer and manufacturing costs of 40 per cent [19], is obtained. Also, because of the smaller size of the Dolos, in inaccessible areas which have no heavy handling equipment (e.g. Tristan da Cunha [38]), the advantage of the smaller blocks would outweigh the extra handling due to more blocks.

Indirectly, because wave run-up is reduced on Dolos breakwaters, a further saving is effected because the whole breakwater structure could be made lower.

CHAPTER 13

PRACTICAL APPLICATIONS OF DOLOSSE:

Since the first use of Dolosse on the East London breakwater in 1964/65, Dolosse have been used extensively locally and internationally. Some of the more important applications are briefly detailed:

Port Elizabeth Shore Protection:

Dolos size	W	= 2,7 tonne
Underlayer	W_u	= 1/4 to 2 tonne
Dolos Numbers	N	= 28000

Cape Town Harbour Extensions:

Design wave heights	H_1	= 2,1 m	H_2	= 4,3 m
Dolos sizes	W_1	= 2,7 tonne	W_2	= 5,4 tonne
			(r	= 0,32)
Underlayer	W_u	= $\frac{1}{2}$ to 2 tonne		
Dolos Numbers	N_1	= 8820	N_2	= 12030

Gansbaai Fishing Harbour:

Design wave height	H	= 6,1 m
Dolos sizes	W_1	= 4,5 tonne; W_2 = 14,4 tonne
	W_3	= 17,1 tonne
Waist ratio	r	= 0,29
Dolos Numbers	N_1	= 2370; N_2 = 860; N_3 = 930.

Richards Bay Harbour:

Design wave heights	H_1	= 5 m H_2 = 7,5 m
Dolos sizes (trunk; head)	W_1	= 5 tonne; W_2 = 15 tonne
	W_3	= 20 tonne; W_4 = 30 tonne
Waist ratios	r_1	= 0,33; r_2 = 0,33; r_3 = 0,33;
	r_4	= 0,37
Dolos Numbers	N_1	= 2800; N_2 = 1200; N_3 = 10500;
	N_4	= 1800.

Humboldt Bay Breakwater (San Francisco):

Design wave height	H	= 12,2 m (breaking)
Dolos size	W_1	= 38 tonne; W_2 = 39 tonne ($r = 0,32$)
Dolos Numbers	N_1	and N_2 = 5000

Bulk Port at Sines (Portugal):

Design wave height	H	= 11 to 12 m
Dolos size	W	= 40 tonne ($r = 0,85$)

Figure 14 shows a typical Dolos armoured rubble mound breakwater.

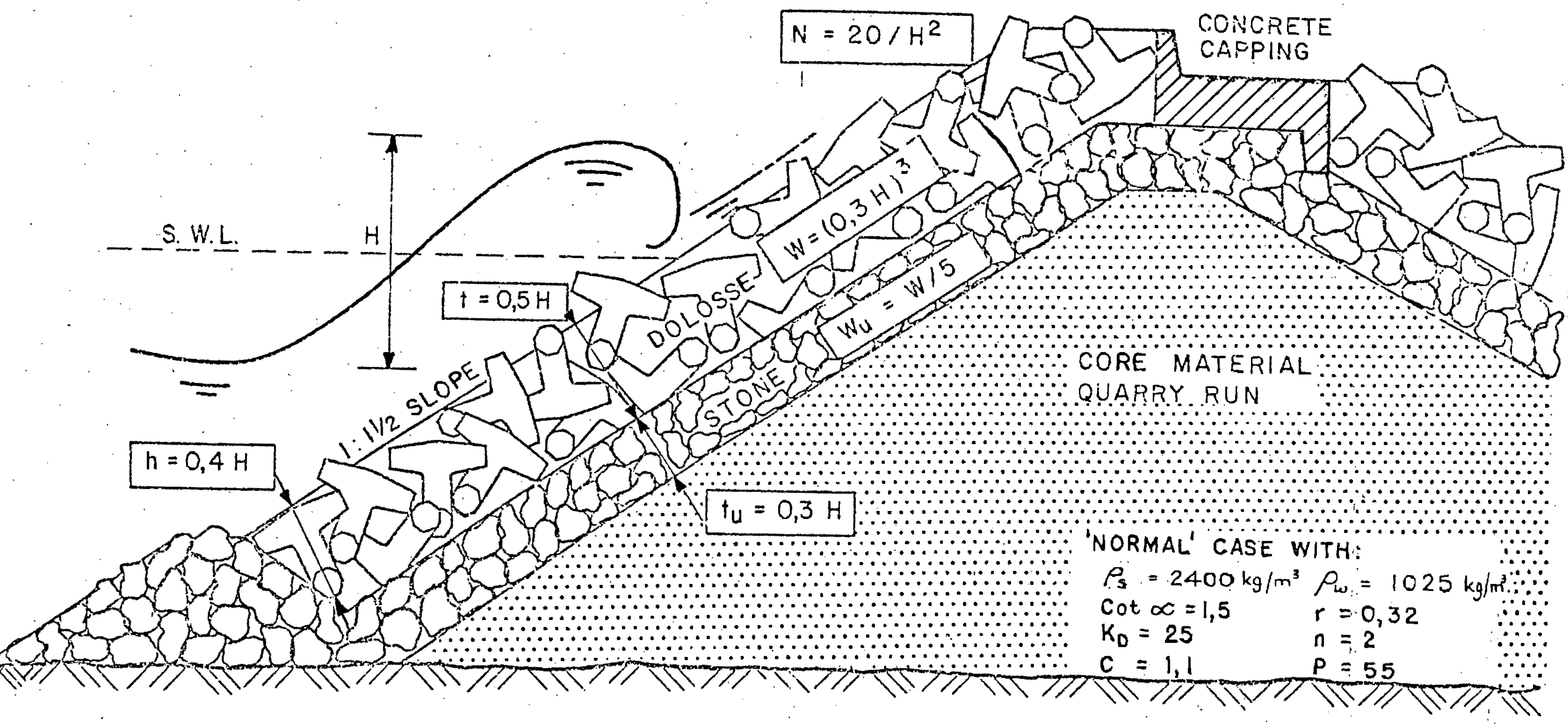

FIGURE 14

ZWAMBORN (1976)

BREAKWATER WITH DOLOS ARMOURING

CHAPTER 14

CONCLUSION:

Dolosse were used in the research of this thesis as they are recognized worldwide as the most effective and economical concrete armour unit available, and because .... " the performance of Dolosse, both in nature and model studies, was found to be excellent in comparison with other specially designed breakwater armour blocks" [19].

*

[A study of the literature on the subject reveals doubt as to the use of the correct H, the Design Wave Height, in the stability Equation (9.1). Merrifield [19,20,21], Zwamborn [19,37,38] and Beute [37] make use of the significant wave height, $H_{\frac{1}{3}}$, i.e. the average height of the highest third of the high waves. Hudson [12] considers H to be the wave height which would result in no damage - no damage is defined by Hudson as a laboratory criterion when waves attack rubble mound breakwaters; a breakwater or jetty subject to waves of certain height for 0,5 hrs. with less than 1 per cent removal of armour units from the cover layer. Morais [22] however, states that the significant wave height should not be used, but offers no alternative as such ...... "The main conclusion is that the significant wave height should not be used as an equivalent parameter for regular and irregular waves. Results are not enough to allow the definition of another parameter, which however should be an exceedance quantile greater than $H_{\frac{1}{3}}$, but not lower than $H_{1/100}$."]

CHAPTER 15

MODEL DOLOS SPECIFICATIONS:

The Dolos models used in the laboratory investigations conformed very closely in detail to the dimensions as given in Figure 13.

They were mass produced from highly accurate moulds manufactured by skilled craftsmen of the C.S.I.R. at Stellenbosch, using the following procedure:

- The first stage is a master, hand carved from wood 2,6 % bigger than the final product to allow for shrinkage when the templet and the moulds are cast.
- The templet, then made in two halves using the master, consists of a mixture of 30 % Crystic Resin and 70 % Barytas (the S.G. Additive).
- Moulds are then cast from Silicon Rubber, encased in either wood or steel. These are filled by pouring the resin mixture in openings in the top of the trunk and the horizontal flukes.
- The models are of the same basic mixture as the templet, but include 2 % by volume accelerator, 2 % by volume catalyst and 100 grams of pigment paste for the colouring. A setting time of 1 hour is normal. They have the following dimensions:

Mass	:	235 grams
Volume	:	97,5 cm^3 (an average value obtained by immersing dolosse in water and measuring the displacement)
Density of Model dolos	:	2,41 g/cm^3
h	:	84 mm

PART III

THE UNDERSCOUR OF RUBBLE MOUND BREAKWATERS BY WAVE ACTION

CHAPTER 16

INTRODUCTION:

The study on the phenomenon of scouring in the vicinity of the toe of rubble mound coastal structures is necessary because it has a close relation with the subsidence of the cover layer units due to wave action. A review of the literature on scouring showed few reports of this phenomenon and this could be due to the complexity of the study and the difficulty of field observations under storm conditions.

The laboratory investigations undertaken in this thesis, conclusively proved, via the use of fluorescent tracing sand particles, that scouring action definitely occurred in the vicinity of the toe of rubble mound breakwaters under the attack of non-breaking waves.

The effect of scour is to reduce the lateral capacity of the underwater foundation and the excessive settlements which may occur reduce the effectiveness of the breakwater in some of the following ways:

- overtopping is likely to be increased,
- armour units may be damaged in the subsidence process, reducing their effectiveness,
- movements of deck traffic (if any) may be adversely affected,

and - the appearance of the structure suffers.

The scour of bed particles adjacent to an obstacle begins when the velocities and accelerations of the water particles cause hydrodynamic forces sufficient to overcome gravity, and cause the bed particles to move. When the bed particles begin to tip from their angle of repose, this is defined as <u>incipient motion</u> and is the point where any study of scour must begin.

Incipient motion and scour have been studied extensively with regard to steady open channel flow, but it has only been in the last two decades that research has been carried out in oscillatory motion.

Because of the difficulty in formulating mathematical equations that represent accurately the phenomena of incipient motion, scour and ultimate scour depth, no formulation of mathematical equations has been attempted in this study. However, the interrelationships and interdependency of the parameters have been experimentally investigated in a two-dimensional wave flume under unidirectional flow regimes of monochromatic waves of various steepness and relative depth to produce the incipient motion and scour results.

CHAPTER 17

BACKGROUND:

The majority of research done on scour in oscillatory motion has been concerned primarily with scour of beaches and littoral sediment transport, but these studies have been few. However, their exists a wealth of knowledge on scour in open channel flows. Since the forces causing scour are somewhat similar for oscillatory flow as for open channel (steady state) flow, the knowledge gained from experiments in open channel flow can be applied with reservations to oscillatory motion. Wells *et al* [34] summarizes all of these previous studies fairly well.

Herbich *et al* [11] studied scour in front of sea walls at various angles and their findings showed that the ultimate depth of scour was a function of wave characteristics as well as the number of waves passing a given point where scour occurred, and scour approached its maximum value asympotically after initially increasing very rapidly.

Roper *et al* [26] showed that for steady state conditions in open channel flow, the depth of scour was a function of the pier Reynolds number, defined as

$$N_{RP} = \frac{U\emptyset}{\gamma} \qquad (17.1)$$

where U = horizontal free stream velocity,
$\emptyset$ = pile diameter
and γ = kinematic viscosity of the fluid.

It was shown that scour is influenced by the type of vortex system caused by the pier. The horseshoe vortex system was the mechanism of scour at the leading edge of blunt-nosed piers. It is possible that a similar effect could occur when waves pass the vertical columns of dolosse at the breakwater toe, but, for oscillatory motion conditions (non-steady state) this horseshoe vortex system may not have time to hold up to an intensity that it is shed and, therefore, the vortex system formed by oscillatory wave motion may not influence the scour.

Roper *et al* also concluded that the bed particle size has a definite influence on local scour. They showed that when the bed particle size is greater than 0,52 millimetres, the particle size influences scour depth and when the particle size is less than 0,52 millimetres, scour depth is independent of particle size.

Carstens [4] made extensive studies of the scour associated with different obstacles. He showed that the rate of scour caused by an object in the flow path was a function of the sediment number N_s, sediment grain geometry, and the ratio of the scour depth to the obstacle size. The sediment number was defined as:

$$N_s = \frac{U}{\sqrt{(S_s - 1)\ gD}} \tag{17.2}$$

where, U = free stream velocity,
S_s = relative density of sediment,
g = acceleration of gravity,
and D = mean sediment particle diameter.

His studies were primarily conducted in steady flow and he presented equations for the ultimate scour depth associated with a vertical cylinder and for the relative scour depth as a function of the sediment number. However, he based these equations on the assumption that the scour hole will have a special shape, that of an inverted frustum of a right circular cone having a base diameter equal to the pile diameter and a side slope equal to the angle of repose of the sediment.

Wells *et al* [34] utilized the knowledge obtained by Roper and Carstens and extended them to scour associated with non-steady oscillatory motion and found that the resulting scour was strongly influenced by the pile and the wave characteristics. Some of his conclusions included:

(a) There was a critical velocity associated with incipient motion and this velocity in oscillatory flow appeared to be lower than that for steady state flow.

(b) In most cases considered, 3000 waves (at periods ranging from 2 to 4 seconds) were sufficient to reach the ultimate scour depth, 6000 being the maximum number. This again indicates that scouring is initially intensive and then reaches a maximum depth asymptotically.

(c) There was an indication that scour would not have occurred had the obstacles in the flow path not been in place.

In previous investigations into the phenomenon of scour at the foot of rubble breakwaters, some parameters affecting the scour phenomenon were established and these will now be discussed.

The damage caused by scour to rubble mound breakwaters founded on sand can be considered to be of the following nature:

(a) The structural damage caused to the core, filter blanket and armour cover in direct contact with the sandy base.

(b) The subsidence (caused by the action of scour) of the armour layer, exposing the core at SWL or at the bottom of the down-rush zone where the damaging forces are at a maximum (see CHAPTER 5).

Parameters which affect the scouring depth in various degrees were found to be:

(i) the void ratio of the permeable face,
(ii) the reflection coefficient,
(iii) the water depth at the toe of the breakwater,
(iv) the sand grain size,
(v) the characteristics of the incoming wave, and
(vi) the slope of the seaward face.

Sawaragi [28] found that the subsidence of the armour cover was more dependent on the scouring depth when the <u>face slope</u> was greater than 30°

and postulated from his results that a seaward slope face of 20° may be considered as stable against subsidence. In the laboratory investigations conducted for this thesis, seaward slopes of $\cot \alpha = 1{,}5$ and $2{,}0$ were used, and it will be later shown that the steeper angled slope resulted in greater damage. The flatter the slope the more uneconomical the breakwater becomes because of its size and slopes of the order of 1:3 are considered to be a practical limit (see CHAPTER 3).

The value of the <u>void ratio</u> as a parameter in determining the amount and the rate of scour to be anticipated lies in its influence on the reflection coefficient and the relative permeability of the structure as a whole. With an increase in the void ratio (i.e. the greater the porosity of the structure) the coefficient of reflection will increase, if this coefficient is defined as the ratio between the incident and reflected wave heights. Sarawagi found this result to be most pronounced when the void ratio was less than 20 %, but ineffectual when the ratio was in the region of 30 %.

It is obvious from the complex nature of the water flow through a rubble mound breakwater that the development of a simple <u>reflection coefficient</u> is extremely difficult and as yet has not been developed. The application of a reflection coefficient developed for a non-permeable structure, viz. the ratio of the incident wave height to the reflected wave height, is unrealistic. However, assuming such a coefficient does exist, Sawaragi found that the scouring depth became larger proportionately to the increment of the coefficient, when the coefficient was greater than 25 %, the scouring depth became remarkably small and in some cases accretion occurred.

Herbich *et al* [11] used the envelope of wave motion to arrive at a value for the reflection coefficient when postulating a theoretical equation for wave scour. This method was used in comparing parameters obtained in the laboratory investigations (see CHAPTER 18, sub-section 18.3 and CHAPTER 25).

From measurements undertaken by various researchers it has become apparent that the reflection coefficient is independent on the position, within the rubble mound, of a theoretical reflecting surface.

Sato *et al* [27] based a lot of importance on this reflecting surface as regards its effect on scour and stated that damage by scour to a rubble mound breakwater was more intensive when this hypothetical reflecting surface approached to the toe of the mound.

Sato *et al* also concluded that a decrease in the water depth at the toe of the breakwater resulted in an increase in the maximum scouring depth. Godfrey [8], however, using waves of similar period to Sato *et al*, contradicted this water depth effect and concluded that accretion in fact occurred when the depth of water at the toe was decreased.

Wave characteristics are shown to be the most critical parameters associated with the scouring phenomena. Godfrey concluded that scouring was very much more intense with short period waves and Sato *et al* reinforced this by stating that the relative maximum scouring depth decreased with the increase in wave steepness.

Finally, the phenomenon which affects the scouring action more than the parameters previously mentioned, is the presence of a longshore current parallel to the breakwater along its outer edge. This could be a wave generated longshore current or the effect of the presence of a fast flowing river close to the breakwater. At Ashod, Israel [16], the effects of this type of current was a scour trench 4,5 m deep and 50 m wide formed alongside the breakwater.

CHAPTER 18

THEORETICAL CONSIDERATIONS OF SCOUR:

The most important forces causing bed particle motion are hydrodynamic, and are a combination of the lift and drag forces. These hydrodynamic forces are opposed by the force of gravity and influenced by bed particle geometry.

The drag force is the combination of the form drag due to pressure differential and the viscous drag due to skin friction. The steady force due to drag as developed in any elementary fluid mechanics text is:

$$F_D = \frac{C_D}{2} \rho_w E U^2 \tag{18.1}$$

where, ρ_w = water density,
E = projected area of object normal to the flow direction,
and C_D = drag coefficient.

The coefficient of drag is a function of the Reynolds number and bed particle geometry and is also influenced by adjacent particles causing anomalies in the flow patterns.

The relationship for the force due to lift is similar to that for form drag and is given by:

$$F_L = \frac{C_L}{2} \rho_w E' U^2 \tag{18.2}$$

where, C_L = coefficient lift,
and E' = projected area perpendicular to flow direction.

This lift force is the resultant due to the pressure differential above and below the body.

In Equations (18.1) and (18.2), U, the velocity, is considered to be the maximum water particle velocity associated with the wave crest for shallow water waves.

The hydrodynamic forces of lift and drag are opposed by the weight of the particle, friction and the intergranular reactions. The latter two are difficult to evaluate, but the gravity force can be represented by the equation:

$$F_G = \frac{\pi D^3}{6} (\rho_s - \rho_w) g \qquad (18.3)$$

where ρ_s = density of sand,

ρ_w = density of water,

and D = mean sediment particle diameter.

18.1 The Mechanics of Motion:

Because sand grains are of varying sizes and angularity, the problem of motion can be simplified by considering sand grains to be spheres of uniform size. From Figure 15, it can be seen that the total hydrodynamic force F_T is the combination of the lift and drag force. For motion to occur, the sum of the moments about point R must be zero or

$$F_r * d = F_g * d \sin \emptyset$$

and where this condition exists, incipient motion can occur.

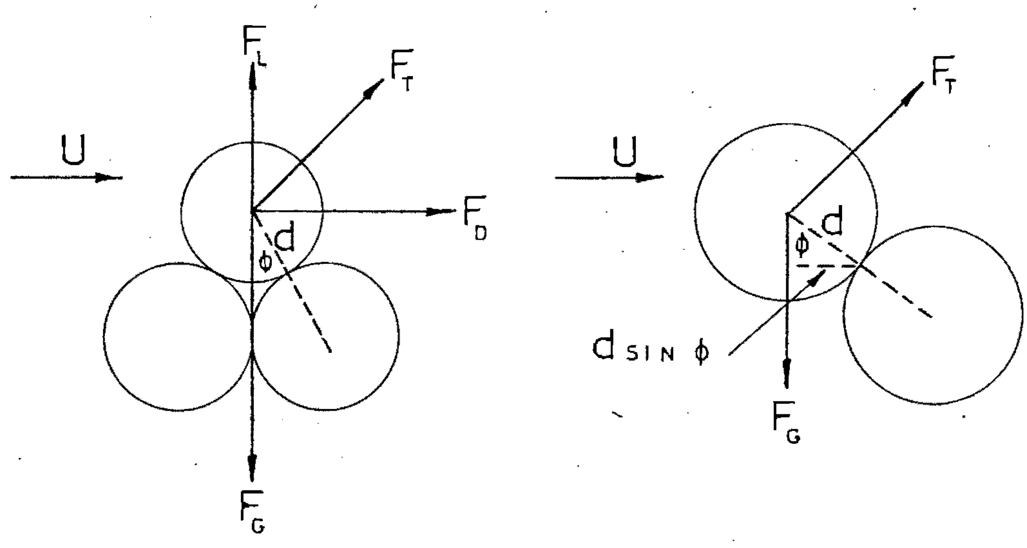

FIGURE 15 Mechanics of Motion

Because of the difficulties in evaluation of lift and drag coefficients and intergranular reactions, mathematical analyses of scour phenomena are few, but Palmer [25] provides a good description of the dynamics of scour about an obstruction in the flow path.

18.2 Scour Dynamics:

A schematic view of the general hydrodynamic situation in the vicinity of an obstruction (Figure 16) reveals the pattern of secondary flows, or turbulence, which accounts for the removal of granular materials through the process of scour.

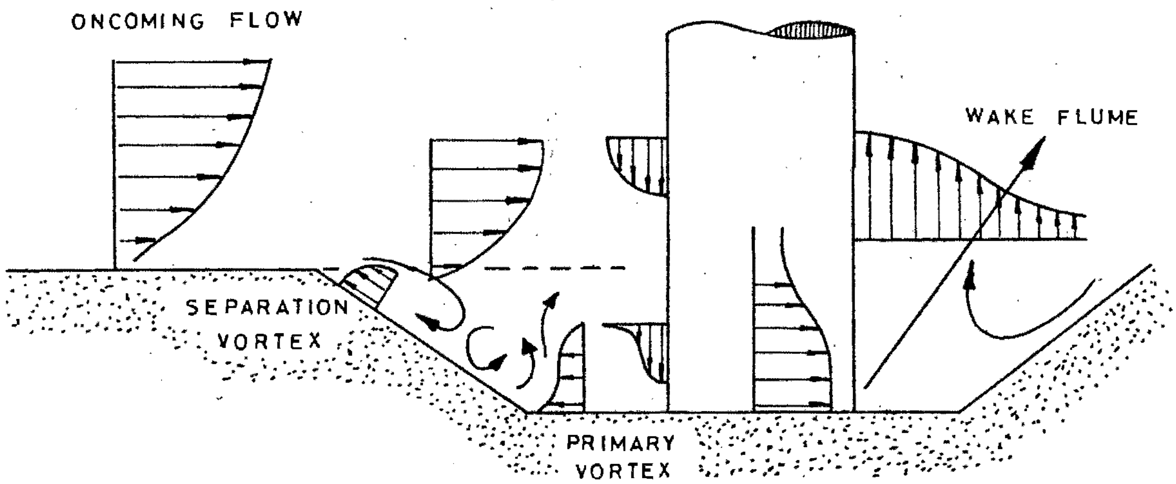

FIGURE 16 Scour Dynamics

PALMER (1969)

The oncoming flow under one surge pulse is represented by the envelope of flow lines at the left. The scour pit is shown as a clearly defined depression around the cylindrical obstruction. The main scouring force is the primary vortex which develops in front of the cylinder. Erosion associated with this primary vortex creates a flat floor within the scour pit adjacent to the walls of the obstruction. Secondary turbulence associated with the separation vortex forms a weak counter-vortex near the rim of the leading edge of the scour pit. Fluid at the sides of the obstruction accelerates to pass round it, and this flow helps to maintain the transport of grains thrown into suspension by the primary vortex. Investigations reveal that the velocity in this region is twice that of the ambient field surge velocity over the sea floor.

The pressure gradient at the rear of the obstruction is the reverse of that developed at the upstream edge. Here, the pressure gradient decreases with increasing height above the bed and this imbalance tends to lift grains out of the scour pit in a turbulent wake flume. Scour equilibrium is achieved for given oceanographic parameters when the volume of material removed by the vortex turbulence is matched by the volume of material introduced into the pit through bed and suspended loads.

18.3 A Theoretical Equation for Wave Scour:

Using shallow water wave theory and boundary layer equations Herbich *et al* [11] provided a mathematical model for the ultimate scour depth in front of a sea wall. The theoretical equation developed was as follows:

$$S = (d - \tfrac{1}{2}A)\left[(1 - C_r)\ u_*(\tfrac{3}{4}C_D \frac{\rho_w \cot \alpha}{gd(\rho_s - \rho_w)})^{\frac{1}{2}} - 1\right] \tag{18.4}$$

where d = still water depth,

A = sum of the incident (H_i) and reflected (H_r) wave heights,

C_r = coefficient of reflection,

u_* = horizontal velocity within the boundary layer,

C_D = drag coefficient,

α = seawall slope angle,

ρ_s = density of sand,

and ρ_w = density of water.

Incident and superimposed waves (resulting from reflection) form an envelope of wave motion and Herbich *et al* noted that the crests and the troughs resulting from the scour formations corresponded to the loops and nodes of the envelopes. The mechanics of the scouring process is explained as follows. Initially, with the approach slope smooth, the horizontal velocity component under the node is affected more than that under the loop resulting in primary scour under the nodes of the envelope. After a period of time, the crests of the sand formation move under the nodes of the envelope and this relative position remains (See Figure 17).

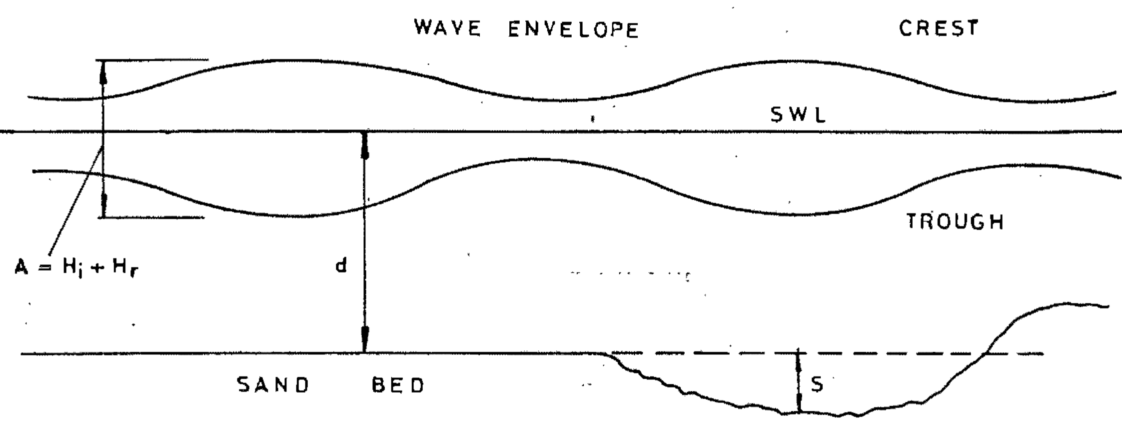

FIGURE 17 Geometry of Sand Scour

The local velocity parallel to the bottom, u_* , is the main factor determining the depth of scour. Therefore, via the continuity theory, this local velocity decreases when the scour depth increases until a point when the ultimate scour is reached. Herbich et al defined u_* as being analogous to U in Equations (18.1) and (18.2).

CHAPTER 19

NATURE OF SCOURING:

The variation of the scouring depth with lapse of time differs with wave characteristics, water depth and position relative to the breakwater. Sato *et al* [27], in his research on scouring at the foot of coastal structures classified this variation into four types:

Type 1: Intense scouring occurs for a short initial period, ceases, and accretion then occurs.

Type 2: A similar initial scouring for an increased period after which an equilibrium position is reached and maintained.

Type 3: Additional slow scouring occurs after the initial rapid scour period.

Type 4: No initial rapid scouring period, but slow scour continues from the beginning.

As could be expected, the variation from one type of scour to another is slight and it is possible to achieve more than one type at any one stage because the bars and trenches formed during the scouring process do affect the wave characteristics. Godfrey [8], however, did identify these four types of scouring in his thesis on rubble mound breakwaters founded on sand and so reinforced the definitions stated by Sato *et al.*

This thesis is primarily concerned with the underscour of a rubble mound breakwater founded on sand and Godfrey, using the same apparatus and a similar model untilized for this study, discovered that most intense scouring occurred at a period setting of 1,85 seconds for the wave paddle, regardless of water depth. Waves of longer period resulted in accretion and shorter period waves dissipated too much energy through breaking to provide any useful results. Therefore, in the proceeding laboratory investigations, the period parameter will be considered a constant at 1,85 seconds, which is a setting of 8 on the wave paddle utilized.

CHAPTER 20

EXPERIMENTAL APPARATUS AND EQUIPMENT:

The apparatus used in the laboratory investigation is shown in Figure 18. The UCT 2-dimensional wave flume is 18,4 m long, 0,6 m wide and 0,55 m deep with perspex panels 0,76 m long encased in steel frames. The flume was considered sufficiently long to study a breakwater model 1,5 m long, with an absorber behind it, placed approximately 13 m from the wave paddle.

The generator consisted of a series of levers leading from an electric motor and the period of the generated regular waves could be adjusted mechanically. Wave heights could be varied by adjusting the eccentricity of the paddle arm on the flywheel. The generator was a simple design, not very practical (e.g. it required several trials for the generation of a wave train of suitable wave height distribution), but it was capable of generating waves of a desired character. It could not generate a wave train exactly as it exists in nature, but a wave train with the same statistical nature could be generated after a few trials. The system worked on the principle that the regular pattern of waves generated by a regular wave generator could be changed and made irregular (if so desired) by the rotation of a lever, attached to the paddle arm, about a slotted wheel. The position of this lever on the slotted wheel could be fixed at any time and in any position. When fixed, the waves were of constant wave height and period, i.e. regular waves.

The periodicity of the wave paddle versus wave generator settings is shown in Figure 19. Most of the laboratory investigations were done at a setting of 8 which corresponded to a wave period of 1,85 seconds, however, a wave height determination was performed for various periods and water depths and this will be discussed later.

Throughout the investigations on scour, a wire-mesh filter (about 1,5 m long, 0,6 m wide and extending the full height of the flume) was placed about 0,6 m in front of the generator in an attempt to

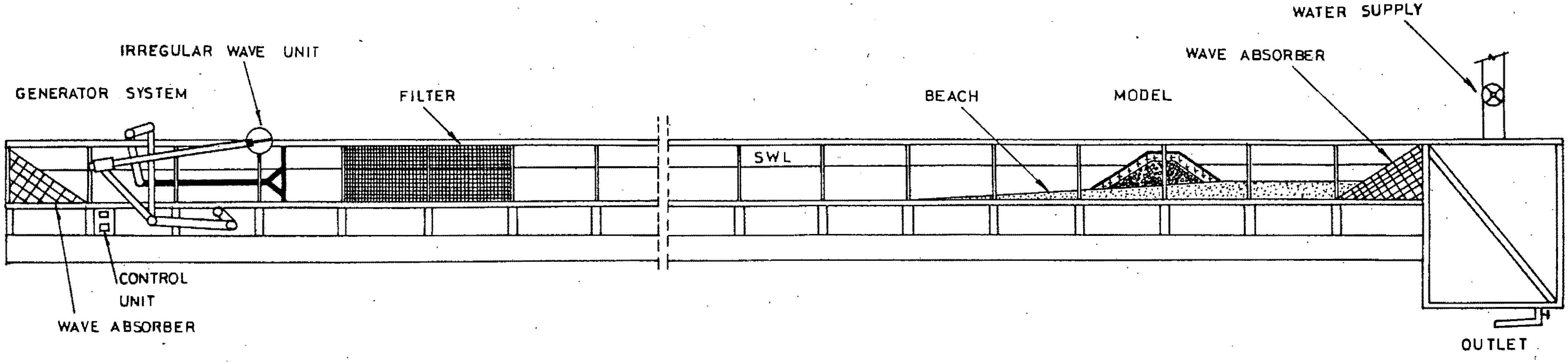

ELEVATION

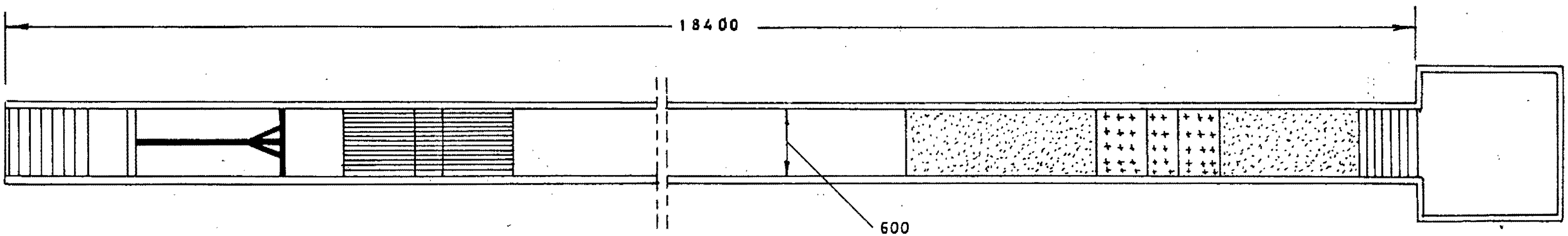

PLAN

FIGURE 18

WAVE FLUME

FIGURE 19

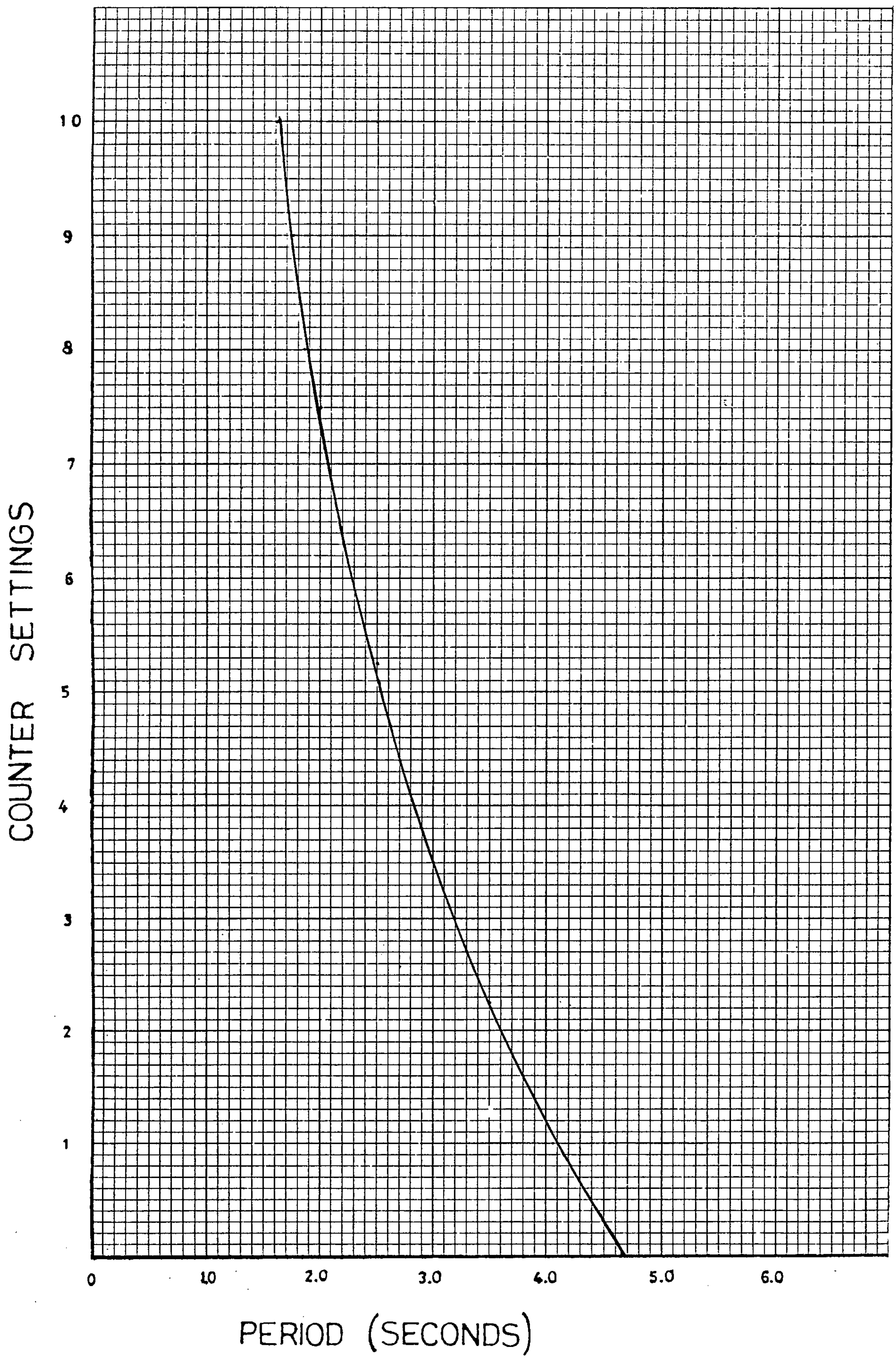
10
9
8
7
6
5
4
3
2
1
COUNTER SETTINGS
0
1.0
2.0
3.0
4.0
5.0
6.0
PERIOD (SECONDS)

reduce the reflected waves hitting the paddle and thus causing re-reflected waves. Unfortunately it was very difficult (if not impossible) to eliminate the reflected waves completely.

along the channel ?

The scour depth measurements were made using a depth probe, resting on the top of the flume walls, and thus measurements could be made along the entire width of the model. The distances of the scour troughs and the bar crests from the toe of the breakwater were made using simple tape measures.

For the actual breakwater model itself, dolosse described in CHAPTER 15 were used, and quarry stone was used for the core and the cover layer, the specified sizes of these are discussed in CHAPTER 24.

Sand of medium particle diameter 200 and 600 microns was used as fine and coarse sand respectively, for the beach profile. Fluorescent sand was also used in establishing the distribution of the scouring action underneath the breakwater. This sand was obtained simply by spraying the normal sand with marine fluorescent paint and allowing it to dry thoroughly before being placed in previously marked areas under the core. Ultra-Violet lamps were then used to trace paths of the fluorescent sand particles. ?

All photographs were taken with a Pentax SPF 35 mm camera, with 135 and 50 mm Takumar lenses. All colour films were Kodak manufactured with ASA's of 64 and 100.

Fresh water was used in the wave flume.

CHAPTER 21

WAVE HEIGHT CALLIBRATION:

The maximum possible wave height that could be generated, at various periods and with or without filtering and shoaling effects, was determined. The measurements were made at the position of the proposed breakwater site with a wave absorber placed at the end of the flume. Severe reflection occurred when the paddle was run continuously which then hampered accurate readings. To reduce this reflection effect, the wave generator was run for not more than 15 seconds and then stopped, and the water level was allowed to settle to its original level. In this manner, first the crests were marked, then the troughs, and then a check was made before the wave heights were recorded. However, even though great care was taken in this measurement, no wave was identical to the one preceding it (i.e. before reflection caused a type of standardized system) and the heights have a tolerance of 5 mm. In all the measurements, the position of the arm on the slotted wheel irregular wave unit was such that the maximum wave was generated at each period setting. This maximum wave corresponded to a paddle displacement of 400 mm.

To establish filtering and shoaling effects on the generated waves, the recordings were done in the following manner:

(a) With the filters removed, the wave heights were measured with a horizontal floor in the flume. Thus a shoal and filter free wave was recorded.

(b) The filters were then introduced to establish their effect on the generated waves.

(c) The waves were recorded with filters and beach in place, the latter having an approach slope of 1 in 15.

67 68

The results obtained can be seen in Table 21.1 and Figure 20.

Without the filter, the wave leaving the paddle was a surging-type breaker at all the periods considered. This breaker eventually formed into swell some distance from the paddle, and these swell heights were

TABLE 21.1

COUNTER READING	T Secs	d_s mm	H(less filter) (less shoaling)	H(with filter) (less shoaling)	H(filter + shoaling) mm
9	1,75	250	-	-	120
		200	-	-	100
		100	-	-	60
8	1,85	250	130	100	145
		200	100	95	120
		100	80	65	80
7	2,05	250	120	110	180
		200	95	105	140
		100	75	70	85
6	2,27	250	115	120	200
		200	90	110	145
		100	70	75	90
5	2,50	250	110	115	210
		200	90	95	150
		100	65	70	95
4	2,80	250	110	105	-
		200	90	90	-
		100	60	60	-

recorded. At very low periods, $\leq$ 1,70 seconds, the swells were very erratic and heights could not be accurately recorded.

With the filter in place, the spilling effect was immediately dampened and a well-defined swell wave left the filter.

Measurements were also recorded at depths of 100 and 200 mm for

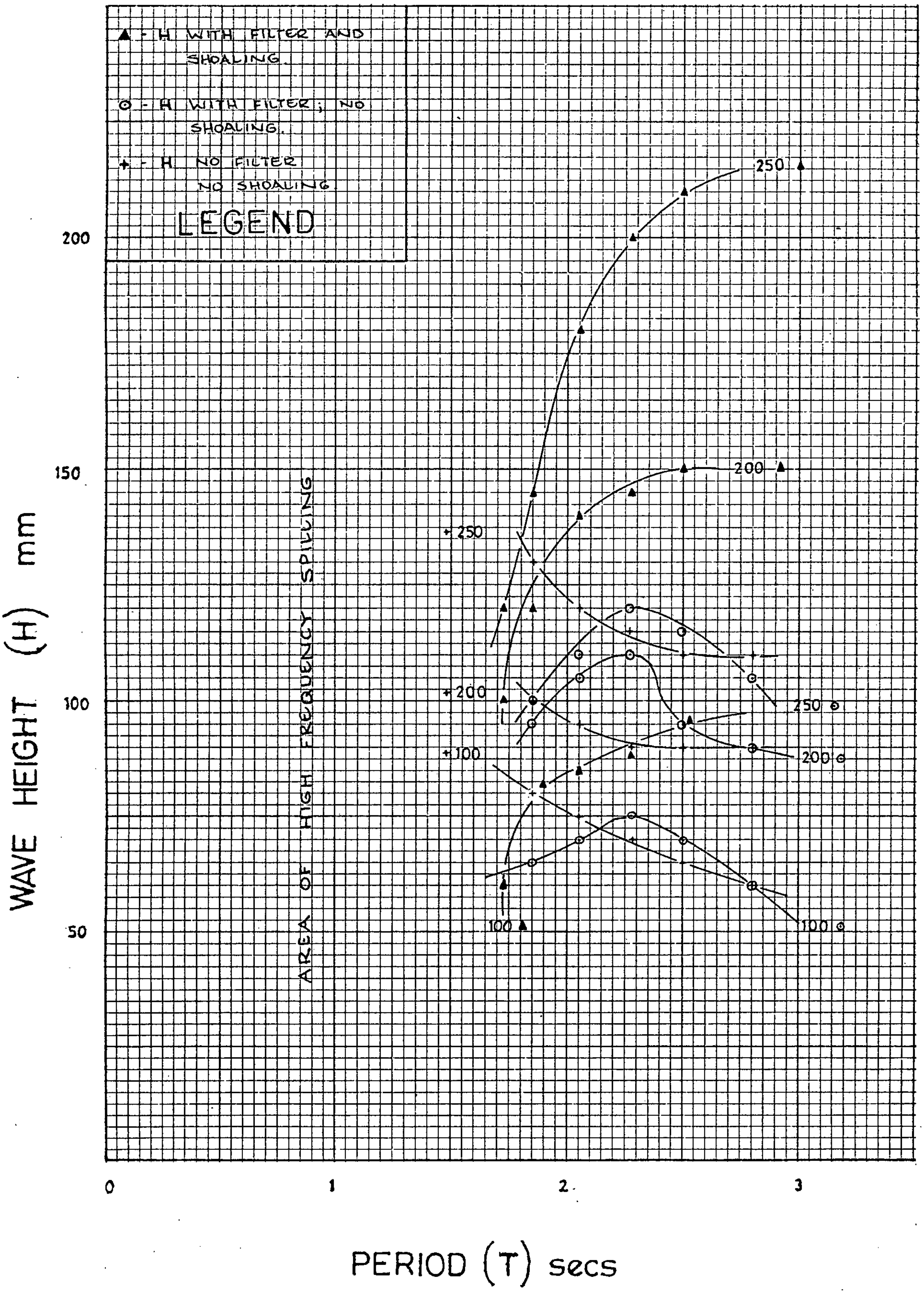
▲ - H WITH FILTER AND SHOALING
⊙ - H WITH FILTER; NO SHOALING.
+ - H NO FILTER NO SHOALING.
LEGEND
AREA OF HIGH FREQUENCY SPILLING
WAVE HEIGHT (H) mm
PERIOD (T) secs
0
1
2
3
50
100
150
200
250
200
100
+250
+200
+100
250 ⊙
200 ⊙
100 ⊙
100 ▲

FIGURE 20

an approach slope of 1 in 10 for the beach, and although the waves peaked more rapidly there was no significant difference in the wave heights in the flume, at the breakwater site. This effect is reinforced when parameters are inserted in Figure 5, PART I.

As can be seen from the table, the maximum wave height obtained was 210 mm, for a depth of 250 mm at the breakwater site. Larger waves could possibly have been obtained, but for the above wave, the crest was about 10 mm lower than the top of the flume and this restricted any further increase.

The main importance in having a wave height callibration for the flume is for determining dimensionless parameters, such as d/L and d/gT^2, etc., which will later be used in the scour analysis. A table of wave parameters, which includes d, H, l, c, l_o, H_o, etc., associated with the wave flume is in Appendix A.

21.1 The Limiting Wave Height:

As this study is primarily concerned with the underscour of the rubble mound breakwater, it must be insured that the stability is not endangered by a wave, larger than the limiting wave height, attacking the breakwater. The limiting wave height, for a particular armour block size can be obtained by the Hudson formula explained in Equation (9.1).

The parameters associated with the model dolosse are as follows from CHAPTER 15:

Largest dimension = 84 mm
Volume = 97,5 cm^3
Mass = 235 g.

$$\therefore \quad \rho_{r(MODEL)} = 2,41 \text{ g/cm}^3 \qquad \text{(i)}$$

and $$S_r = 2,41 \qquad \text{(ii)}$$

assuming ρ_w for fresh water.

K_D = 25 for 2 % damage and for non-breaking wave conditions (see Table 9.1) (iii)

α = arc cot 1,5. (iv)

From Equation (9.1),

$$W = 235 = \frac{2,41 * H^3}{25\ (2,41 - 1)\ 1,5} \text{ (grams)} \qquad (21.1)$$

$$\therefore \quad H = 172,8 \text{ mm}$$

which is the non-breaking wave height which would cause stability problems in the armour layer of 235 gram dolosse.

Therefore, in the proceeding investigations on scour, the above maximum limiting wave height had to be adhered to. It can be seen from the wave height callibration test for the flume, that a wave height exceeding 173 mm only occurred for depths of 250 mm at periods $\geq$ 2,05 seconds.

As the scour investigations were conducted at a wave period of 1,85 seconds the dolos armour unit layer would be unaffected by stability problems caused by this non-breaking wave.

CHAPTER 22

THE NATURE OF THE SEDIMENT:

A review of the literature on sediment transport studies revealed from experience with small scale movable bed models, that for investigations involving sediment transfer via shear velocities or longshore transport, the use of lightweight material such as anthracite dust, lead to exaggerated behaviour of the model with respect to the prototype. Le Méhauté [18] stated that the use of sand in the case of beach studies was not always recommended as it lends to too large a distortion and, subsequently to large scale effects. He recommended lighter materials such as pumice, coal and plastics.

However, in studies on the onshore-offshore transport of sediment, Swart [29,30] found a relationship defining the dimensionless form of the equilibrium beach profile in a zone up to a water depth of approximately twice the wave height in deep water. From this relationship it was derived that the equilibrium beach profiles in the model and a prototype could only obtain an exact geometrical similarity when the scale of the sediment size equalled unity. In practical terms this result suggested a median particle diameter of approximately

$$200\ \mu m \leq D_{50} \leq 250\ \mu m$$

Although this study does not conform to any particular prototype, it was however decided to use natural sand as the beach material.

Therefore, the results of this study are limited by the following restrictions as regards the beach and beach material:

(i) The bed is considered to be composed of non-cohesive material.

(ii) The bed material is described by its grain size.

(iii) There is no inflow or outflow from the ground water acquifer to significantly affect the scour.

Fine sand (D_{50} = 200 μm) and coarse sand (D_{50} = 600 μm) were used in the laboratory investigations.

CHAPTER 23

MODEL SCALES:

A design wave height is defined by Ergin *et al* [6] as the maximum wave height measured at the location of the proposed breakwater, before it is constructed, which will not damage the cover layer. The removal of up to one per cent of the total number of armour units in the cover layer is considered to be no damage. This is based on the Hudson criteria discussed in CHAPTER 9.

The model dolosse chosen for the laboratory investigations were of a particular weight, size and relative density such that a model scale had to be chosen to accommodate them so as not to have scale effects in the results.

As the model in no way depicted a particular prototype there was no recorded significant wave height which could be used as the design wave. What was important however, was that a wave of height 173 mm in the wave flume was the maximum design wave for no damage in the model (see sub-section 21.1) so this wave would affect the model scale chosen, i.e. a prototype wave of 3.00 m would be modelled by a scale of approximately 1 in 18, if undistorted scales were chosen, for the wave flume utilized.

Therefore, for an undistorted scaling system, the only factor determining the length scales was the working area available in the flume as the fine sand size of 200 µm median diameter did not have any effect.

A scale of 1 in 20 allowed a close investigation of the mechanics of scour under the structure and was the easiest workable scale in the wave flume considered.

When using the coarse sand as beach material (D_{50} = 600 µm) a distorted scaling system may be necessary to achieve realistic results and because wave height is the important parameter, the vertical scale would then be 1 in 20 and the distortion for the horizontal scale would have to be estimated. Zwamborn [36] states that distortion is necessary to have sufficient water depth in a model of practical size to ensure fully turbulent flow and sufficient tractive force to move the larger sediment. He suggests vertical and horizontal scales between 20 to 100 and 80 to 300 respectively.

For the undistorted scaled model, the length scales were then:

$$\frac{\lambda_m}{\lambda_p} = \frac{1}{20} = H_q = L_q = d_q \qquad (23.1)$$

where H_q = wave height scale
L_q = wave length scale
d_q = water depth scale
and q = donates prototype to model ratio.

This also implies the correct reproduction of wave steepness and breaking and thus a maximum design wave height for zero damage of 3.46 m in a prototype. period 8,27 s ?

As in nearly all hydraulic models the gravitational and inertial forces are the governing forces in the action of waves. Therefore, the Froude Law was used in determining the model dimensions and in the interpretation of the results.

With the length scales as chosen above, the resulting time scale was:

$$T_q = \left(\frac{1}{20}\right)^{\frac{1}{2}} = \frac{1}{4{,}47} \qquad (23.2)$$

The mass scale was:

$$W_q = \left(\frac{1}{20}\right)^3 = \frac{1}{8000} \qquad (23.3)$$

The wave celerity according to first order wave theory is given by

$$C^2 = \frac{gL}{2\pi} \tanh \frac{2\pi d}{L}$$

Thus for $L_q = d_q$ it followed that the wave celerity scale was

$$C_q = (d_q)^{\frac{1}{2}} = \frac{1}{4,47} \qquad (23,4)$$

The transport of bed material is to a large extent determined by the resultant bed shear, while the bed shear in itself is determined by the resultant velocity at the bed. The orbital velocity produced by the waves will also be in accordance with Froude's law, viz:

$$\underline{\text{orbital velocity scale}} \quad u_q = (d_q)^{\frac{1}{2}} = \frac{1}{4,47} \qquad (23.5)$$

A scale for gravity is associated with Equations (23.2, 3, 4 and 5) but because water is used as the fluid, this gravity scale is unity. However, as regards the mass scale, Lé Méhauté [18] indicates a very important scale effect due to the fact that in the water tank, fresh water is used instead of salt water, and the slight difference in density of approximately 3 % produces an error in the armour mass approximation, (if the model and prototype densities are the same) of about 10 - 15 %. in what?

Distortion of scales for the coarse sand model tests create complex problems in correctly simulating the scour phenomena and this is considered beyond the scope of this thesis. Therefore, the coarse sand test was conducted under undistorted scales (as above) and a comparison with the fine sand results was made.

23.1 The Time Scale for Two-Dimensional Scour:

The construction of civil engineering works such as breakwaters on sand foundations causes disturbances in the local flow and consequently generates conditions for the development of local scour. Prevention of scour is costly and hence some scour must be accepted and predicted.

Breusers [2] states that the time scale of the scouring process in non-cohesive sediments should be estimated from considerations on the sediment transport and the flow pattern in the scouring hole. The flow pattern however is very complicated so that a prediction of velocities or bottom-shear stresses at any time and place is very complex and little is also known on the amount of sediment transport in highly turbulent conditions. Practical relations for time scale must be derived mainly from model experiments with different scales.

For a suitable definition of the time scale of the scouring process he states that it is necessary that in scale tests with similar flow configuration the following relationship is valid:

$$\frac{S(x,t)}{d_s} = \xi\left(\frac{t}{t_o}, \frac{x}{d_s}\right) \qquad (23.6)$$

where S = scouring depth,
d_s = water depth at the end of the bottom protection,
x = distance from the end of the bottom protection,
t = time,
t_o = a characteristic time of the scouring process,
and ξ = the same function in both tests.

Breusers, conducted tests with undistorted model scales to arrive at a time scale for two-dimensional local scour and found that the maximum scouring depth varied exponentially with time

$$\text{i.e. } \frac{S_{max}}{d_s} = \left(\frac{t}{t_1}\right)^{0,38} \qquad (23.7)$$

where t_1 = t at which $S_{max} = d_s$.

applies

This result, however, conforms to uni-directional flow regimes and may not apply to oscillatory flow conditions.

To obtain a characteristic time value of the scouring process under oscillatory flow conditions, i.e. t_o in Equation (23.6) and t_1 in Equation (23.7) a series of tests was conducted in the wave flume, using a simulated rubble mound breakwater.

23.1.1 Time of Test Duration - An Estimation:

To simulate a dolos protected rubble mound breakwater, a piece of wood with the necessary voids for the correct porosity, was utilized. Porosity is defined as a volume dependent parameter (see Equation (10.1))of the cover layer, but if this cover layer is considered to be of unit depth, then the porosity becomes area dependent. Therefore, for the porosity value of 60 % for a dolos armour layer, 60 % of the sloping face of the simulated breakwater had to be voids. This was achieved by holes drilled into the wood. (See photograph (23.1))

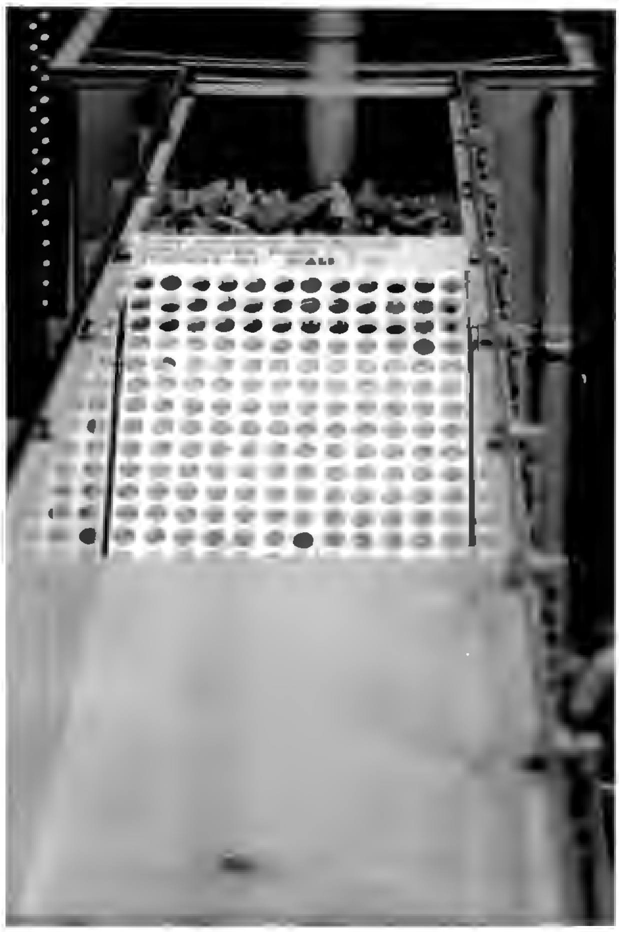

Photograph 23·1

The layout of the apparatus can be seen in photograph (23.2) taken before the tests. Not shown on the photograph is a sand depth at the toe of 100 mm, and a sand size of D_{50} = 200 µm.

The aim of the investigation was to measure the depth of the scour hole and its distance from the toe, as a function of time. The axes used for these measurements are shown in photograph (23.2). The distance of the origin from the furthest forward position of the wave paddle is 12,60 m.

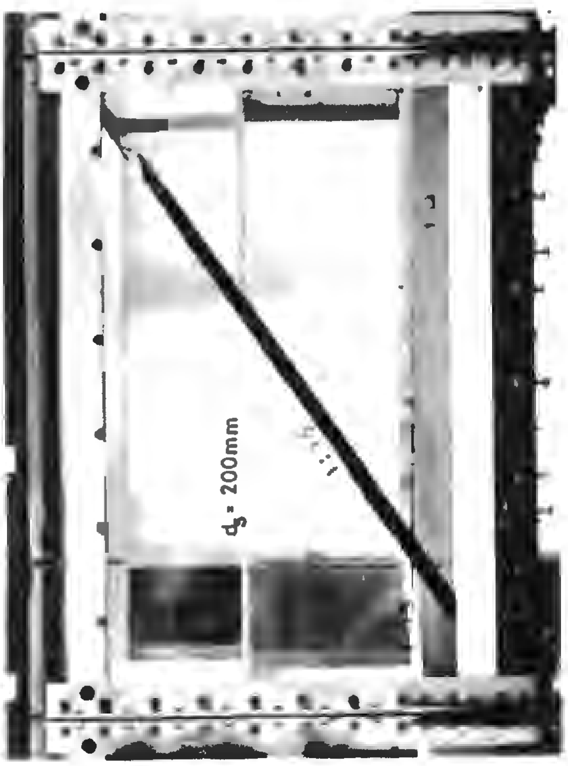

23·2

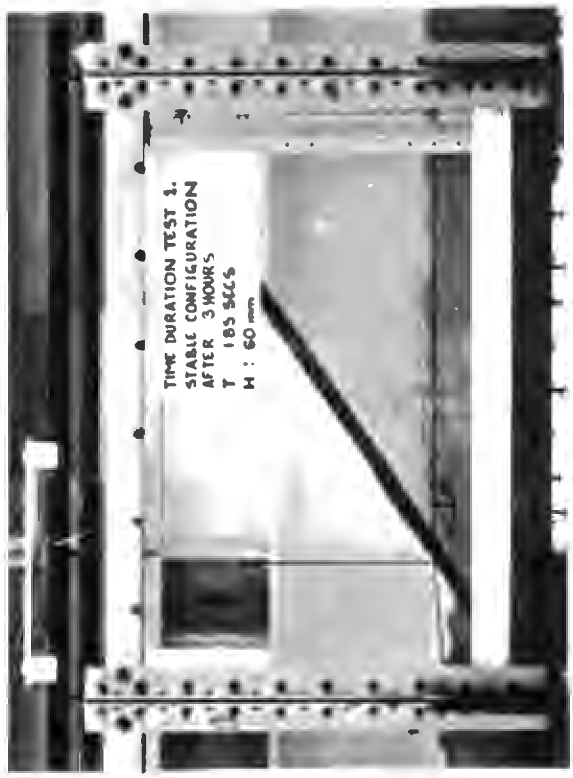

23·3

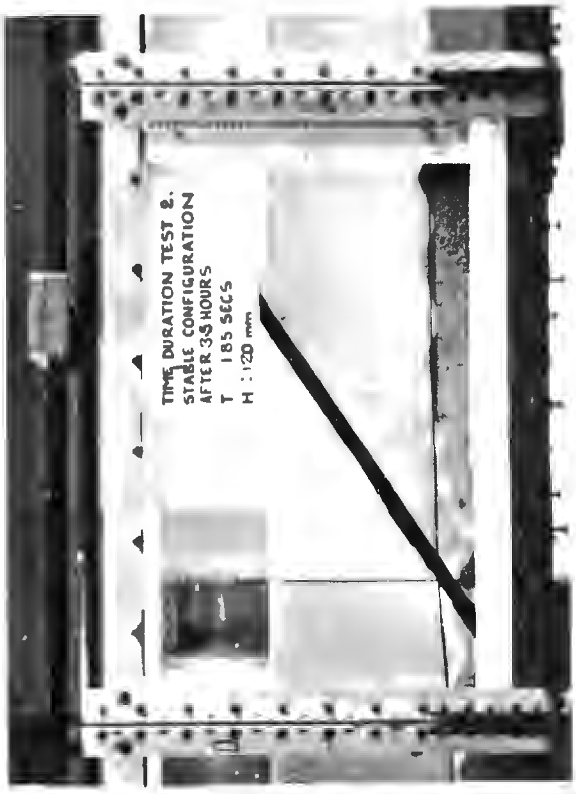

23·4

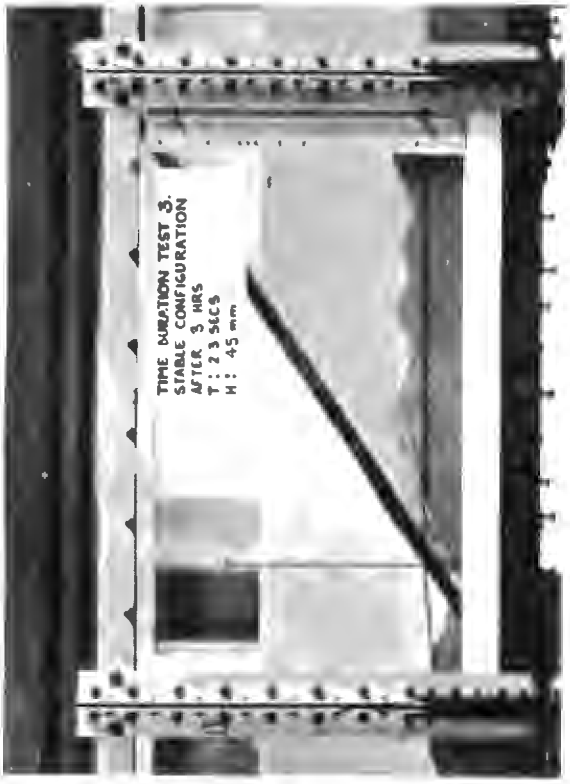

23·5

Three tests were conducted, two at a period setting of 1,85 seconds and one at a 2,3 second setting. The parameters associated with the three tests are shown below.

Test No.	T (sec)	d_s (mm)	H (mm)
1	1,85	200	60
2	1,85	200	120
3	2,30	200	145

The difference in wave height (H) between tests 1 and 2 occurred because test 1 was conducted using the minimum wave paddle displacement and test 2 the maximum.

The results of the tests are shown in Figure 21 and the final stable configurations can be seen in photographs (23.3,4 and 5. Tests 1 and 2 showed very similar results. The basic sand configuration after the tests were the same except that the scour in test 2 was more intense and it took longer for conditions to stabilize. Indications are that at the same water depth and wave period, the scour intensity is proportional to the wave height in that, the larger the wave height, the more intensive the scour is.

Test 3 indicated the dependence of scour on the period of the incoming waves. With the wave period at 2,3 seconds, rapid scour occurred initially, followed by accretion into the scour hole. When the test was terminated accretion was still occurring and the scour hole was decreasing in depth. Another major difference between test 3 and, 1 and 2 was the ripple migration. In the latter two, the ripple migration was away from the toe, initially very rapid (80 mm per 15 minutes) and slowing down to 20 mm per 15 minutes when the stable configuration was reached. In test 3, initially no migration occurred, but after an hour, the ripples moved towards the toe at a steady rate of 30 mm per half hour.

A characteristic time value of the scouring process was

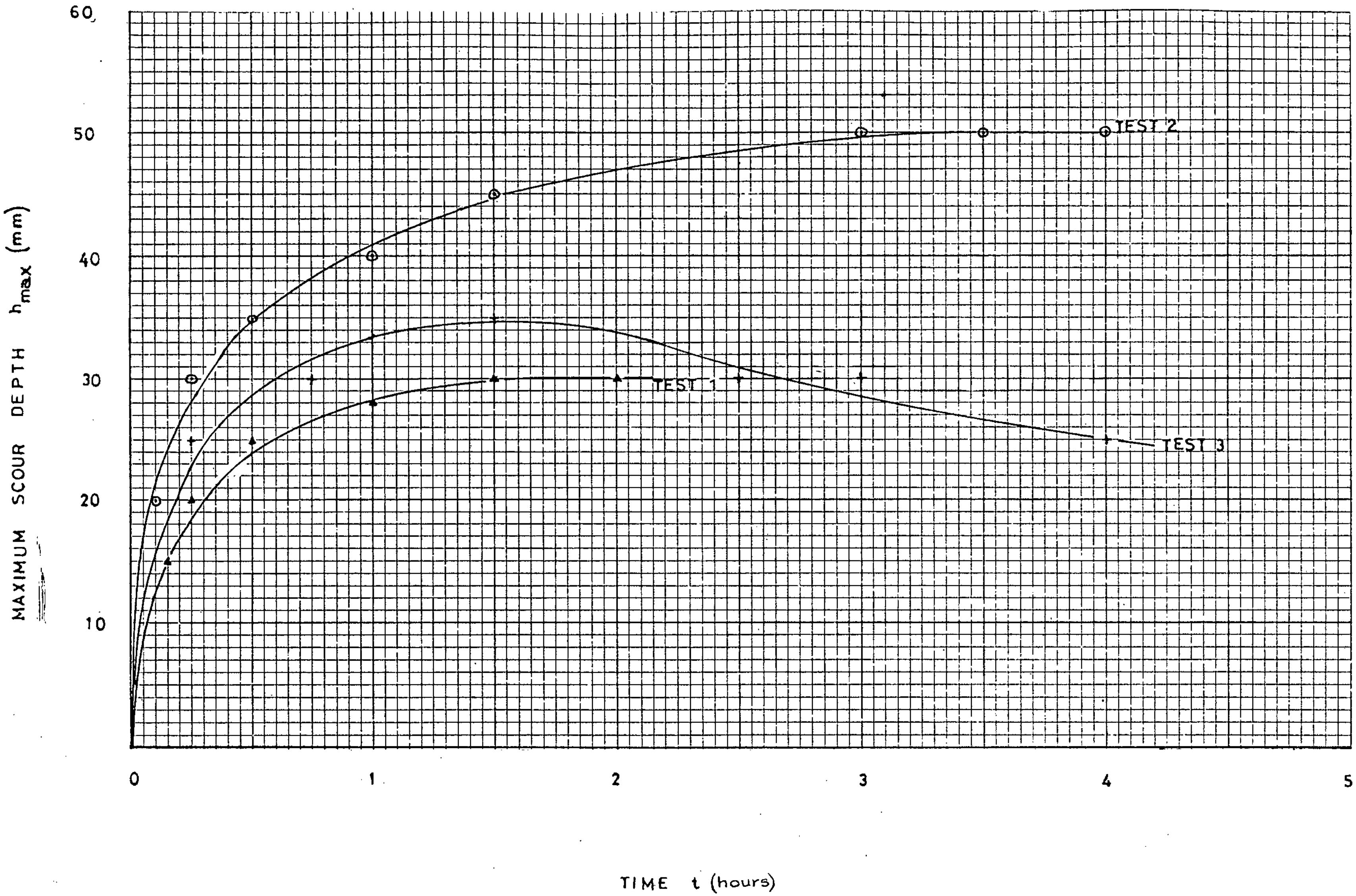
MAXIMUM SCOUR DEPTH h_{max} (mm)
60
50
40
30
20
10
0
1
2
3
4
5
TIME t (hours)
TEST 1
TEST 2
TEST 3

FIGURE 21

defined as the time at which the beach configuration in the area of the toe became relatively stable. Figure 21 shows this occurring at $2\frac{1}{2}$ and $3\frac{1}{2}$ hours for Tests 1 and 2 respectively. Stability did not occur in Test 3 due to the increased accretion as the time increased.

Therefore, when testing the dolos protected rubble mound model breakwater under maximum scour conditions, a test time duration of not less than $3\frac{1}{2}$ hours had to be employed. This value agrees fairly well with the literature on scour where it was found that a 4 hour duration was necessary when testing with sand of the size D_{50} = 200 μm.

CHAPTER 24

THE BREAKWATER MODEL:

The three-layered section as recommended by the Shore Protection Manual (CERC) [32] for non-breaking wave and moderate overtopping conditions, was used. (See Figure 8 in PART I). Two slopes were used, 1 in 2 and 1 in 1,5. Page 20

upstream

page 39

The crest width, as defined by Equation (11.5), resulted in a dimension of 95 mm (equivalent to 1,8 m in practice, at a scale of 1 in 20) which practically was not feasible. It was decided that this dimension would be governed by the minimum width allowing access of heavy dump vehicles in practice, i.e. 5 metres, or 250 mm in the model.

In assuming no overtopping, the highest level of the model was H, the design wave height, above the maximum still water level. At a wave period of 1,85 seconds and a water depth at the model toe of 200 mm, H was 120 mm (see Table 21.1). page 67

Initially, a filter layer was not used and the armour and under-layers extended directly to the sea bed.

The water depth in front of the breakwater, 200 mm, gave a relative depth, d/L, sufficient to prevent waves from breaking due to shoaling.

page 20

24.1 The Core, Underlayer and Cover Layer:

page 40

The weights of the rubble in the core and the underlayer were obtained from Figure 8 and Equation (11.6) respectively. If W is the weight of the individual dolos armour units, the weight therefore of the underlayer rubble is

$$W/5 \; = \; 47 \text{ grams if } W \; = \; 235 \text{ grams,}$$

and for the core material,

W/200 to W/6000 = 1,2 to 0,04 grams.

Quarry stone was used for both the core and the underlayer and average weights of the individual stones were obtained by weighing batches of 40 stones. In this way, weights of 49 and 1,70 grams were obtained for the underlayer and core material respectively, which compare favourably with the design weights. a little high

24.2 Layer Thicknesses: Pg 39

The dolos armour layer thickness is defined from Equation (11.3) as:

$$Z = nC(V)^{\frac{1}{3}}$$

where, n = 2 (double layer)
C = 1,1 (and average between 0,9 and 1,3),
and V = 97,5 cm^3,

which gave Z = 101 mm, measured perpendicular to the slope. Pg 40

The underlayer thickness follows from Equation (11.7), and

thus Z_u = 60 mm.

The cross-sections of the models used for the scour investigations are shown in Figures 22 (a) and (b). page 83

24.3 The Dolos Number Required:

The number of blocks required to cover a unit area is given by Equation (11.2) as page 39

$$N = nC(1 - P/100)\ V^{-\frac{2}{3}} \text{ per } m^2$$

where

P = 60 % (Pg 34) and n, C and V follow from before,

which gave

N = 424 per square metre.

The exposed area of the model, in the flume considered, was 0,4 m^2

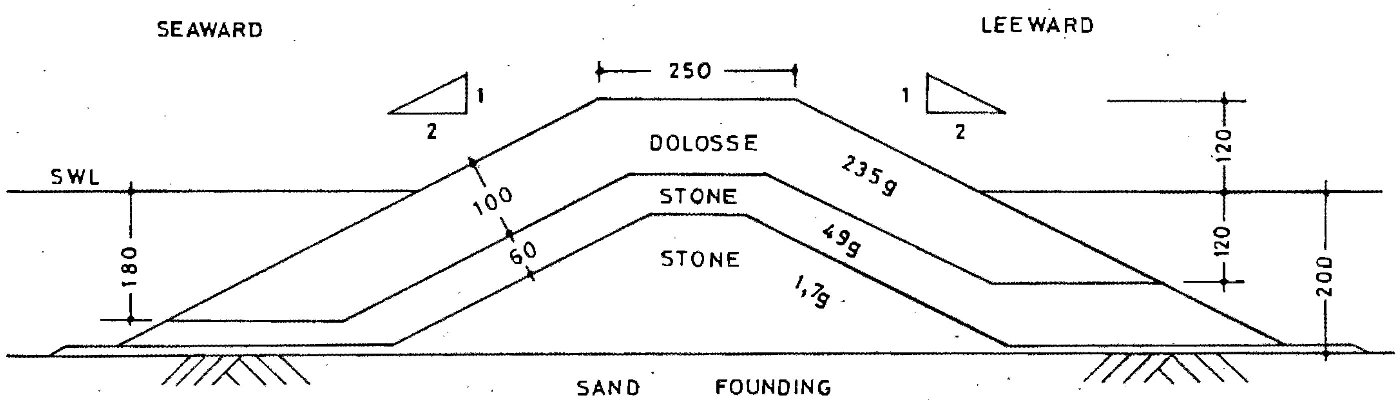

FIGURE 22a

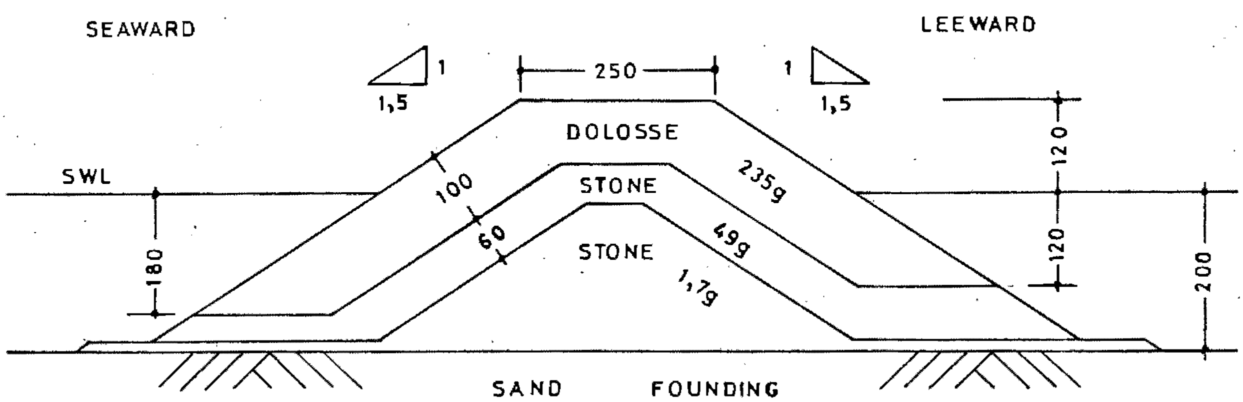

FIGURE 22b

at a front slope of 1:2 so that the number of dolos required reduces to 180, placed in a double layer.

24.4 Method of Constructing Test Sections:

The breakwater test sections were constructed in the wave flume on the sand base, 12,60 m from the furthest forward position of the wave paddle.

The sand was dumped wet into the flume and hand trowelled and compacted to the desired slope.

The core material and the underlayer, from the base of the test section to the crown of the core, were placed with the flume de-watered. The core material was wetted with a hose and then compacted with hand trowels to simulate the natural consolidation effected by wave action during construction of full scale structures. The under-layer stones were then placed by shovel and dressed by hand, between the desired limits.

The dolos armour units were placed as shown in Figure 23. The first rows were placed so that the horizontal legs formed a type of wall perpendicular to the direction of the wave attack. Thereafter, the dolosse were placed randomly by hand, with at least 60 per cent of the vertical flukes facing seaward. This was done to prevent some units performing a half rotation down the slope when too many have their horizontal flukes facing seaward. This method of randomly placing dolos armour units has been observed at actual breakwater locations (Port Elizabeth and Cape Town Harbour extensions), and is also recommended by Merrifield [20]. ?

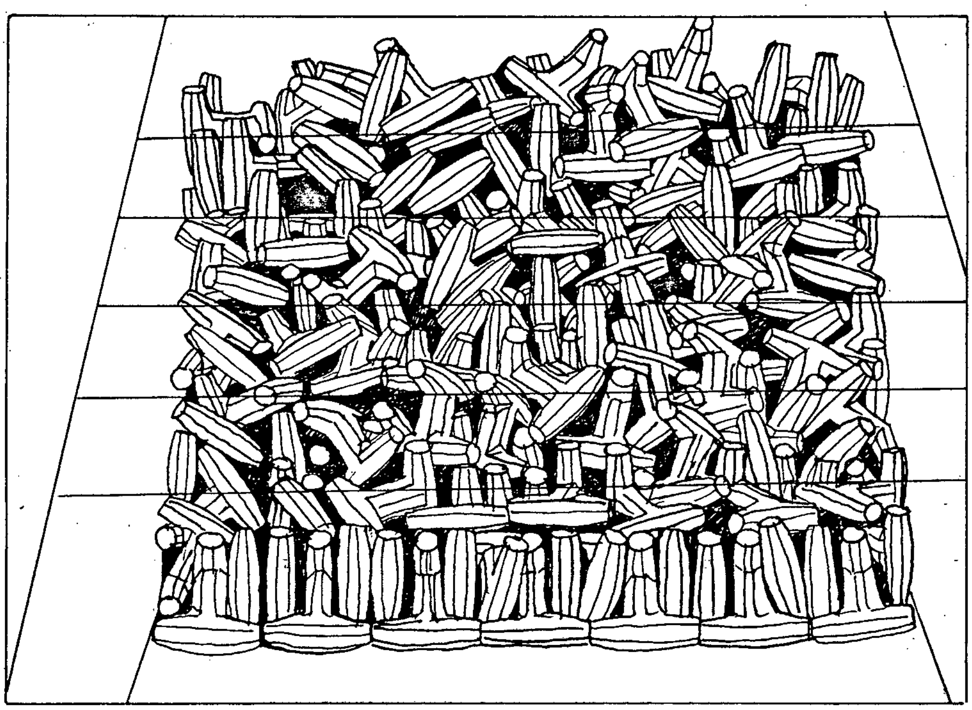

FIGURE 23

CHAPTER 25

TESTING PROCEDURES:

Before each experiment, the sand bed was carefully levelled, the breakwater model reconstructed with parameters varied as required, and colour photographs were taken from the side and the front views. The water depths and periods were checked and note of the time was taken. The experiment could then proceed.

Throughout the test runs, the beach profile and the shape of the scour were measured with a point gauge at intervals of 15 minutes at the beginning of the tests and 1 hour near the end, until the steady state of the scour was established after 4 hours of wave run.

For some cases, fluorescent tracers were placed in carefully marked positions under the breakwater and the movement of the bed materials was established under ultra-violet light.

The subsidence of the armour blocks was recorded in two ways:

(a) Physical measurements were taken throughout the test run, and

(b) Colour photographs were taken (again from the front and side views) after the experiments, and comparisons were made with those taken before, to establish the overall subsidence.

The characteristics of the motion of water particles when short period waves encounter a rubble mound breakwater were described by determining the wave steepness (H/L), the relative depth (d/L), the depth of water at the toe of the breakwater (d_s), the angle of the beach slope forward of the breakwater (δ), and the angle of the sea-side slope of the breakwater with the horizontal (α).

It is emphasised that the wave heights, H, are the heights of the waves that occurred at the position of the proposed breakwater before it was constructed in the flume, and not the heights of the waves moving up, or breaking on, the breakwater slope. Also, it is pointed out that the angle (α) is the angle of the breakwater slope as first constructed and not the angle of the breakwater slope after the breakwater has been stabilized after subsidence.

In order to establish the reflection coefficients, the wave envelopes were observed and the method described by Herbich *et al*[11] was utilized in this respect. He used a method whereby a system of oscillatory waves progressing towards a sea-wall, forms another system of waves due to reflection, after impinging on the wall. These two wave systems form a third wave system as the reflected wave is superimposed on the incident wave. It is this superimposition which forms the wave envelope which was recorded during the tests for this thesis. A schematic explanation of the parameters associated with this method is shown in Figure 24. Page 88

Figure 24 also broadly defines the dimensions associated with sand scour.

The parameters associated with the various tests undertaken are shown in Appendix C.

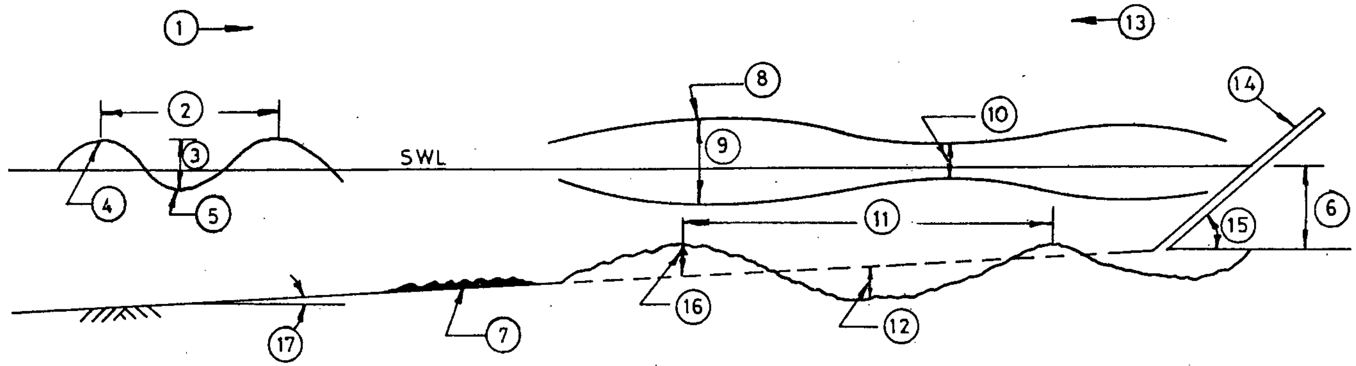

1 INCIDENT WAVE

2 WAVELENGTH

3 WAVE HEIGHT

4 WAVE CREST

5 WAVE TROUGH

6 WATER DEPTH

7 RIPPLES

8 WAVE ENVELOPE

9 LOOP OF ENVELOPE

10 NODE OF ENVELOPE

11 SAND SCOUR LENGTH

12 SAND SCOUR DEPTH

13 REFLECTED WAVE

14 BREAKWATER

15 ANGLE OF SLOPE

16 SAND MOUND HEIGHT

17 BEACH SLOPE

FIGURE 24 SCHEMATIC EXPLANATION OF TERMINOLOGY

CHAPTER 26

RESULTS AND DISCUSSIONS:

The amount of sediment that can be transported from the scour hole is a function of the vortex strength and the bed material characteristics. When the amount of sediment inflow (as bed load, since initially the suspended load does not seem to affect the scour) is equal to the amount that the vortex can transport, an equilibrium condition is achieved. But this equilibrium is only a time averaged condition as the bed movement and the vortex transport capacity are not at all steady. In this thesis, maximum scour is defined as the depth of the scour hole when there is no significant bed load motion, i.e. migration of the ripples within the scour hole still occurs, but the depth of the scour pit remains unchanged over a period of time. Note that no attempt has been made to distinguish between clear water scour and scour with considerable sediment motion.

26.1 Establishing the Wave Period and Water Depth causing Scour:

TABLE 26.1

d (mm)	T (sec)	d/L*	Time (t) (hrs)	S (mm)	S/H_o^*	$t/T^*\ 10^{-3}$
200	$\leq 1,75$	0,085	0,80	Accretion	-	1,50
200	1,85	0,080	0,25	- 35	- 0,32	0,49
			0,50	- 45	- 0,41	0,97
			2,00	- 60	- 0,54	3,89
200	2,05	0,072	0,25	- 25	- 0,20	0,44
			1,00	- 35	- 0,28	1,76
			2,00	- 40	- 0,32	3,51
200	$\geq 2,27$	0,065	0,25	- 15	- 0,12	0,40
			0,75	Accretion	-	0,71

*The values of H_o and d/L are from Appendix A.

In his initial investigations into breakwaters on sand, Godfrey [8] conducted tests in the wave flume and recorded scour action with respect to water depth at the toe, and wave period.

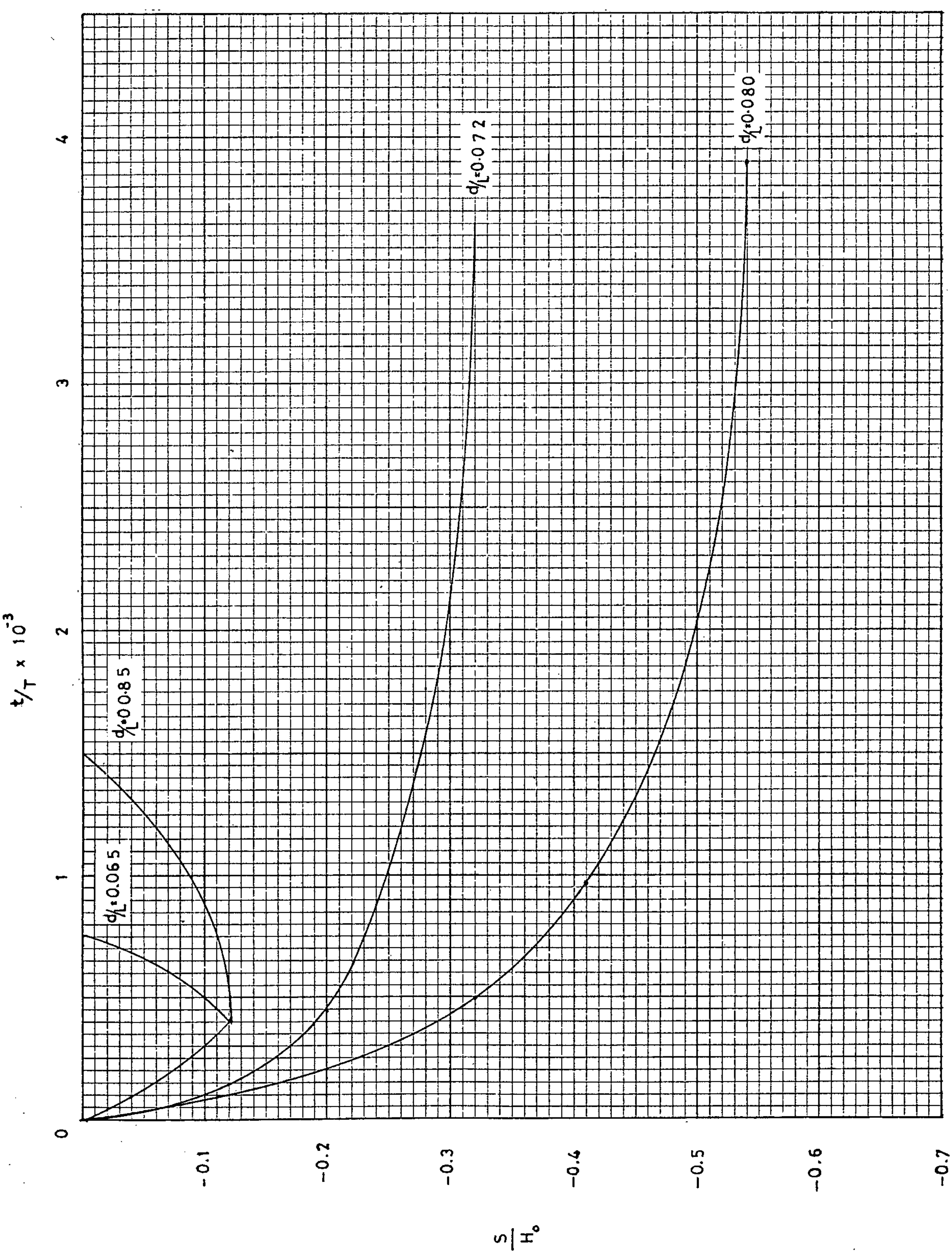

FIGURE 25

It was possible to extract Table 26.1 and Figure 25 from the results of these initial experiments and also from personal observations made at the time. It was discovered that maximum scour occurred at a relative depth of 0,080, or at a wave period of 1,85 seconds and a depth of water at the structure of 200 mm. A depth of 100 mm at the structure and a waver period of 1,85 seconds resulted in minor scour, nowhere near as intensive as for the 200 mm water depth. Wave periods of $1{,}75_s > T > 2{,}75_s$ resulted in minor initial scour followed immediately by accretion, until almost the entire first row of dolosse were covered by the build up of sand.

26.2 Establishing the Movement of Bed Material during Scour:

In the previous sub-section a wave period with a water depth was found which resulted in scour in front and under the breakwater. To establish that the subsidence of the armour which occurs during the scouring action (see sub-section 26.3.3) is mainly due to the removal of bed material beneath the breakwater, it was necessary to trace the movement of this bed material to prove that scour was in fact occurring.

Fluorescent sand tracers were placed in the positions shown in photograph 34 in Appendix F (a photograph taken after the test and showing the original sand levels also), the red tracer in front and the yellow at the back. Waves then attacked the breakwater for 4 hours and photographs were taken under ultra-violet light which established the movement of the fluorescent tracers. page 150

It was found that the mound which forms on the approach beach consists of a mixture of sand removed from the scour trench in front of the breakwater, and from beneath the breakwater. Photograph 35 indicates that the scouring action migrates from the toe area towards the core as time progresses, because first red then yellow tracers were deposited on the mound. The white line in the photograph is the original approach beach level. Photograph 36 is a daylight view of the sand mound, showing the demarcation of tracers above the white line and the level of deposition of tracers in the scour trench. As the depth of the scour trench has approached equilibrium, this implies that migration of sand away from the core area still persists. There is also an implication that the original sand from the area in front of the toe has been removed and deposited at the mound (before the scouring action approached the tracer areas) and has then migrated to an area further down the beach. This is shown in a later section.

To indicate that the above removal and deposition of the sand tracers is not merely a boundary effect of the flume walls, a trench 20 – 30 mm deep was cut into the mound, and photograph 37 shows the yellow surface sand either side of the red sand in the trench.

26.3 <u>An Explanation of Sand Scour at the Breakwater</u>:

Experiments were conducted with the rubble mound breakwater founded directly on sand, on graded rubble filters and on plastic filters. A comparison of results from these three situations and general comments on the effects of scour will now be discussed.

26.3.1 <u>The Relationship between Scour and Water Depth at the Structure</u>:

Figure 26 shows dimensionless parameters S/H_o plotted against d_s/H_o from results obtained by Sawaragi [28], Sato *et al* [27] and Godfrey [8]. No conclusive relationship could be drawn from a study of the plot and it is felt that a reason for this is that the three authors did not keep the same constants. Godfrey kept the wave period constant and altered the water depth and wave height; Sato *et al* kept the wave period and wave height constant and altered the water depth; Sawaragi kept the wave height constant and altered the wave period and water depth, a feature not possible in the flume used by Godfrey and for this thesis. A comparison of the relative depths at which the tests were carried out showed that Godfrey and Sato *et al* worked mainly in the intermediate water depth range and Sawaragi in the shallow range. Therefore, Godfrey and Sato *et al* seemed to have worked under similar conditions, and although no correlation between the parameters is obtained from the plot, it is felt that scour initially increases with water depth and then rapidly decreases as the water depth increases, all from the same deep water wave height.

26.3.2 <u>Maximum Scour as a Function of Time</u>:

In all the tests conducted, except those with plastic filters

FIGURE 26 Maximum Scour vs Water Depth at the Structure

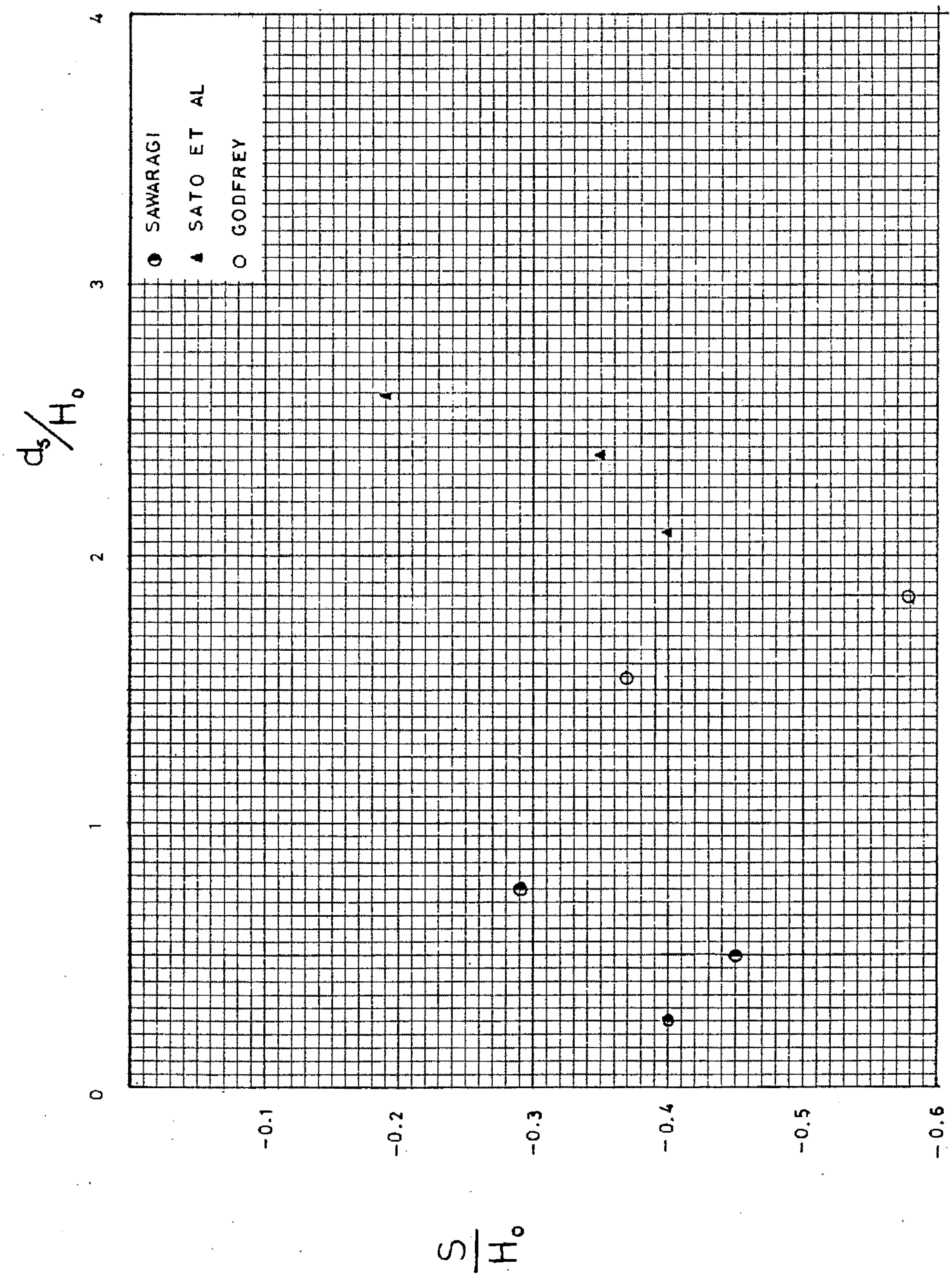

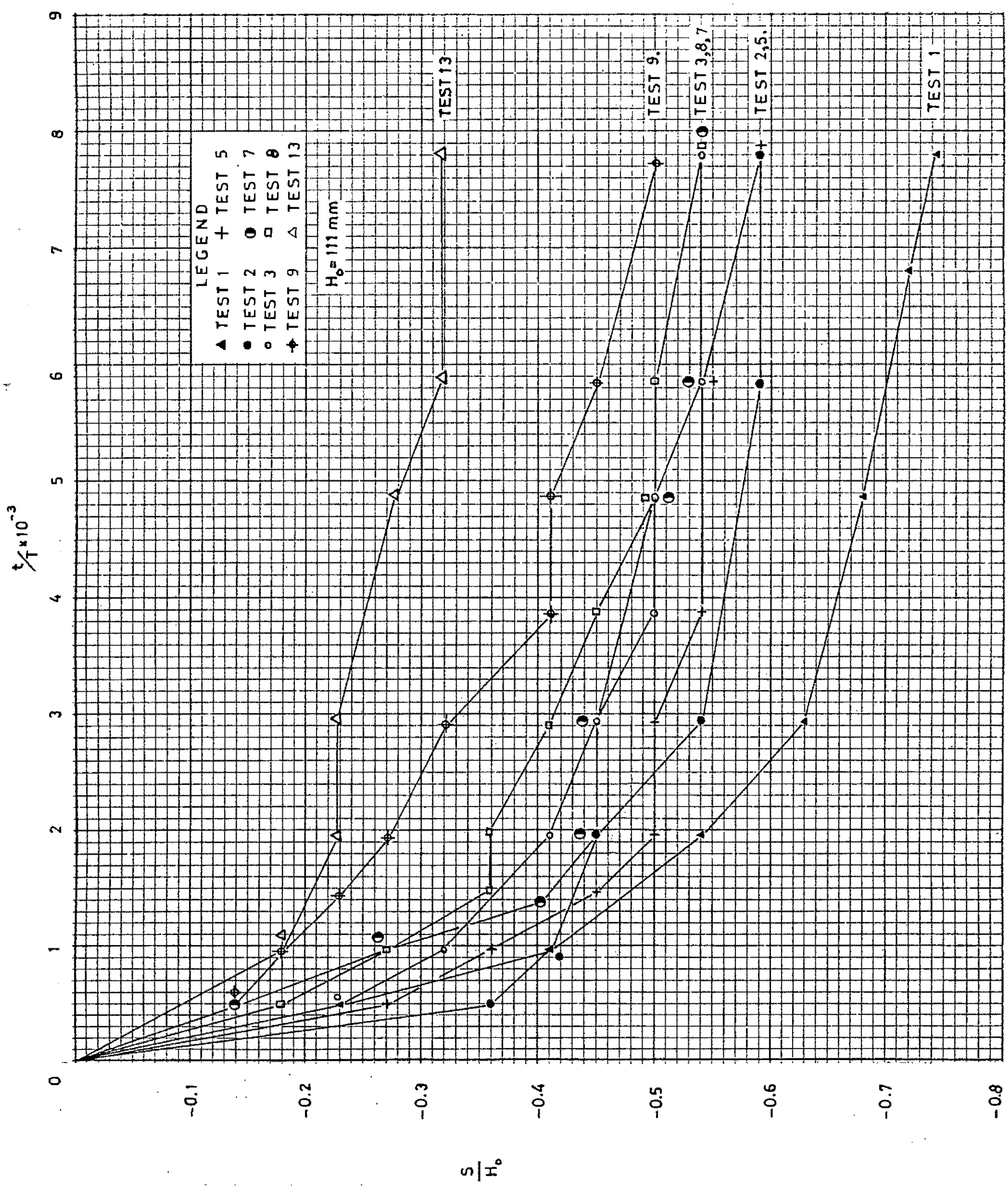

FIGURE 27 Scour Depth versus Time

under the breakwater where very little scour, if at all, was observed, it was found that scour initially increased very rapidly with time, and then slowed down until a steady scour rate continued for a long period of time. This implies that scour approaches its maximum depth asymptotically. Figure 27 shows the relations between Maximum Scour and Time.

page 75

In attempting to arrive at a correlation with the results obtained by Breusers [2] in his study on two dimensional local scour (see sub-section 23.1), maximum scour depth, non-dimensionilized by the water depth at the structure, was plotted against time on a log-log plot (see Figure 28). For clarification all the tests were not drawn in, but the equations for the graphs, obtained by the Least Squares Approximation, can be seen in Appendix E. page 135

page 96

It was found that the maximum scour depth varied exponentially with time and if an average slope was deduced from all the equations obtained, a fair correlation with Breusers' result was achieved, and the equation explaining the relationship was found to be:

$$\frac{S_{max}}{d_s} = \left(\frac{t}{t_1}\right)^{0,33} \qquad (26.1)$$

where, $t_1 = t$ at which S_{max} tended to a maximum.

26.3.3 Relationship between the Amount of Subsidence of Blocks and Scouring Depth:

It must be confirmed whether the subsidence of the blocks is dominated by the scouring action in the vicinity of the breakwater toe. Figure 29 shows the relationship between Block Subsidence, S_b (measured down the slope) and Maximum Scour, S, both non-dimensionlized by the deep water wave height H_o.

It is clear that the steeper seaward breakwater slope of $\cot \alpha = 1,5$ results in more block subsidence, even though the maximum scour depth is similar in magnitude. This occurs because of the difference in the shape of the scour hole. Photographs

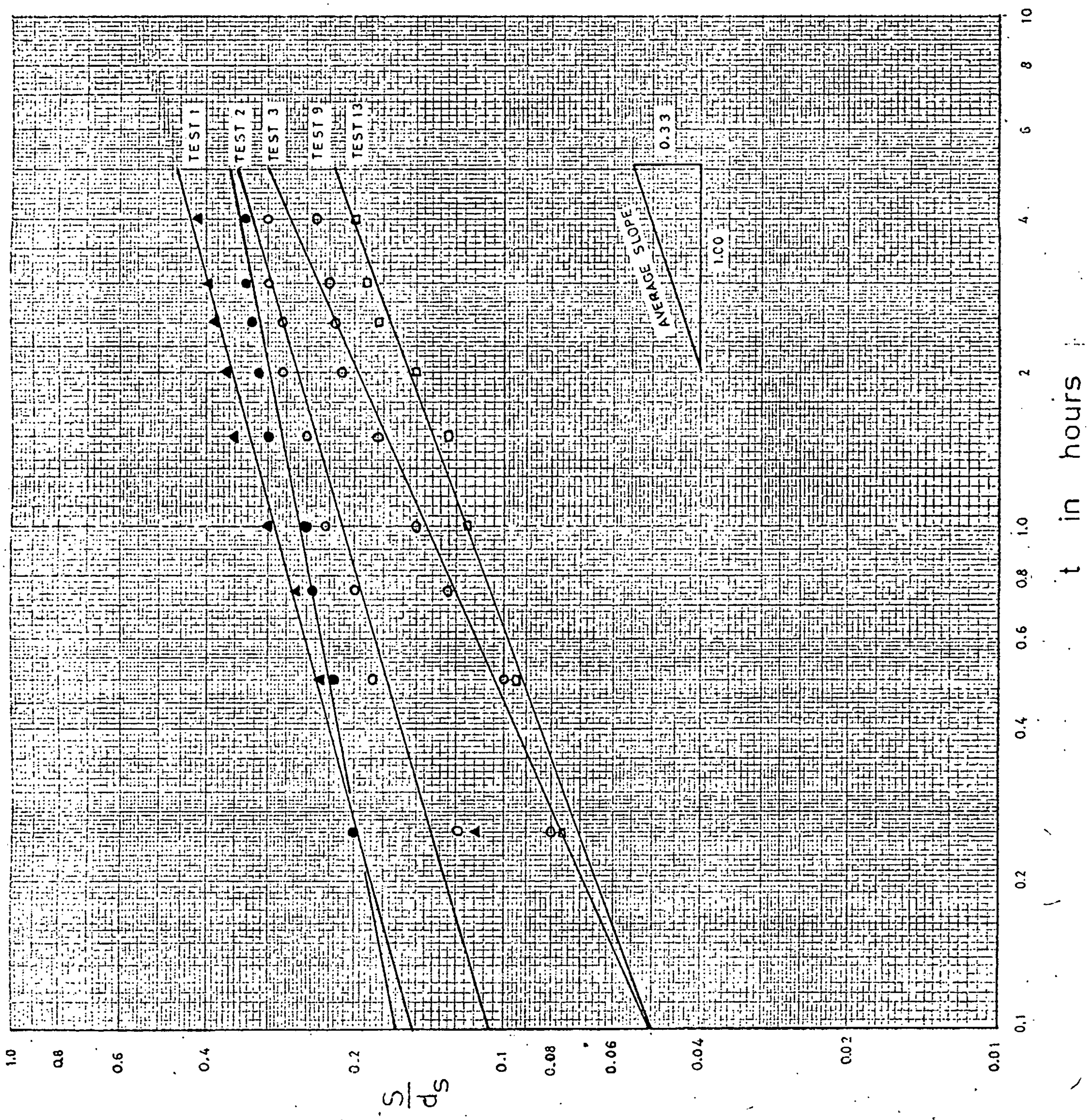

FIGURE 28 Scouring Depth as a Function of Time

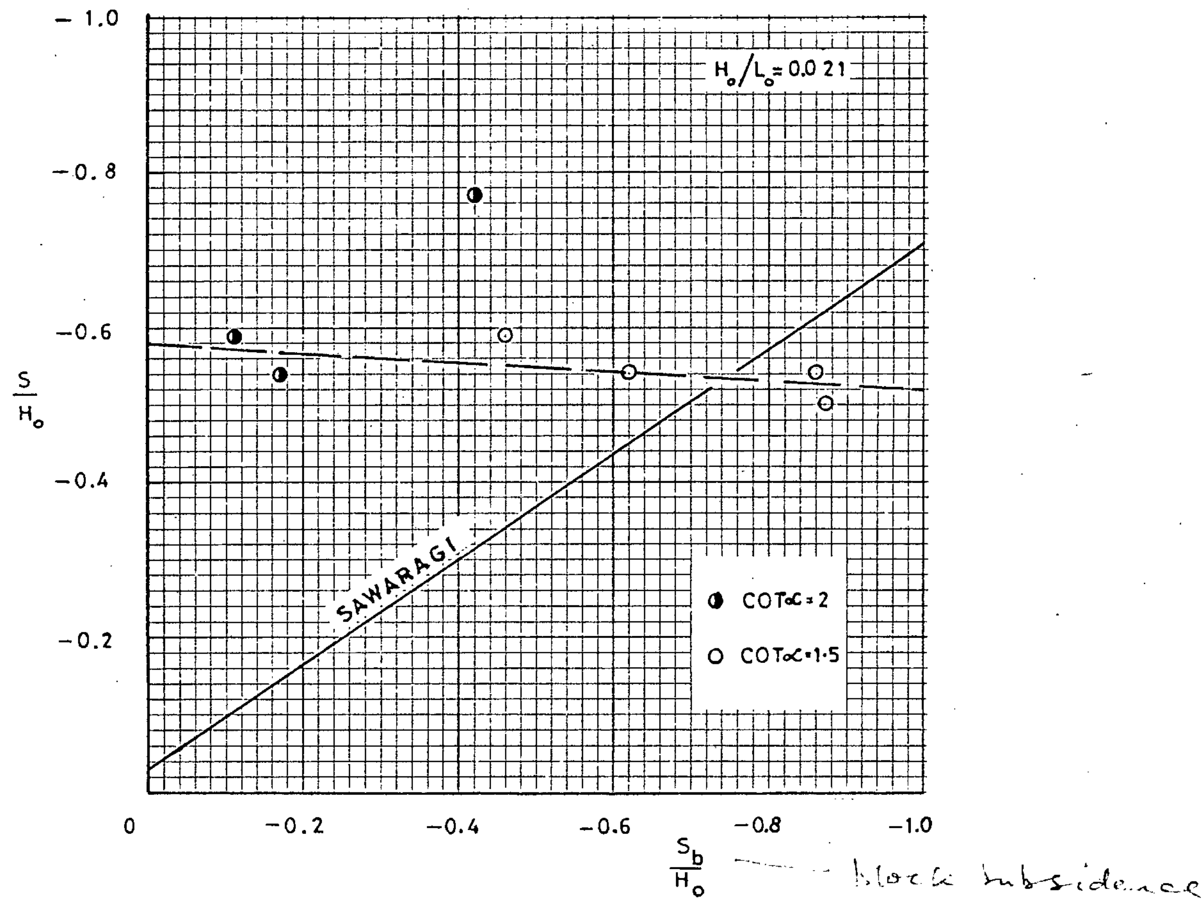

FIGURE 29 Relationship between Block Subsidence and Maximum Scour

1, 2, 19 and 23 in Appendix F, show that for a breakwater seaward along flume slope of cot $\alpha = 2$, the scour hole has a definite maximum and the scour wave length is 850 mm whereas for the slope cot $\alpha = 1{,}5$ the maximum scour depth is less, but the scour hole much wider, 1230 mm wave length, and stretching to under the core. This resulted in a mass subsidence of the underlayer and subsequently all the dolosse subsided a similar magnitude in the latter case. Appendix D shows that for Test 1 (cot $\alpha = 2$), the Green Dolosse subsided 90 mm and the Blue, 10 mm yielding a 46,3 mm average, whereas for Test 9 (cot $\alpha = 1{,}5$), the Green Dolosse subsided 90 mm and the blue 75 mm, yielding an 86,3 mm average. This can also be seen on Figure 30.

Similar comparisons of seaward slope were made after a graded filter was placed under the breakwater and the steeper slope

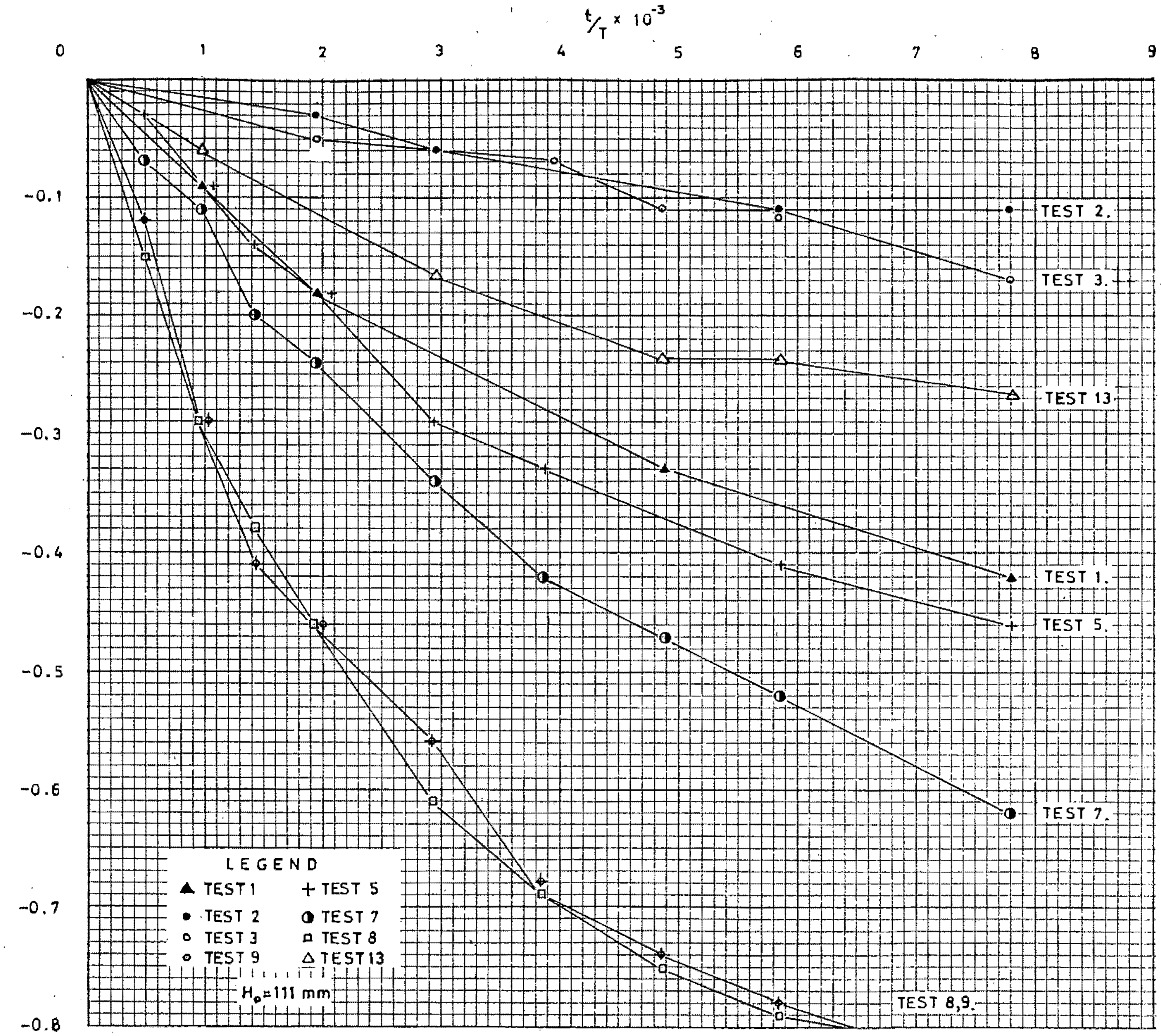

FIGURE 30 Block Subsidence versus Time

again yielded larger block subsidence. This was done in Tests 2 and 5 and the resulting photographs 6, 7, 14 and 15 in Appendix F show this clearly, as does Figure 30.

Figure 29 also implies that there can be scour without block subsidence. This is attributed to two reasons:

(i) In the case of graded filters under the breakwater it can be seen from the photographs mentioned above and others in Appendix F, that the scour hole forms ahead of the toe and then migrates towards the core with time. This would then yield values for scour depth, but no block subsidence.

(ii) The remarkable interlocking capabilities of the dolos armour units allow no subsidence even though sand has been scoured away from underneath them. This is highlighted when comparing Figure 29 with the results obtained by Sawaragi [28]. Sawaragi's graph almost goes through the origin which implies immediate block subsidence with scour, but he used glass balls of 2 cm in diameter which have no interlocking capabilities.

26.3.4 <u>The Relationship between Scour Depth and Mound Height</u>:

The depth of the scour trough below and the height of the sand mound above, the original beach profile were measured and their ratio plotted against time (non-dimensionilized by the wave period $T * 10^3$) in Figure 31. Although there are variations, it can be seen that there is a definite tendency for an equilibrium condition that is achieved after the time interval of 4 hours utilized for the tests.

This was observed during the experimental investigations where it was found that the trough and the mound reached equilibrium magnitude, both vertically and horizontally, and that a steady slow scour rate continued by the action of ripple migration, away from the breakwater. This action resulted in the original beach profile being flattened so that sand was eventually deposited 500 mm from the end of the beach (see photograph 5 in Appendix F).

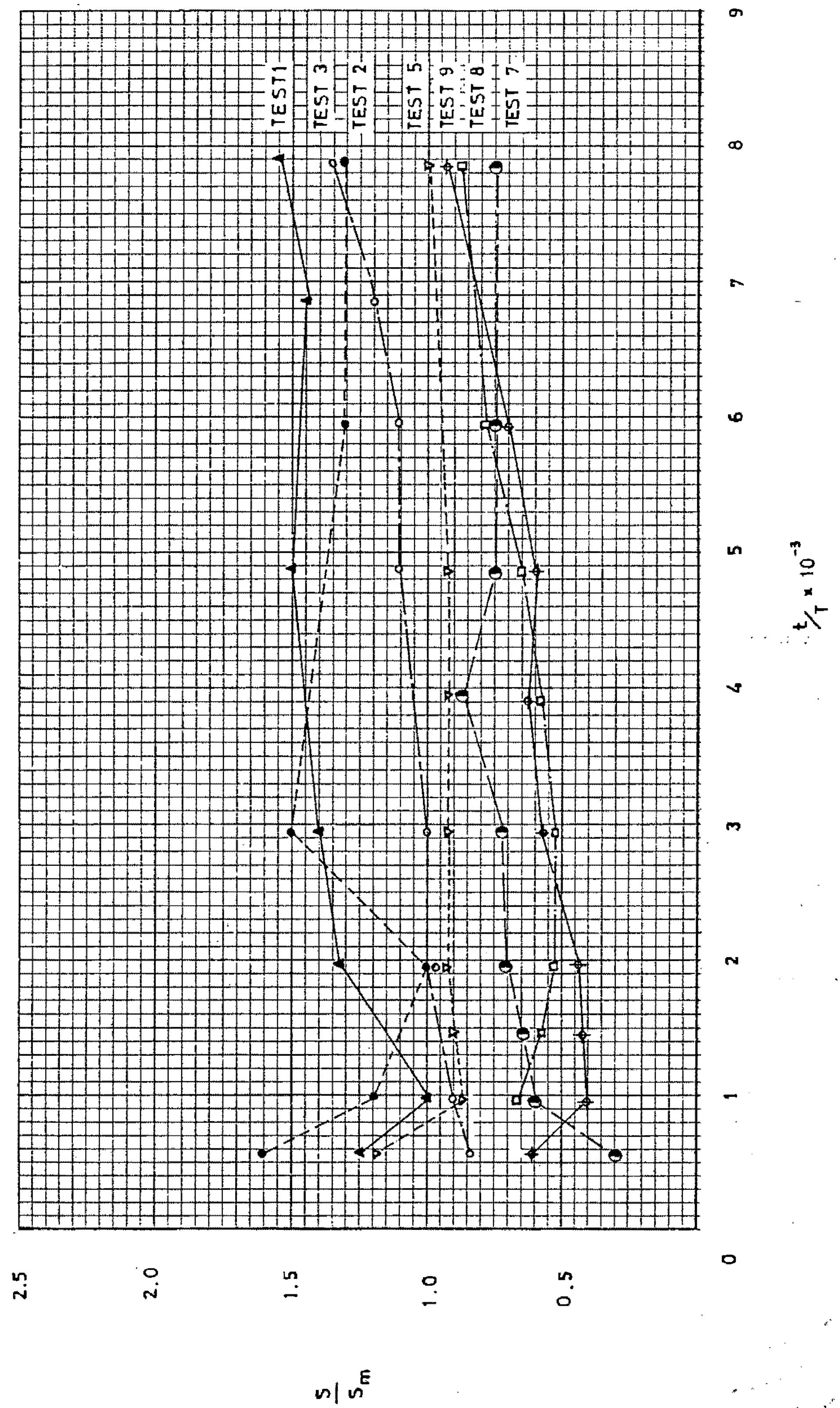

FIGURE 31 Scour Depth vs Mound Height

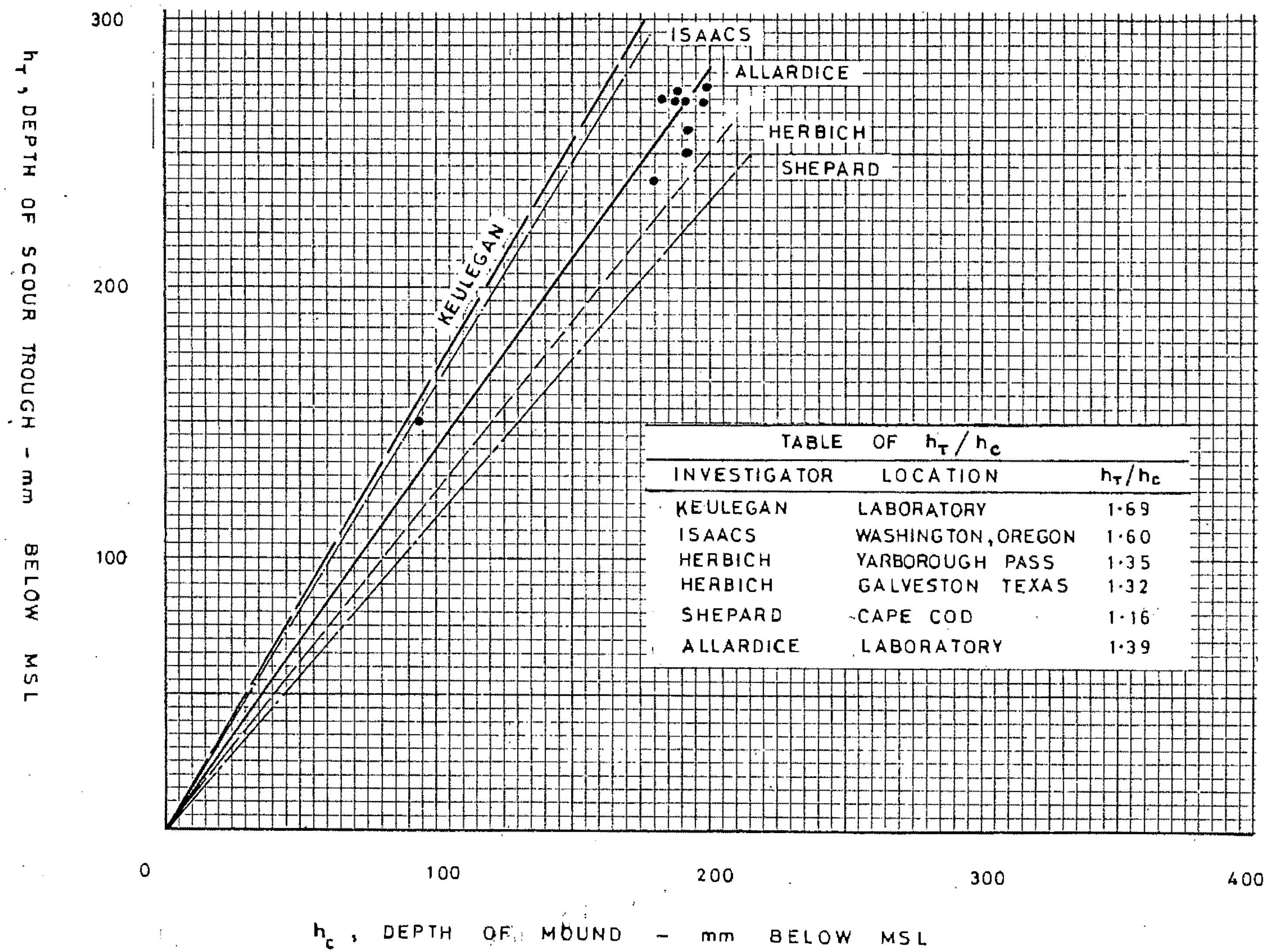

TABLE OF h_T / h_c

INVESTIGATOR	LOCATION	h_T/h_c
KEULEGAN	LABORATORY	1·69
ISAACS	WASHINGTON, OREGON	1·60
HERBICH	YARBOROUGH PASS	1·35
HERBICH	GALVESTON TEXAS	1·32
SHEPARD	CAPE COD	1·16
ALLARDICE	LABORATORY	1·39

FIGURE 32 Relationship between Depth of Trough and Depth of Mound

A variation of Figure 31 is Figure 32 where the depths below Mean Sea Level (MSL) of the scour trough (h_T) and mound (h_c) were plotted against each other. This was done to arrive at a comparison with the results obtained by Herbich [10] in his study on model and beach scour patterns. He concluded that the ratio tended towards an equilibrium value characteristic of each location, but at times, significant deviations occurred.

It can be seen that all the results obtained in this thesis for values of h_T/h_c, compare favourably with those obtained by Herbich and other authors, both in field and laboratory studies.

This consistency in results with investigations on natural beach patterns indicates that the scouring action in front of an artificial barrier, e.g. a rubble mound breakwater in this case, is a combination of forces present in natural beach scouring patterns and those associated with the presence of the breakwater.

26.3.5 <u>Relationship between Scour Depth and Sand Crest Wave Length</u>:

Scour depth readings, S, and scour wave length measurements,

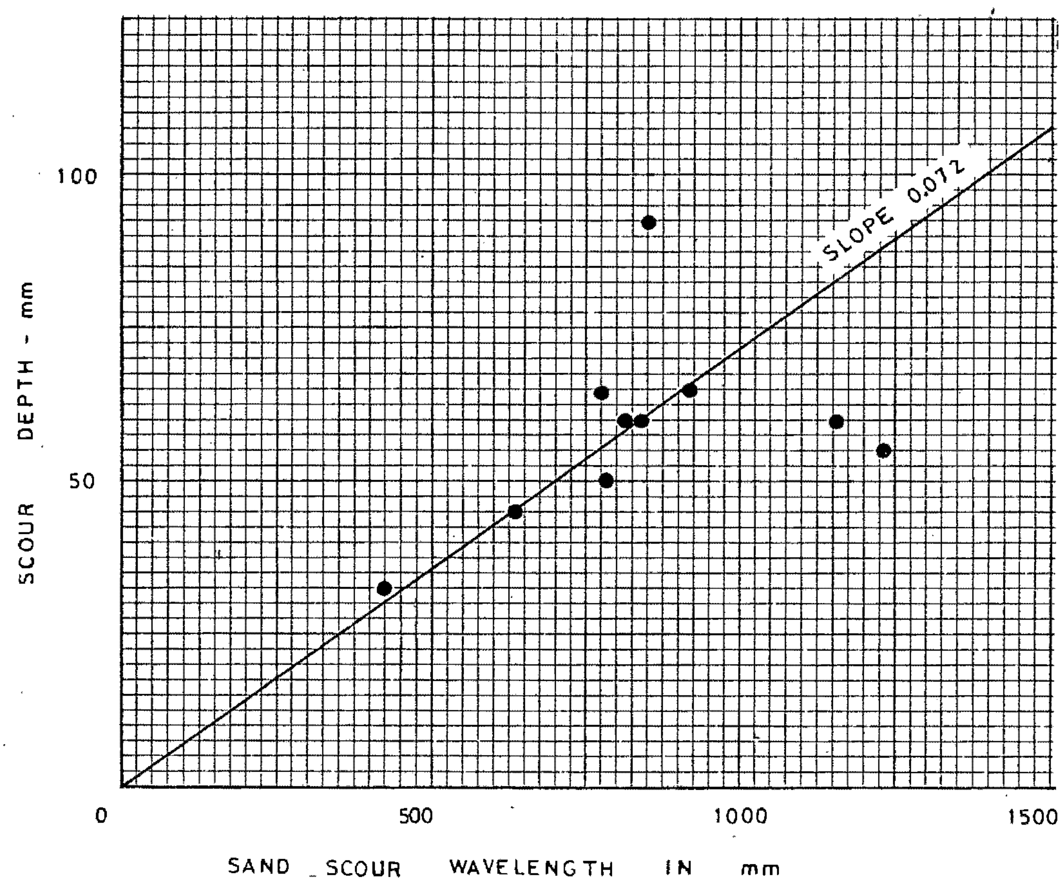

FIGURE 33 Depth of Scour vs Sand Scour Wavelength

S_L, were recorded for all tests and in Figure 33 they have been plotted against each other. Although the scatter is considerable (as may be expected) the relationship may be approximated by a straight line passing through the origin and having a slope of 0,072.

Laboratory experiments by Herbich *et al* [11] and Sato [27] have revealed that the distance between succeeding bar crests, i.e. the sand scour wave length as in Figure 24, is a function of the wave length of the incoming waves, and was generally equal to one half the wave length generated. From Figure 33, 70 % of the results have a wave length between 600 mm and 900 mm and from Appendix A, the theoretical incoming wave length is 2487 mm so although there appears to be a relationship there is not a good correlation with the results obtained by Herbich *et al* and Sato.

26.3.6 The Relationship between Scour Depth and the Reflection Coefficient:

Figure 34 is a plot of S/K as a function of the reflection coefficient, C_r, for $\cot \alpha = 2$ and 1,5, where,

S = Scour Depth
and $K = d_s - \frac{1}{2}A$ and d_s = water depth at the structure
and A = wave envelopé loop dimension.
(See Figure 24 and Appendix D)

It appears that the scour depth is only a random function of the reflection coefficient. This is probably due to the fact that the reflection coefficient depends on wave characteristics, breakwater slope and the kinematic behaviour upon hitting the breakwater. It must also be noted that average reflected wave heights were used when calculating C_r.

This result is in agreement with that obtained by Herbich and Ko [11] in their investigations into scouring of sand beaches in front of seawalls, but disagrees with Sawaragi [28] who found that the scouring depth increased with C_r when C_r was greater than 25 %.

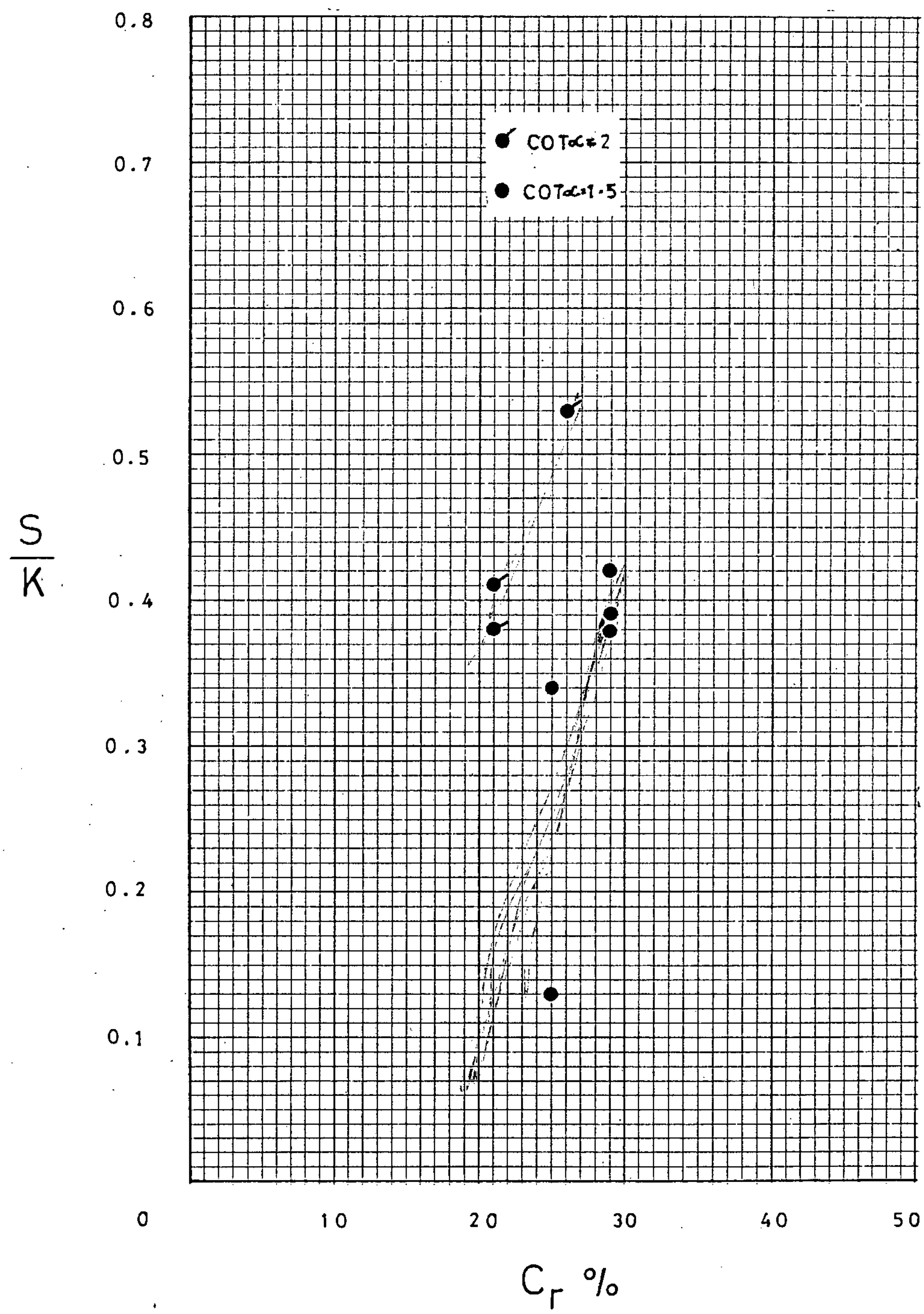

FIGURE 34 A Relation between Scour Depth and Reflection Coefficient

He in fact registered values of the reflection coefficient in excess of 50 % and this was impossible to obtain with the rubble mound breakwater model used in this investigation.

Figure 34 does however show that generally, the reflection coefficient increased with the increase in the seaward slope of the model breakwater.

26.3.7 The Effect of an Irregular Wave Attack on the Scouring Action:

An irregular wave train of wave heights varying from 120 mm to 80 mm attacked the breakwater in a water depth of 200 mm (Test 6 in Appendix C). The test was started at the maximum wave height and a full cycle of waves took 250 seconds.

The results showed a similar tendency to those obtained for a constant wave height but that the irregular wave attack had the ultimate effect of slowing down the scouring, and therefore the subsidence processes. This slowing down occurred mainly when the smaller waves were generated which was expected in lieu of previous observations.

Figures 35 (a) and (b) show scour depth and block subsidence plotted against time and the less intense effect of the irregular wave attack (Test 6) against a regular wave attack (Test 5) can clearly be seen.

Ergin and Pora [6] have shown that the effect of an irregular wave train on a rubble mound breakwater can be compared with that of a periodic wave height equal to the significant wave height of the spectrum. This agrees with the findings of Ouellet [24] in his paper on Breakwater Models. This may also be so in this case, but a comparison cannot be made because the periodic wave attack in Test 5 and other tests had a wave height equal to the maximum wave height for the irregular wave train.

26.3.8 The Effects of a Tidal Range on Scour:

A Tidal Range of 100 mm at a Tidal Cycle of 2,5 hours was

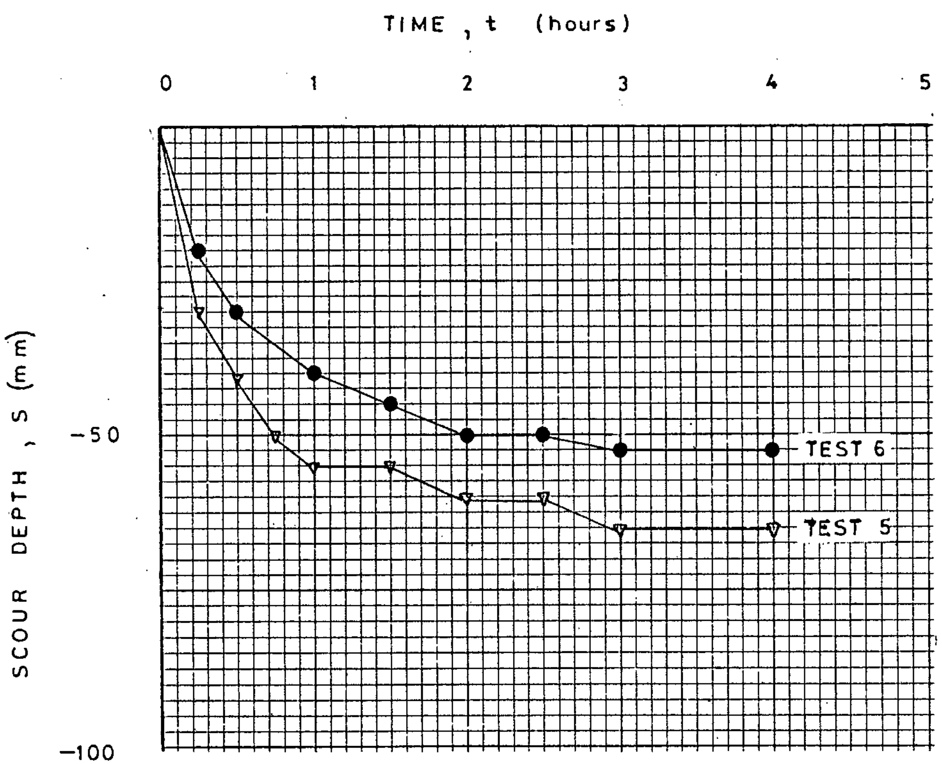

FIGURE 35a Scour Depth vs Time

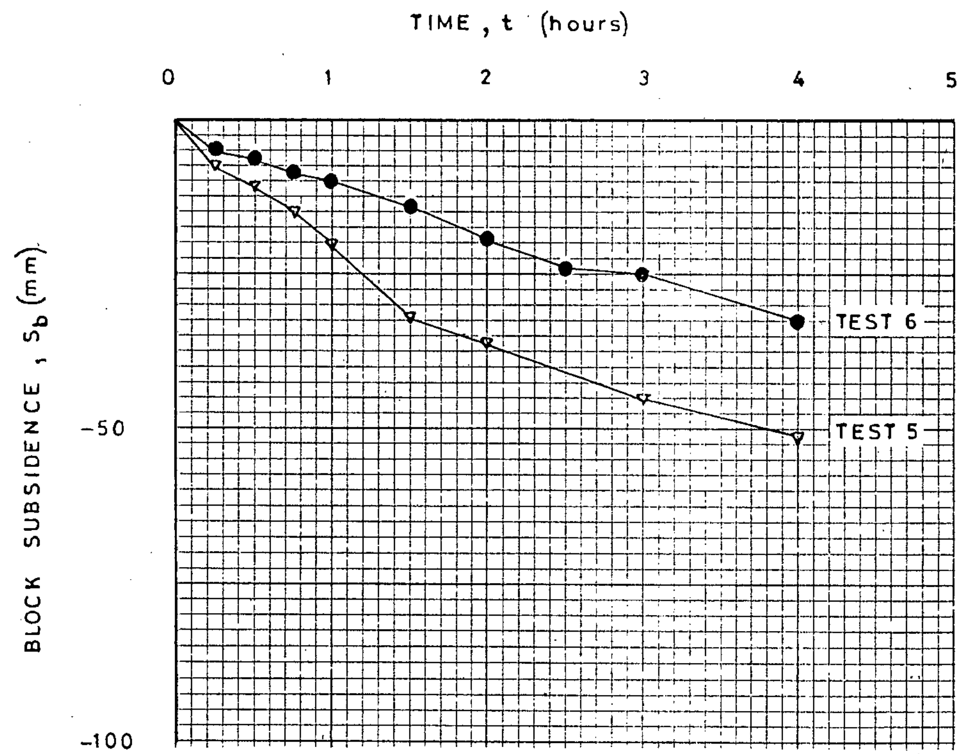

FIGURE 35b Block Subsidence vs Time

introduced. (See Figure 36.)

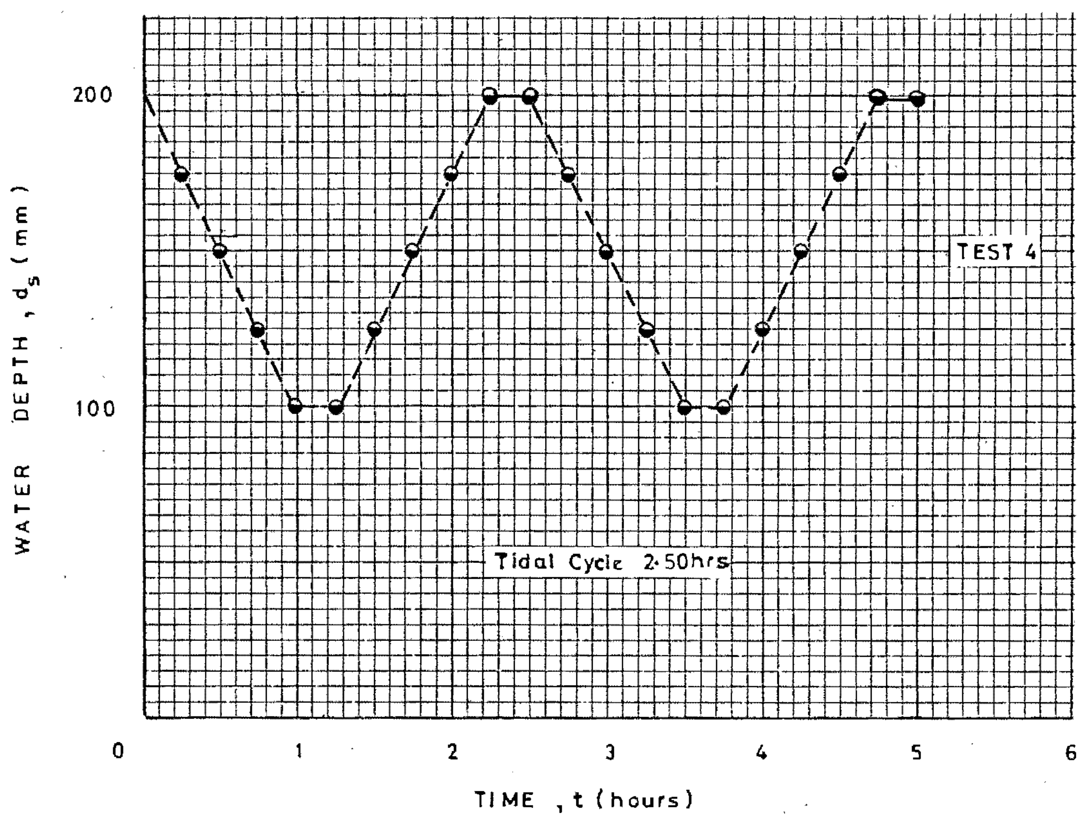

FIGURE 36 Tidal Range

The test was started at high tide and continued through two cycles so that the test duration was 5 hours and not 4 hours as for other tests. Figures 37 (a) and (b) show the results of the Tidal test (Test 4), compared with a test having similar parameters, but at a constant depth of water (Test 3). It can be seen that the ultimate effect of the scouring action is similar, in that the scour trench is approximately of similar depth, and that there is relatively no difference in the block subsidence. This can also be seen by comparing photographs 8, 11, 12 and 13 in Appendix F.

At the <u>high tides</u>, the scour was as intense as for the other tests at water depths of 200 mm, but the effect of the <u>low tide</u> was to change the wave form which resulted in a change in the scouring process. Figure 37 (a) shows that at high tides, the scour trench

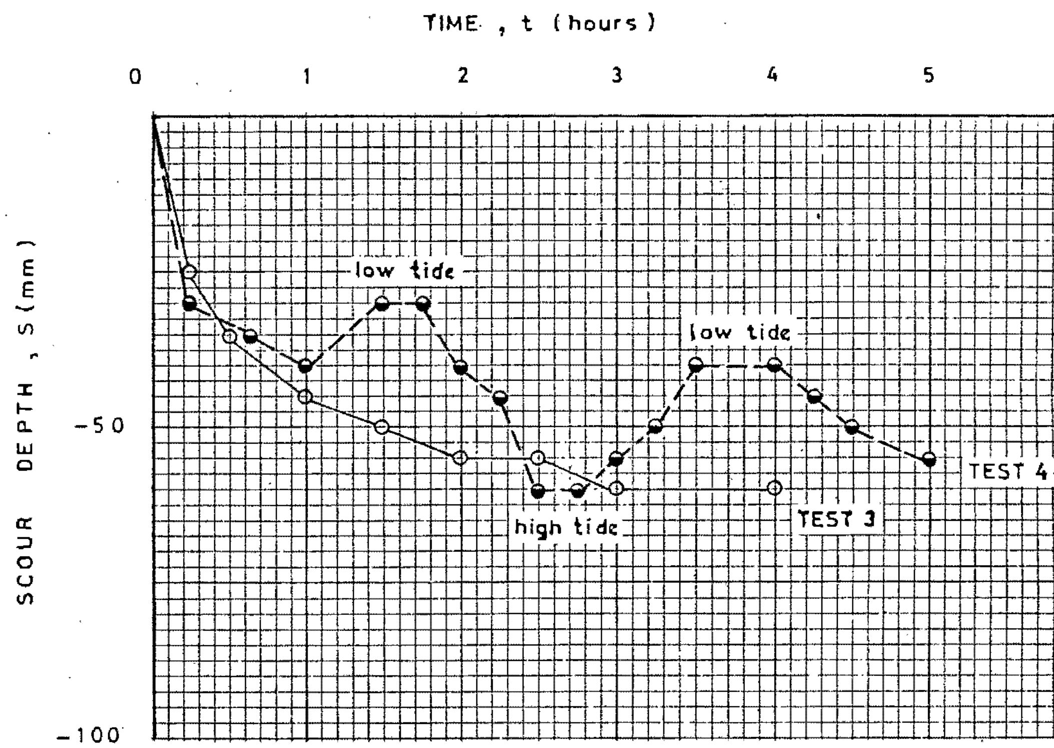

FIGURE 37a Scour Depth vs Time

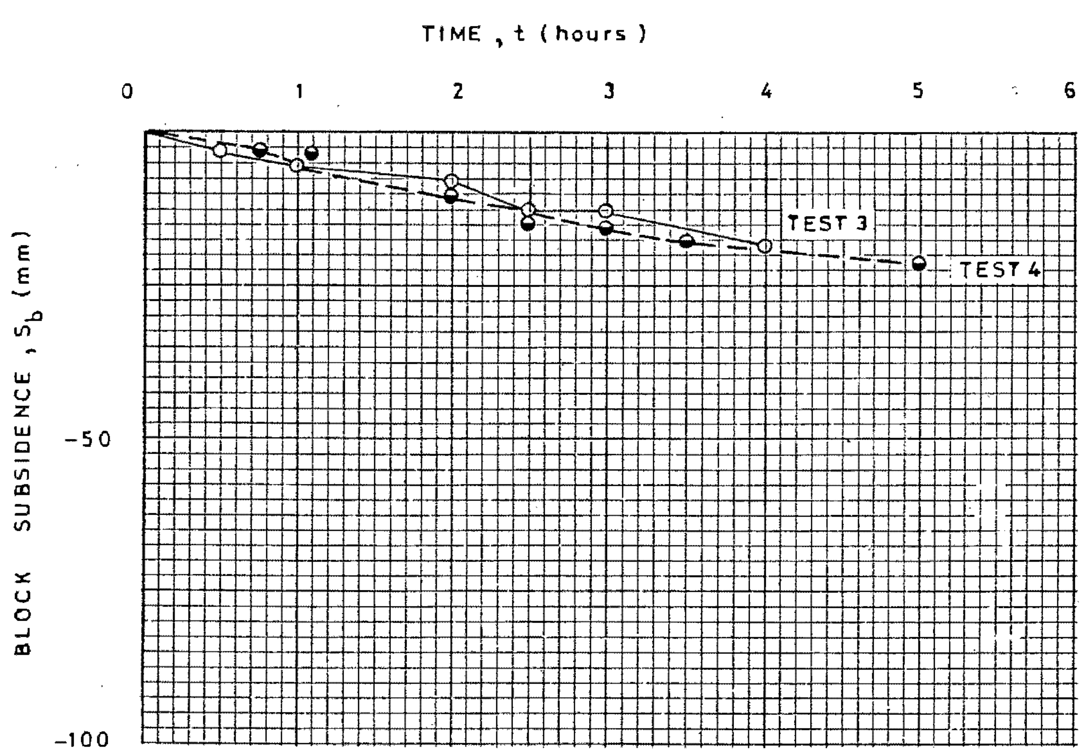

FIGURE 37b Block Subsidence vs Time

became deeper, and at low tides, shallower. This is a direct result of the wave form changing from swell to breaker which had the effect of flattening the sand bar, thus widening it in both directions, and thus filling the scour trench.

However, Figure 37 (b) suggests that block subsidence persisted throughout the tidal range which implied that scour continued at all tides. This is explained by the action of scour under the breakwater at all tides. At higher tides, scour was more towards the core centre and sand was deposited around and behind the toe region. At lower tides, this material was removed and deposited in the trench for transportation to the bar at the higher tides again. This cycle of events persisted throughout the test.

Finally, the findings of a tidal range on scour agree with results obtained by Godfrey [8] who found that at deeper waters, the scouring action was observed further towards the core centre, than at shallower waters.

26.3.9 Overtopping of the Breakwater - A Result of Scour:

The primary function of most breakwaters is to provide a sheltered anchorage on the lee side of the structure. Therefore, breakwaters are usually designed to prevent overtopping by the design wave. In all the tests conducted, no overtopping occurred with the initial shapes of the breakwater, but after the test duration, definite waves were observed behind the breakwater which were not due to transmission through the breakwater but due to the overtopping action. Estimation of the overtopping depth was difficult, owing to the turbulence and aeration associated with the wave spilling over the crest of the breakwater, but photographs were taken in an attempt to record the phenomenon.

Photographs 9 and 10 show the approaching wave at its maximum uprush and downrush positions at the commencement of a test and photograph 20 shows the water level behind the breakwater after the approaching wave has been transmitted through the core. It can be seen that there is very little water movement in the lee of the breakwater.

The scouring action under the breakwater resulted in the crest level subsiding 30 mm to 50 mm (see Appendix D, Tests 7, 8 and 9) and this allowed overtopping to occur. Photographs 21 and 22 show the water profile behind the breakwater after the passing of a wave, and they indicate the substantial height (estimated at 20 mm in some cases) of the overtopped wave. Photograph 21 also indicates the turbulence associated with the passage of the wave over the breakwater crest.

23.3.10 Dune Scour:

In the discussion to Herbich *et al*'s [11] findings on scour of sand beaches in front of sea walls, Zwamborn inquired whether similar vertical scour patterns would be observed in front of natural coastal structures such as sand dunes.

In sub-section 26.3.4 it was concluded that scour in front of an artificial barrier, e.g. a rubble mound breakwater, was a combination of forces present in natural beach scouring patterns and those associated with the presence of the breakwater.

From observations taken during the tests conducted for this thesis, it was generally felt that scour in front of natural barriers, e.g. sand bars, occurred. Photograph 5 distinctly shows two sand bars. The larger one was formed first (from sand removed from the breakwater area) and the smaller bar was formed from sediment removed from the outer edge of the larger bar and deposited some 700 mm away. The ultimate effect of this action was to have a flattened beach of uniform height, from the toe area to the outer bar.

26.3.11 The Overall Damage to the Rubble Mound Breakwater as a Result of Scour:

An extract from Jacob Feld's book - Construction Failures [7] - reads, ".... failures can be said to be a behaviour not in agreement with the expected conditions of stability, or as lacking freedom from necessary repair, or as non-compliance with the desired use of the completed structure".

A definition of damage to a rubble mound breakwater is based on the volume of the armour units displaced from the zone of active armour unit removal for a specific design wave height. This zone extends from the middle of the breakwater crest down the seaward face to a depth equivalent to one zero damage wave height below the still water level. This is in accordance with the definitions based on Hudson's [12] findings.

To accurately assess the extent of the damage caused by subsidence due to scour in this thesis, visual observations and photographs had to be relied upon. As described in Chapter 25, colour photographs were taken before and after the tests, the coloured dolosse and a series of grid lines making the damage assessment fairly simple. These photographs are shown in Appendix F. Not all the frontal and the initial side photographs have been included, as the initial photographs in the tests were very similar.

If damage is defined as it is by Hudson, then little damage occurred to the breakwater because armour units were not really removed from the zone of active armour unit removal, although in Tests 1, 5, 7, 8 and 9 subsidences larger than the lengths of the dolosse were recorded, and this could be defined as damage. But, if Jacob Feld's definition is used, then scour definitely resulted in failure of the rubble mound breakwaters used in the tests.

26.3.12 General Comments on Scour:

The results of the tests showed that maximum scour occurred at a definite wave period and water depth, and that a swell type wave was more damaging than a breaking wave.

Although only one test was conducted using coarse sand (D_{50} = 600 μm) i.e. Test 13, results, when compared to tests having similar parameters, showed far less effects of scour on the breakwater (see Figures 27 and 30). This was probably due to reasons described in Chapter 22, in that scale effects are present when conducting movable bed studies using grain sizes greater than 250 μm. A possible solution to these effects is a distorted scaling system but an accurate assessment of the distortion can only be obtained by juggling the scales in successive model tests.

Two tests were also conducted to establish the effect of the approaching beach slope on scour. A comparison of the results from Tests 8 and 9 from Appendix C and D and Figures 27 and 30, show that a steeper slope of 1 in 10 for the approaching beach, has very similar results to those for an approach in beach slope of 1 in 15. (See also, Photographs 17 and 23 in Appendix F). However, Godfrey's [8] results showed that scour was more intense for a beach slope of 1 in 15 than for 1 in 30 so it is felt that scour would be the most intense for slopes of 1 in 10 to 1 in 15 and definitely more intense than for a horizontal approach beach.

In Test 3, it was decided to extend the approach beach slope of 1 in 15 under the breakwater, and a comparison was then made with the results from Test 2. From Figures 27 and 30 and Appendix D, it can be seen that a sloping sea bed under the breakwater has no marked effect on scour or block subsidence. It is however felt that a slope of 1 in 15 is the maximum allowable to make practical construction of a rubble mound breakwater feasible.

CHAPTER 27

THREE DIMENSIONAL SCOUR:

Investigations in the field and in the laboratory have shown that the effects of three dimensional scour are far more serious than two dimensional scour.

In his experiments on the flow characteristics of vortices in three dimensional scour, Vinje [33] compared three dimensional and two dimensional local scour as a function of time and concluded that: "Local scour due to three dimensional flow is more serious than local scour associated with two dimensional flow under the same conditions (discharge, water depth, roughness, etc.)"

In the field, the main cause of the third dimension to the scour phenomenon has been a littoral current, resulting from either an oblique swell attack on the breakwater, or from a river discharge close to the breakwater, or from both.

At Ashdod [16], Israel, winter storms attacked a tetrapod-protected breakwater obliquely causing littoral currents and the effect of this and the presence of a strong flowing river which put the sand into suspension in the vicinity of the breakwater, resulted in a scour pit 4,5 m deep, 50 m wide and 180 m long, parallel to the breakwater. The berm rocks slipped into the erosion pit and the tetrapods, no longer sustained, collapsed, thus exposing the crown wall and setting a serious problem to the safety of the breakwater.

Merrifield [20] experienced similar problems at some of his first dolos-protected breakwater sites. In one case, beach subsidence at the toe of the bank due to scour by a littoral current, caused the toe to drop some 1,5 m, the top of the bank to swing over 10 m horizontally, and subsequently altered the seaward slope of the breakwater from $1\frac{1}{2}$ to 1 to $\frac{3}{4}$ to 1. This resulted in about 2 per cent dolos breakage.

Zwamborn [39], in his paper on the design and construction of rubble mound breakwaters, provides a theoretical expression for the velocity of wave generated longshore currents, and warns that these currents will be deflected by breakwaters, causing either accretion or scour, depending on local conditions and breakwater design.

A three dimensional experimental program was envisaged for this thesis, but problems concerning the availability of more dolos models, the size of the existing wave basin in the U.C.T. Civil Engineering Laboratories and the extra costs, resulted in the program being terminated.

The kind of experimental set-up desired is shown in Figure 38. Problems were encountered with the University of Cape Town wave basin in that the wave generator extended the entire width of the basin which made wave spending revetments relatively inefficient in absorbing the reflected waves from the breakwater and the direct waves from the generator. A length of breakwater of 3,0 m was considered a minimum for a thorough investigation into three dimensional scour at the toe and this left a mere 3,5 m for a spending area in the U.C.T. basin, so the test section would have been attacked by a mixture of direct, reflected and re-reflected waves, which would have made the investigation unrealistic and extremely complex.

However, it is felt that a laboratory investigation into three dimensional scour at the toe of rubble mound breakwaters on sand foundations, would yield interesting results and a possible correlation to the results of the two dimensional scour investigated in this thesis, and it is proposed that future studies be conducted in this field.

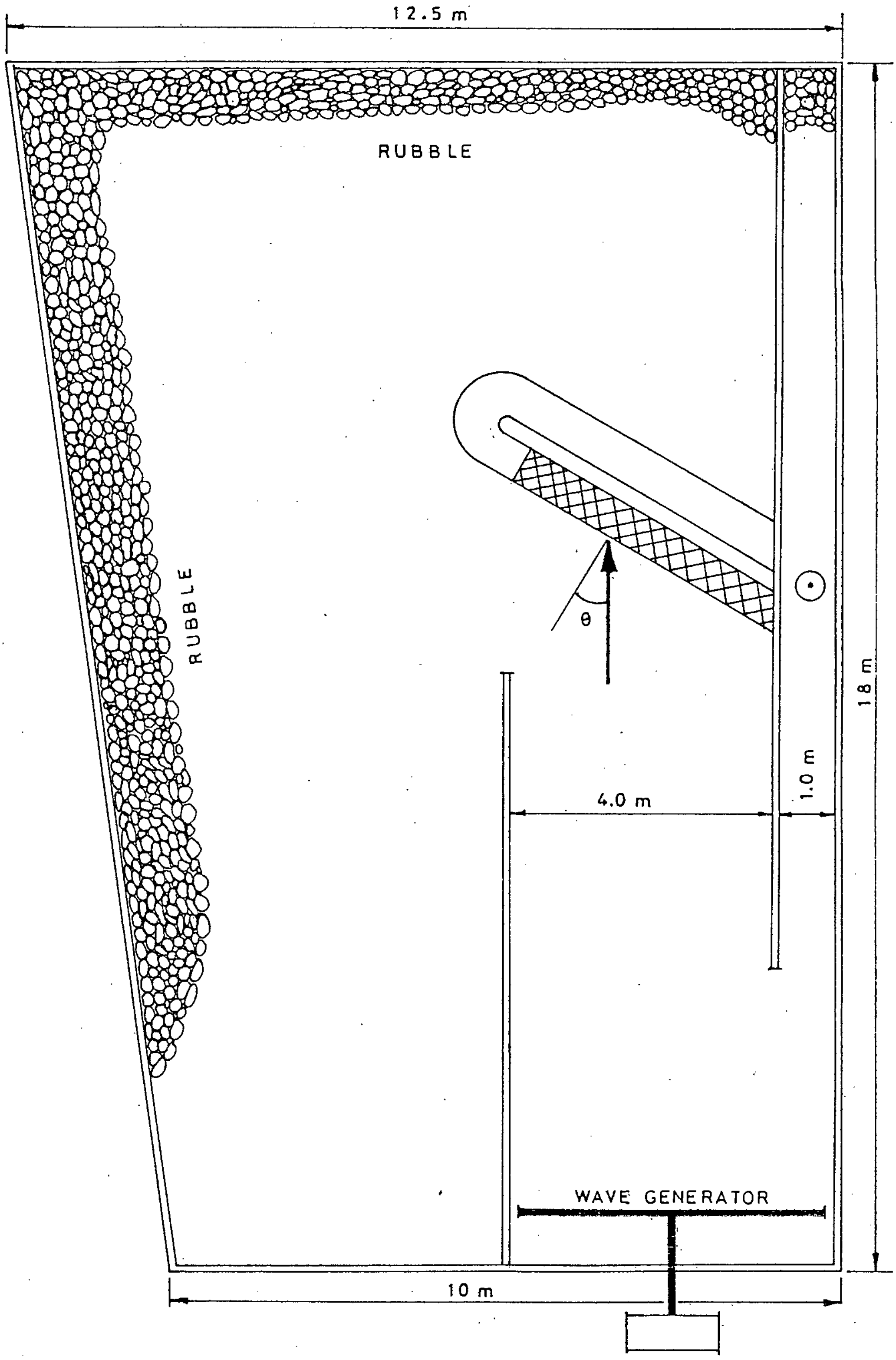

⊙ WAVE MEASURING DEVICE

θ ANGLE OF WAVE INCIDENCE

▨ TEST SECTION

SCALE : 1 in 100

FIGURE 38 Experimental Set-up

CHAPTER 28

FILTER SYSTEMS FOR RUBBLE MOUND BREAKWATERS FOUNDED ON SAND:

An extract from Barrett's[1] paper reads: "Due to the granular soils on which most coastal structures are constructed, filters are necessary for the stability of the structure.

Filter systems must be permeable to prevent a build-up of hydrostatic pressure by allowing the water to pass through without significant head loss. They must be impermeable to soil to prevent the soil leaching through the structure causing it to become unstable and/or to settle."

28.1 Graded Filter System:

In an attempt to lessen the damaging effect of scour on rubble mound breakwaters founded on sand, graded rock filters were introduced. This procedure consisted of extending the core and the underlayer to positions past the breakwater toe, as recommended in the Shore Protection Manual [32] and as shown in Figure 8. Graded filters were employed in Tests 2 to 7 and the results and effects of these filters are shown in Appendix D and in the photographs in Appendix F.

The main effect of the graded filters was a sharp decrease in the block subsidence as shown when comparing results of tests with and without graded filter blankets, but having similar parameters, i.e.

Compare: Tests 2 and 3 with Test 1 (Photographs 7 and 11 with 2)
Test 5 with Test 9 (Photographs 15 with 23), and
Test 7 with Test 8 (Photographs 16 with 17).

It must be noted however, that although graded rock filter blankets greatly reduced the relative amount of subsidence, subsidence of a fairly large magnitude still occurred, (65 mm downslope and still increasing after the 4 hours test duration in Test 7).

The most important effect of the graded filters on the scour trench was a displacement seaward, of the trough of the trench, from the breakwater toe. What this means is that scour still occurred, and a trench still formed (as shown by measurements in Appendix D and Figure 27), but the damaging effect of the armour- and under-layers subsiding into the scour pit was greatly reduced as the trough of the scour pit was as much as 150 mm from the breakwater toe in some cases. (See the photographs mentioned above).

It is therefore felt that although graded rock filters reduced the damaging effects of scour on rubble mound breakwaters founded on sand, they were not the solution to the problem.

28.2 Plastic Filter System:

In a further attempt to alleviate the scour problem, plastic filters were introduced under the breakwater. The term "plastic filters" refers to cloths woven of modern synthetic fibres. In this thesis, two types of plastic filters were investigated and they have been identified by code names,

i.e. Type 1 - a filter manufactured from 75 % polypropylene and 25 % nylon yarns woven into cloths,

and Type 2 - a non-woven, spun-bonded, needle-punched continuous filament polyester fabric.

In his paper on the design of filter systems for rubble mound structures, Lee [17] stated that plastic filters should be designed, to be effective in retaining soil, but remain permeable to water under both laminar and turbulent flow conditions. It was with these main intentions that plastic filters were introduced in this investigation.

Brief specifications of the two types of plastic filters investigated are as follows.

CHARACTERISTIC	TYPE 1	TYPE 2
Coefficient of Permeability	$1,6 \times 10^{-3}$ m/s	3×10^{-3} m/s
Tensile Strength	4807* N/m	5900* N/m
Fabric Thickness	0,5 mm	± 2 mm

*Figures quoted apply under wet and dry conditions.

The filters were extended 900 mm seaward from the centre of the core, i.e. approximately 300 mm past the breakwater toe. The end of the filters on the approach beach was anchored with rocks (see photograph 29 in Appendix F) to prevent lifting under wave action. Conditions which had previously resulted in the worst combination of scour and subsidence were provided for the tests on the filters. These parameters are shown in Appendix C for Tests 10 and 11.

The following photographs in Appendix F depict before and after views of the results of a wave attack on the plastic filtered rubble mound breakwater:

Photographs 24, 25, 26 and 27 - Test 10, Type 1 Filter
and 28, 30, 31, 32 and 33 - Test 11, Type 2 Filter.

It can be seen that relatively no subsidence occurred and that which did - Test 10 - occurred at the flume wall sides, the reason being, the filter was not flush with the wall sides so that sand was able to percolate out thus causing the two outermost dolosse to subside. This problem was alleviated in Test 11 where the sides of the filter were turned up against the glass wall of the flume.

Photographs for Test 11 clearly show, that for the filter with the higher coefficient of permeability, i.e. Type 2 with $0,3 \times 10^{-3}$ m/s, sand movement still occurred, away from the breakwater toe and under the filter, and a sand build-up can be observed behind the anchored section of the filter. It can also be seen that a scour trench still formed at the end of the filtered section but if the end of the filter is extended far enough away from the breakwater, as it was in this case, this trench has no effect on the stability of the structure.

It has therefore been shown that plastic filters are instrumental in preventing scour, and therefore subsidence, of the sand beneath rubble mound breakwaters. Readers are however cautioned about the scale effects of the scour prevention characteristics of the plastic filters as model dolosse were used on full scale type filters.

CHAPTER 29

CONCLUSIONS AND RECOMMENDATIONS:

It is concluded from the results of two dimensional scour tests completed on small scale rubble mound breakwaters, consisting of quarry stone and dolos-shaped armour units, founded on sand, that:

(i) Scour is a function of the wavelength of the incoming waves and a relative depth of $d/L = 0,080$ resulted in maximum scour.

(ii) The ultimate scour depth is approached asymptotically, and a relationship, explaining the exponential growth of scour with time, was developed.

(iii) Breakwater seaward slopes of $\cot \alpha = 1,5$ produced larger block subsidence due to scour than for flatter slopes of $\cot \alpha = 2$. The steeper slope of $\cot \alpha = 1,5$ was considered to be the maximum practical slope.

(iv) A direct relationship exists between the depth of the scour trough and the depth of the mound, both measured from MSL.

(v) No conclusive evidence exists connecting the extent of the scour to the water depth at the structure, although it became clear that, providing the wave period was kept constant, scour was of greater intensity and occurred more towards the core centre, with deeper water.

(vi) A direct relationship exists between the scour trough depth and the sand crest wavelength.

(vii) The scour depth is only a random function of the reflection coefficient.

(viii) If the effects of an irregular wave train on the breakwater are compared with those of a periodic wave train of wave height equal to the maximum wave height of the spectrum, it is found that the scouring process was less intensified for the former. Similar results were obtained when a tidal range was introduced.

(ix) The most important damaging effects on the breakwater because of scour are in the form of mass subsidence of the armour and the core, and therefore overtopping.

(x) The main cause of sand scour in the vicinity of the breakwater toe was considered to be a combination of forces present in natural beach scouring patterns, and those associated with downrush forces within the breakwater slope. The forces associated with downrush have been explained by Bruun *et al* [3], who developed a flow net which revealed that the outflow was concentrated at the lowest level of wave retreat, which caused strong normal forces along the stream lines of the flow. These stream lines extend to the sea bed.

Although no three dimensional scour investigation is included in this thesis, it is the writer's opinion that a third dimension such as a littoral current parallel to the breakwater would have a greater damaging effect due to scour than the two dimensional effects discussed. It is therefore recommended that the results obtained in this thesis be instrumental in an attempt on a three dimensional investigation.

The introduction of filters and especially plastic filters were very effective for the prevention of sand scour, but further studies would be necessary on their durability.

It is recommended that a further study be undertaken to investigate the possibility of scale effects in the results obtained in the scour investigation, especially those obtained using coarse sand of size $D_{50} = 600$ μm, as a full understanding of this was not achieved.

To try and predict scour depths and subsidence for a prototype case or to relate the results obtained to a prototype, would be presumptious. To predict happenings or occurrences of a phenomenon in a prototype requires that there be similitude, both geometric and dynamic, between the model and the prototype. This requires that similitude exists between the orbital velocities and orbital lengths (i.e. wave characteristics are similar), grain size and grain distribution in the bed, roughness of the beds, and translation of the orbit due to drift. Without these similitudes, erroneous conclusions could be reached in attempting to predict prototype conditions.

However, it is the belief of the writer that meaningful results have been obtained and it is his sincere opinion that they should be given consideration in every structure in which sand scour poses a possible threat.

BIBLIOGRAPHY

1. BARRETT, R.J., "The use of plastic filters in coastal structures", Proc. 10th Conference on Coastal Engineering, Tokyo, Chapter 62, pp 1048-1067, 1966.

2. BREUSERS, H.N.C., "Time scale for two-dimensional local scour", Proc. 12th Congress, International Association for Hydraulic Research, Vol. 3, Section C32, pp 1-8, 1967.

3. BRUUN, P and JOHANNESSON, P., "Parameters affecting stability of rubble mounds", J. Waterw. Harb. and Coastal Eng. Div., Proc. ASCE, Vol. 102, n WW2, pp 141-164, 1976.

4. CARSTENS, M.R., "Similarity laws for localized scour", J. Hydr. Div., ASCE, Vol. 92, n HY3, Proc. p 4818, pp 13-36, 1966.

5. COURSEY, G.E., "A new shape in shore protection", Civil Eng., ASCE Vol. 43, n 12, pp 68-71, 1973.

6. ERGIN, A. and PORA, S., "Irregular wave attack on rubble mound breakwaters", J. Waterw. Harb. and Coastal Eng. Div., Proc. ASCE, Vol. 97, n WW2, p 8114, pp 279-293, 1971.

7. FELD, J., "Construction Failure", John Wiley and Sons, 1968.

8. GODFREY, M., "Breakwaters on sand", B.Sc.(Eng.) Thesis Document, Dept. of Civil Eng., University of Cape Town, 1976 (Unpublished).

9. HARSHKUMAR, C.D., "Volume and strength of a dolos", J. Waterw. Harb. and Coastal Eng. Div., Proc. ASCE, Vol. 102, n WW1, p 11928, pp 79-88, 1976.

10. HERBICH, J.B., "Comparison of model and beach scour patterns", Proc. 12th Conference on Coastal Engineering, Washington D.C., Chapter 80, pp 1281-1302, 1970.

11. HERBICH, J.B. and KO, S.C., "Scour of sand beaches in front of seawalls", Proc. 11th Conference on Coastal Engineering, London, Chapter 40, pp 622-643, 1968.

12. HUDSON, R.Y., "Laboratory investigation of rubble mound breakwaters", J. Waterw., Harb. and Coastal Eng. Div., Proc. ASCE, Vol. 85, n WW3, pp 93-121, 1959.

13. HUDSON, R.Y., "Wave forces on rubble mound breakwaters and jetties", Misc. paper n 2-453, U.S. Army Eng. Waterw. Exp. Station, Vicksburg, 1961.

14. JACKSON, R.A., "Limiting heights of breaking and non-breaking waves on rubble mound breakwaters", Tech. Rep. n H-68-3, U.S. Army Corps of Engineers, Waterw. Exp. Station, Vicksburg, 1968.

15. JOHANNESSON, P. and BRUUN, P.M., "Hydraulic performance of rubble mound breakwaters; reasons for failure", Port and Ocean Engineering under Arctic Conditions, Technical University of Norway, Vol. 1, pp 326-358, 1971.

16. KAPLAN, N., "Design of breakwaters on a sandy seabed", Dock and Harb. Auth., Vol. 52, n 615, pp 376-378, 1972.

17. LEE, T.T., "Design of filter systems for rubble mound structures", Proc. 13th Conference on Coastal Engineering, Vancouver, B.C., Chapter 109, pp 1917-1933, 1972.

18. LE MÉHAUTÉ, B., "Similitude in coastal engineering", J. Waterw., Harb. and Coastal Eng. Div., Proc. ASCE, Vol. 102, n WW3, p 12293, pp 317-335, 1976.

19. MERRIFIELD, E.M. and ZWAMBORN, J.A., "The economic value of the new breakwater unit, the dolos", Proc. 10th Conference on Coastal Engineering, Tokyo, Chapter 51, pp 885-912, 1966.

20. MERRIFIELD, E.M., "Dolos concrete armour protection", Civil Eng., ASCE, pp 38-41, December, 1968.

21. MERRIFIELD, E.M., "A new breakwater and coastal protection block", Dock and Harb. Auth., Vol. 50, n 594, pp 490-493, 1970.

22. MORAIS, C.C., "Irregular wave attack on a dolos breakwater", Proc. 14th Conference on Coastal Engineering, Copenhagen, Chapter 98, pp 1677-1690, 1974.

23. OUELLET, Y., "The effects of irregular wave trains on a rubble mound breakwater", J. Waterw., Harb. and Coastal Eng. Div., Proc. ASCE, Vol. 98, n WW1, p 8693, pp 1-14, 1972.

24. OUELLET, Y., "Considerations on factors in breakwater model tests", Proc. 13th Conference on Coastal Engineering, Vancouver, B.C., Chapter 106, pp 1873-1884, 1972.

25. PALMER, H.D., "Wave-induced scour on the sea floor", Civil Engineering in the Oceans, Part II, pp 706-716, 1969.

26. ROPER, A.T., SCHNEIDER, V.R. and WEN SHEN, S., "Analytical approach to local scour", Proc. 12th Congress, Int. Assoc. for Hydraulic Research, Vol. 3, section C18, pp 1-11, 1967.

27. SATO, S., TANAKA, N. and IRIE, I., "Study of scour at the foot of coastal structures", Proc. 11th Conference on Coastal Engineering, London, Chapter 37, pp 579-598, 1968.

28. SAWARAGI, T., "Scouring due to wave action at the toe of a permeable structure", Proc. 10th Conference on Coastal Engineering, Tokyo, Chapter 61, pp 1036-1047, 1966.

29. SWART, D.H., "A schematization of onshore-offshore transport", Delft Hydraulics Lab., Publ. n 134, 1974.

30. SWART, D.H., "Offshore transport and equilibrium beach profiles", Delft Hydraulics Lab., Publ. n 131, 1974.

31. TOWNSON, J.W., "History of breakwaters", Dock and Harb. Auth., Vol. 54, n 633, pp 98-101, 1973.

32. U.S. ARMY COASTAL ENGINEERING RESEARCH CENTRE, Shore Protection Manual, Vol. II, Chapters 5-8, Second Printing, 1973.

33. VINJE, J.J., "The flow characteristics of vortices in three-dimensional local scour", Proc. 12th Congress, Int. Assoc. for Hydraulic Research, Vol. 3, section C25, pp 1-11, 1967.

34. WELLS, D.R. and SORENSEN, R.M., "Scour around a circular cylinder due to wave motion", Proc. 12th Conference on Coastal Engineering, Washington, D.C. Chapter 79, pp 1263-1280, 1970.

35. WILSON, K.W. and CROSS, R.H., "Scale effects in rubble mound breakwaters", Proc. 13th Conference on Coastal Engineering, Vancouver, B.C., Chapter 106, pp 1873-1884, 1972.

36. ZWAMBORN, J.A., "Hydraulic Models", CSIR Report, MEG 795, Hydraulics Research Unit, Stellenbosch, South Africa, 1969.

37. ZWAMBORN, J.A. and BEUTE, J., "Stability of dolos armour units", ECOR Symposium S71, Stellenbosch, S.A., 1972.

38. ZWAMBORN, J.A., "Dolosse for coastal works", A paper presented to the E.P. Society of Civil Engineers, November 1975.

39. ZWAMBORN, J.A., "Design and construction of rubble mound breakwaters", Lecture notes for Coastal Engineering Course, ECOR, Port Elizabeth, July 1976.

APPENDIX A

WAVE PARAMETERS FOR U.C.T. WAVE FLUME

WAVE PARAMETERS FOR U.C.T. WAVE FLUME

d (mm)	T (mm)	d/gT^2	C^2/gd	C (mm/s)	L = CT (mm)	d/L	d/L_o	L_o (mm)	H (mm)	H/H_o	H_o (mm)
100	1,75	0,0033	0,958	969,4	1696,5	0,059	0,021	4761,9	60	1,22	49
	1,85	0,0030	0,960	970,4	1795,2	0,056	0,019	5263,2	80	1,25	64
	2,05	0,0024	0,968	874,5	1997,7	0,050	0,015	6666.7	85	1,30	65
	2,27	0,0020	0,972	976,5	2216,7	0,045	0,012	8333,3	90	1,35	67
	2,50	0,0016	0,980	980,5	2451,3	0,041	0,009	11111,1	95	1,46	65
200	1,75	0,0067	0,914	1339,1	2343,4	0,085	0,041	4878,1	100	1,05	95
	1,85	0,0060	0,921	1344,3	2487,0	0,080	0,038	5263,2	120	1,08	111
	2,05	0,0049	0,939	1357,3	2782,5	0,072	0,031	6451,6	140	1,13	124
	2,27	0,0040	0,948	1363,8	3095,8	0,065	0,025	8000,0	145	1,17	124
	2,50	0,0033	0,958	1371,0	3427,5	0,058	0,021	9523,8	150	1,22	123
250	1,75	0,0083	0,890	1477,4	2585,5	0,097	0,052	4807,7	120	1,01	119
	1,85	0,0074	0,905	1489,8	2756,1	0,091	0,047	5319,2	145	1,04	140
	2,05	0,0061	0,920	1502,1	3079,3	0,081	0,039	6410,3	180	1,07	168
	2,27	0,0049	0,939	1517,5	3444,7	0,073	0,031	8064,5	200	1,13	177
	2,50	0,0041	0,948	1524,8	3812,0	0,066	0,026	9615,4	210	1,16	181

The above table was obtained with the aid of the Dimensionless Wave Characteristics nomogram reproduced in Appendix B, by courtesy of Professor F.A. Kilner of the Department of Civil Engineering at the University of Cape Town.

APPENDIX B

DIMENSIONLESS WAVE CHARACTERISTICS

DIMENSIONLESS WAVE CHARACTERISTICS

Used for wave shoaling with wave crests parallel to the shoreline.

c = phase velocity
c_g = group velocity
L = wave length
d = undisturbed depth
T = wave period
H_o = deep water wave height
H = general wave height

Based on small amplitude wave theory and constant power transmission

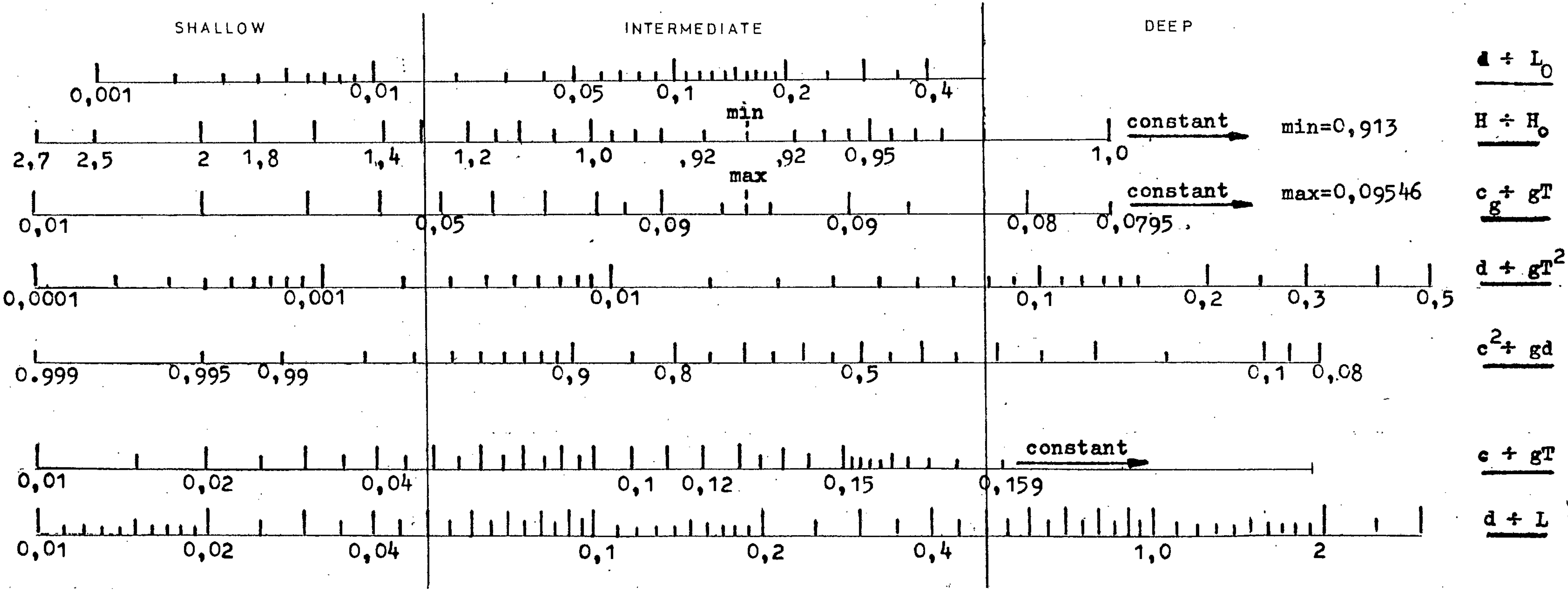

1
8.
9
12
13

A P P E N D I X C

EXPERIMENTAL PROGRAM

EXPERIMENTAL PROGRAM

TEST NO.	BREAKWATER SLOPE	BEACH SLOPE	T (Secs)	H (mm)	d_s (mm)	SAND SIZE (μm)	REMARKS
1	1 in 2	1 in 15	1,85	120	200	200	No filter - Breakwater founded directly on sand. Horizontal sea floor under breakwater.
2	1 in 2	1 in 15	1,85	120	200	200	Graded filter under the breakwater. Horizontal sea floor under breakwater.
3	1 in 2	1 in 15	1,85	120	200	200	Graded filter under the breakwater. Sea bed sloping 1 in 15 under breakwater.
4	1 in 2	1 in 15	1,85	variable	variable 100-200	200	Graded filter under breakwater. Sea bed sloping 1 in 15 under breakwater. Tidal influence.
5	1 in 1,5	1 in 15	1,85	120	200	200	Graded filter under breakwater. Sea bed sloping 1 in 15 under breakwater.
6	1 in 1,5	1 in 15	1,85	variable	200	200	Graded filter under breakwater. Sea bed sloping 1 in 15 under breakwater.
		irregular wave attack					
7	1 in 1,5	1 in 10	1,85	120	200	200	Graded filter under breakwater. Sea bed sloping 1 in 15 under breakwater.
8	1 in 1,5	1 in 10	1,85	120	200	200	No filter - Breakwater founded directly on sand. Sea bed sloping 1 in 15 under breakwater.
9	1 in 1,5	1 in 15	1,85	120	200	200	As for Test 8
10	1 in 1,5	1 in 15	1,85	120	200	200	Type 1 plastic filter placed beneath breakwater. Sea bed sloping 1 in 15 under breakwater.
11	1 in 1,5	1 in 15	1,85	120	200	200	Type 2 plastic filter placed beneath breakwater. Sea bed sloping 1 in 15 under breakwater.
12	1 in 1,5	1 in 15	1,85	120	200	200	No filters - Breakwater founded on sand. Sea bed sloping 1 in 15 under breakwater. Fluorescent sand tracers used.
13	1 in 1,5	1 in 15	1,85	120	200	600	As for Test 12.

APPENDIX D

EXPERIMENTAL RESULTS

EXPERIMENTAL RESULTS

TEST NO.	DOLOS SUBSIDENCE (DOWNSLOPE)(mm) GREEN	YELLOW	RED	BLUE	MEAN	TRENCH DEPTH S (mm)	BAR HEIGHT S_m (mm)	SAND SCOUR LENGTH S_L (mm)	WAVE ENVELOPE DIMENSIONS (mm) NODE (B)	LOOP (A)	H_i	H_r (Average)
1	90	60	25	10	46,3	85	50	850	80	144	120	32
2	40	10	–	–	12,5	65	50	775	80	130	120	25
3	30	20	15	10	18,8	60	45	820	80	130	120	25
4	35	20	20	10	21,3	45	45	635	80	130	120	25
5	120	40	30	15	51,3	65	65	920	70	140	120	35
6	65	40	20	15	35,0	55	55	780	80	130	120 (H_{max})	25
									50	90	80 (H_{min})	20
7	105	65	55	50	69,8	60	80	830	70	140	120	35
8	95	95	95	95	95,0	60	80	1165	70	140	120	35
9 and 12	90	90	90	75	86,3	55	60	1230	80	140	120	30
13	35	35	30	20	30,0	35	30	450	80	140	120	30

Note: Tests 10 and 11 resulted in no marked trench near the structure, and relatively no armour subsidence. Wave characteristics are as for Tests 7 to 13.

APPENDIX E

STRAIGHT LINE EQUATIONS ASSOCIATED WITH FIGURE 28

STRAIGHT LINE EQUATIONS ASSOCIATED WITH FIGURE 28

The equations are obtained by LINEAR REGRESSION of the transform variables of the parameters involved, whereby S/d_s and t are transformed into natural logs.

The equations are of the form:

$$y = e^{bx+c} \quad \text{or} \quad y = At^{b}$$

where,

b = the slope of the graphs

c = y-intercept,

x = $\log_e t$,

and A = $1/e^{c}$.

TEST 1 : $y = 0,291\ t^{0,280}$

TEST 2 : $y = 0,262\ t^{0,200}$

TEST 3 : $y = 0,215\ t^{0,303}$

TEST 5 : $y = 0,244\ t^{0,260}$

TEST 6 : $y = 0,194\ t^{0,253}$

TEST 7 : $y = 0,197\ t^{0,430}$

TEST 8 : $y = 0,189\ t^{0,388}$

TEST 9 : $y = 0,150\ t^{0,480}$

TEST 13 : $y = 0,122\ t^{0,368}$

The average slope is 0,326, as shown in Equation (26.1).

A P P E N D I X   F

PHOTOGRAPH CATALOGUE

PHOTOGRAPH CATALOGUE

Photograph Number	Description
1	TEST 1 - before testing; side view.
2	TEST 1 - after testing; side view.
3	TEST 1 - before testing; front view.
4	TEST 1 - after testing; front view.
5	View showing scour trough and mounds.
6	TEST 2 - before testing; side view.
7	TEST 2 - after testing; side view.
8	TEST 3 - before testing; side view.
9	View showing wave uprush on slope.
10	View showing wave downrush on slope.
11	TEST 3 - after testing; side view.
12	TEST 4 - before testing; side view.
13	TEST 4 - after testing; side view.
14	TEST 5 - before testing; side view.
15	TEST 5 - after testing; side view.
16	TEST 7 - after testing; side view.
17	TEST 8 - after testing; side view.
18	TEST 8 - view showing large mound and trough.
19	TEST 9 - before testing; side view.
20	TEST 9 - view showing water profile behind breakwater after wave impinges on breakwater at beginning of test.
21	TEST 9 - view, at end of test, showing water profile behind breakwater after passing of transmitted wave - note turbulence.
22	TEST 9 - view showing distinct form of the transmitted wave (after testing).
23	TEST 9 - after testing; side view.
24	TEST 10 - before testing; front view.
25	TEST 10 - after testing; front view.
26	TEST 10 - before testing; side view.
27	TEST 10 - after testing; side view.
28	TEST 11 - before testing; side view.
29	TEST 11 - view showing plastic filter and anchor.

Photograph Number	Description
30	TEST 11 - before testing; front view.
31	TEST 11 - after testing; front view.
32	TEST 11 - after testing; side view.
33	TEST 11 - view showing trench in front of plastic filter and anchor.
34	TEST 12 - after test side view also showing sand tracer initial positions.
35	TEST 12 - after testing; side view of mound under ultra-violet light showing tracers.
36	TEST 12 - after testing; daylight side view of sand mound.
37	TEST 12 - after testing; front view of a trench cut into the sand mound showing red tracers in the trench and yellow tracers on the edges on top.


SCOUR INVESTIGATION
BREAKWATER SLOPE 1:2
BEACH SLOPE 1:15
SCALE 1:20
T: 1·85 s H: 120 mm
W15
W200

1


SCOUR INVESTIGATION
BREAKWATER SLOPE 1:2
BEACH SLOPE 1:15
SCALE 1:20
T: 1·85 s H: 120 mm
W15
W200

2

3

4

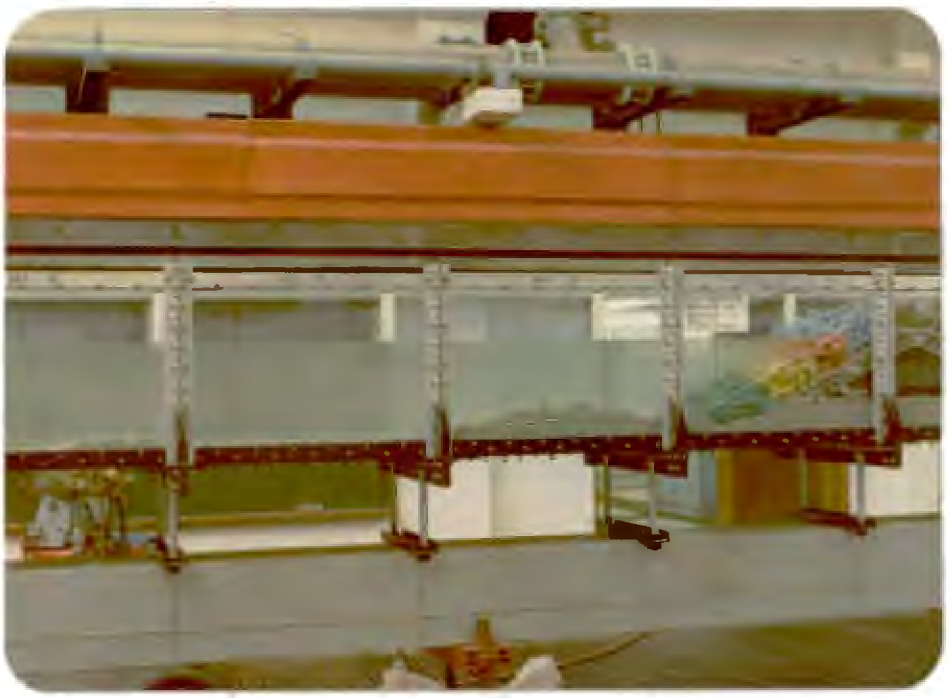

5


SCOUR INVESTIGATION
BREAKWATER SLOPE 1 2
BEACH SLOPE 1 15
SCALE 1 20
T 1 85 s H 120 mm

6


SCOUR INVESTIGATION
BREAKWATER SLOPE 1 2
W/5
W/200

7


SCOUR INVESTIGATION
BREAKWATER SLOPE 1 2
BEACH SLOPE 1 15
SCALE 1 20
T 1.85 s H 120 mm
W
W/5
W/200

8


BREAKWATER SLOPE 1 2
BEACH SLOPE 1 15
SCALE 1 20
T 1.85 s H 120 mm
W
W/5

9


SCOUR INVESTIGATION
BREAKWATER SLOPE 1 2
BEACH SLOPE 1.15
SCALE 1 20
T 185 s H 120 mm
W
W/5

10


SCOUR INVESTIGATION
BREAKWATER SLOPE 1 2
BEACH SLOPE 1 15
SCALE 1 20
T. 185 s H 120 mm
W/5

11


SCOUR INVESTIGATION
BREAKWATER SLOPE 1 2
BEACH SLOPE 1 15
SCALE 1 20
T 185 s H. 120 mm
W/5
W/200

12


SCOUR INVESTIGATION
BREAKWATER SLOPE 1:2
BEACH SLOPE 1:15
SCALE 1:20
T 1·85s H VARIABLE
W/5

13


SCOUR INVESTIGATION
BREAKWATER SLOPE 1:15
EACH SLOPE 1:15
SCALE 1:20
T 1·85s H 120 mm
W/5
W/200

14


OUR INVESTIGATION
EAKWATER SLOPE 1:15
ACH SLOPE 1:15
ALE 1:20
T 1·85s H 120 mm
W/5
W/200

15


SCOUR INVESTIGATION
BREAKWATER SLOPE
BEACH SLOPE
SCALE
W/5
W/200

16


SCOUR INVESTIGATION
BREAKWATER SLOPE
BEACH SLOPE
W/5
W/200

17


W/200

18

145


SCOUR INVESTIGATION
BREAKWATER SLOPE 1:1·5
BEACH SLOPE 1:15
SCALE 1:20
T 1·85s H 120mm
W/5
W/200

19

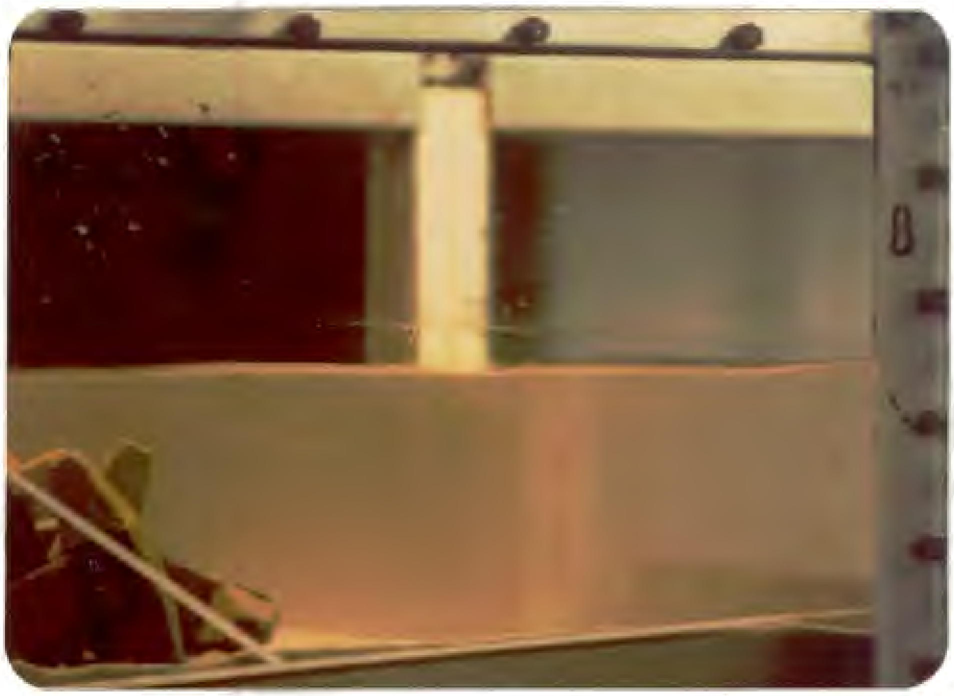

20

21

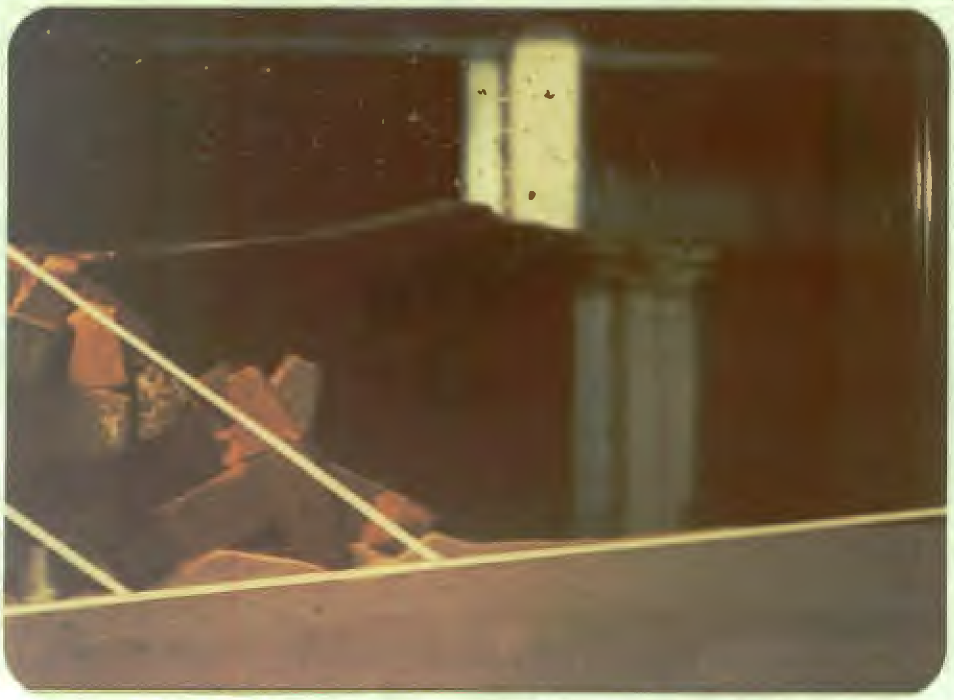

22


SCOUR INVESTIGATION
BREAKWATER SLOPE 1:1.5
BEACH SLOPE 1:15
SCALE 1:20
T 1.85s H 120mm
W5
W200

23

24

25


SCOUR INVESTIGATION
W
W/5
W/200

26


SCOUR INVESTIGATION
BREAKWATER SLOPE 1:1.5
BEACH SLOPE 1:15
SCALE 1:20
W
W/5
W/200

27


SCOUR INVESTIGATION
BREAKWATER SLOPE 1 15
BEACH SLOPE 1 15
SCALE 1 20
T 1.85s H 120mm
W/5
W/200

28

29

30

31

32


W5
W/200

33


SCOUR INVESTIGATION
BREAKWATER SLOPE 1 1.5
BEACH SLOPE 1 15
SCALE 1 20
T 1.85s H 120mm
W5
W/200

34

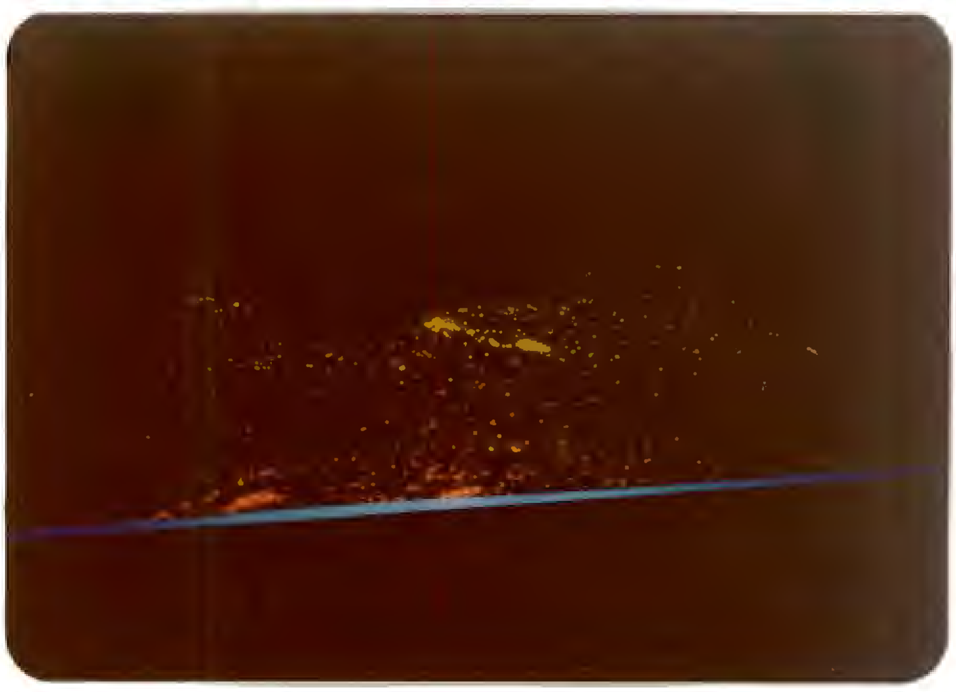

35

36

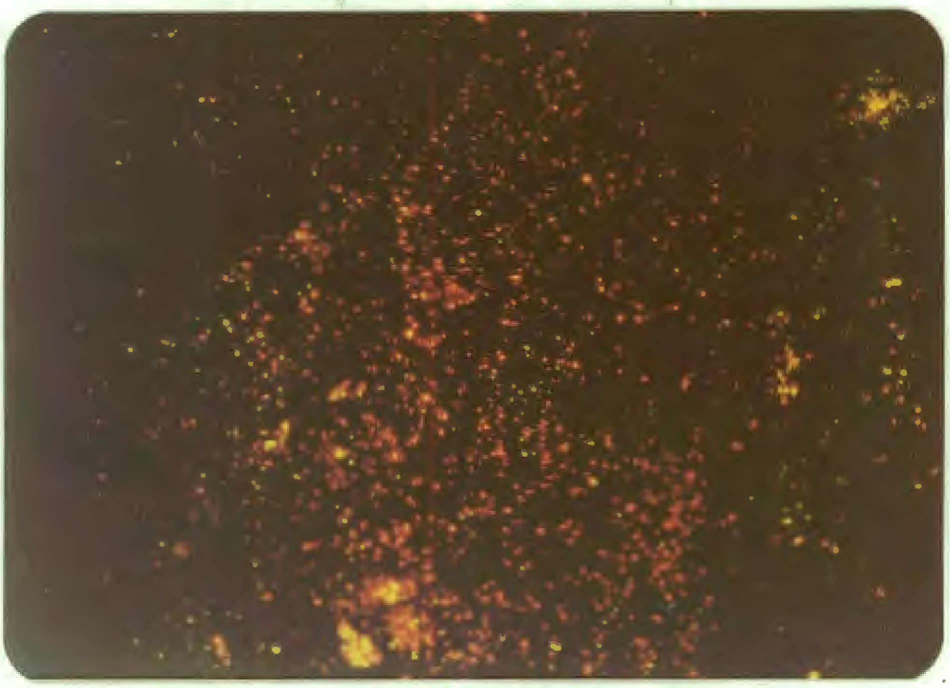

37

COURSES COMPLETED IN PARTIAL FULFILMENT OF THE M.Sc. (ENG.) DEGREE AT THE UNIVERSITY OF CAPE TOWN

COURSE	DATE CREDITED	CREDIT VALUE
Oceanography 'A'	July 1976	5
Oceanography 'B'	November 1976	5
Turbulent Diffusion	December 1976	5
Sediment Transport	May 1977	5
Coastal Hydraulics	November 1977	5
Coastal Engineering Practice	Outstanding	5
	Total	30.

Total credit requirements for the M.Sc. (Eng.) Degree: 40

Quarter Thesis: 10
Course Credits: 30

Total: 40

UNIVERSITY OF CAPE TOWN

UNIVERSITY EXAMINATIONS : JUNE 1976

PHYSICAL OCEANOGRAPHY Ia

PAPER I

Time: 2 hours

Attempt ALL questions

1. (a) What is meant by the standard ocean and the dynamic height anomaly?

   (b) The dynamic topography of a region at 30°S is displayed on a chart on which the contours of equal dynamic heights above a reference level are spaced at intervals of 0,1 dyn. m.
   Construct a graph from which the geostrophic velocity of the relative surface current can be determined from the distance between the isobars. Use spacings of 10, 20, 50 and 100 km. Assume the angular velocity of the earth is $0{,}7 \times 10^{-4}$ rad/sec.

(25)

2. Discuss as fully as you can the meteorological and dynamical reasons why the mean near-surface temperatures of the coastal waters off Cape Town are lower in the summer than the winter.

(35)

3. Assume you were asked to accompany a research ship to a position 30°S and 20°W in the South Atlantic and report on the temperature and salinity in the water column.

   (a) describe the equipment and methods you would employ,

   (b) what results would you anticipate?

(30)

4. Write about 3 of the following:

   (a) Exchange coefficients,

   (b) Coriolis force,

   (c) The role of infra-red radiation in the regulation of the sea surface temperature,

   (d) The meridional (vertical) circulations in the Atlantic Ocean.

(30)

UNIVERSITY OF CAPE TOWN

UNIVERSITY EXAMINATIONS : JUNE 1976

PHYSICAL OCEANOGRAPHY Ia

PAPER 2

Time: 2 Hours

Attempt ALL questions

1. Outline briefly notable characteristics of the bathymetry, tides and currents in South African waters. (30)

2. (a) Given the phase velocity equation $C^2 = \frac{g}{k} \tanh (kd)$ where $k = \frac{2\pi}{L}$, and the group velocity relation $C_g = \frac{d\sigma}{dk}$, find the group velocity in "deep" and "shallow" water for Airy Waves. (15)

   (b) Discuss the wave prediction problem with respect to the spectral formulation of Pierson and Neumann. (15)

3. (a) Describe the nearshore circulation system. (10)

   (b) What factors influence breaking waves and how are they classified? (10)

   (c) If $q = \frac{4H^2}{\sqrt{3\gamma^3}}$ is the incoming wave discharge volume per unit crest length calculate the longshore volume for 1 m wave amplitude, 10 second wave period, incident at 30° to the beach normal. Assume $\gamma = 0.78$ (10)

4. (a) Explain how and why the oxygen concentration changes with depth in the Tropical North Pacific Ocean. (7)

   (b) Account for the seasonal and diurnal variations of the carbon dioxide concentrations in the surface water of the oceans. (8)

   (c) Write short notes on processes which control the concentration of the major elements in sea water. (15)

UNIVERSITY OF CAPE TOWN

UNIVERSITY EXAMINATIONS - OCTOBER, 1976

PHYSICAL OCEANOGRAPHY Ib (PAPER I)

Time - TWO Hours

Attempt ALL questions

1. (a) Given a dimensionally consistent wave energy spectrum depending only on gravity, windspeed U, fetch X and duration T as

$$E(\sigma,t,x) = \alpha g^2\sigma^{-5} f\left(\frac{\sigma_o}{\sigma}, \frac{U}{\sigma_o X}, \frac{1}{T\sigma_o}\right)$$

where $\sigma_o = \frac{G}{U}$, explain the concept of a fully developed wave spectrum. Give the functions and sketches that describe the high and low frequency ends of this spectrum.

(b) Explain the basic problems involved in predicting surface gravity waves at a given point.

(30)

2. (a) You are given that the phase velocity of waves at the interface of a two layered fluid obeys the equation

$$C^2 = \frac{(\rho''-\rho')\frac{g}{k}}{\rho'\coth(kh') + \rho''\coth(kh'')}$$

where the upper layer has density ρ' and depth h' and the lower layer has density ρ'' and depth h''. Also $\rho'<\rho''$. By making the relevant approximations deduce the phase velocity of internal waves when the depth of both layers is large compared to one wavelength. If $\rho'-\rho'' = 10^{-3}$, calculate the ratio of the velocity of the internal wave to that of a surface wave of the same wavelength.

(b) Explain Defant's classification of tidal character. The amplitudes of some of the principal components of a tide are O_1 = 0,02m, M_2 = 0,50m, K_1 = 0,06m, S_2 = 0,2m. What is the nature of this tide and what is the mean range of the spring tide?

(30)

3. (a) Explain the terms relative, planetary, absolute and potential vorticity. By using the conservation of potential vorticity examine the subsequent motion of a north flowing current in the N. Hemisphere, initially at 30°N with zero relative velocity. The depth decreases slowly in a northerly direction.

(b) Describe the assumptions applied to the equations of motion that lead to inertial currents. Given these equations in the form

$$\frac{du}{dt} - fv = 0$$

$$\frac{dv}{dt} + fu = 0$$

Show that inertial currents have a constant speed but changing direction.

(35)

4. Using concepts defined in question 3, show how Stommel explained the intensification of western boundary currents for an ocean of uniform depth.

(25)

UNIVERSITY OF CAPE TOWN

UNIVERSITY EXAMINATIONS, NOVEMBER, 1976.

PHYSICAL OCEANOGRAPHY IB - PAPER 2

TIME: 2 Hours

Attempt ALL Questions

1. (a) A water mass of density ρ_1 and velocity V_1 overlies one of density ρ_2 at rest at latitude ϕ. Derive an expression for the slope (γ) of the density interface.

   (b) Using (a) above derive an expression for the ratio of the slopes of the isopycnals and the isobars.

   (c) Sketch and explain the isopycnal distribution in a section across the Pacific Equatorial undercurrent.

(34)

2. (a) Describe the dynamics of a hurricane and explain its effects on the underlying water. Give equations where possible.

   (b) Compare and contrast hurricanes and extra tropical cyclones.

(32)

3. (a) Give a reasoned identification of the accompanying vertical sections from the same region of an ocean.

   (b) Sketch the T-S diagrams of typical water columns on the east and west sides of the South Pacific. Explain the outstanding differences.

   (c) Briefly describe the probable mode of formation of North Pacific Intermediate Water.

(32)

4. (a) Estuaries may be classified according to stratification. What differences in regimes makes this possible?

   (b) Derive an expression from which the inflow from the sea to a basin can be calculated in terms of salinities and evaporation - precipitation differences.

(22)

UNIVERSITY OF CAPE TOWN

DEPARTMENT OF APPLIED MATHEMATICS

UNIVERSITY EXAMINATION: TURBULENT DIFFUSION

Project to be completed in fulfilment of course credit requirements:

Due date: 28th November, 1976.

Lecturer: Professor J. Brundrit

Question 1:

Experimental evidence suggests that the dissipation rate is not evenly distributed over the volume occupied by a turbulent flow. The distribution of the dissipation rate appears to be intermittent, with large dissipation rates occupying a small volume fraction. Make a model of this phenomenon by assuming that all of the dissipation occurs in thin vortex tubes (diameter η, characteristic velocity $\mu = [\frac{1}{3} u_i u_i]^{\frac{1}{2}}$). What is the volume fraction occupied by these tubes? Verify if the approximate vorticity budget indeed holds for these vortex tubes.

Question 2:

A fully developed turbulent pipe flow of fluid with a Prandtl number equal to one is being cooled by the addition of a small volume of slightly cooler fluid over a cross-section. Estimate the initial temperature fluctuation level. How many pipe diameters downstream are required before the temperature fluctuations have decayed to 1 % of the initial level? For the purpose of this calculation, it may be assumed that the mean velocity in the pipe is approximately independent of position. Also, an estimation of the dissipation rate ϵ is needed; it can be obtained from momentum and energy integrals for pipe flow. For a prescribed decrease in mean temperature in the pipe, should one increase the volume flow of coolant and reduce the temperature difference or vice versa in order to reduce the temperature fluctuations?

UNIVERSITY OF CAPE TOWN

DEPARTMENT OF CIVIL ENGINEERING

UNIVERSITY EXAMINATION: FEBRUARY, 1977

COURSE CE 511 - SEDIMENT TRANSPORTATION

Note: This is an 'open book' examination. Scripts are to be collected at 5.30 p.m. on Thursday, 24th February 1977 and returned by 9.00 a.m. on Monday, 28th February, 1977. The attached affidavit is to be signed by each student on receipt of the examination script.

Answer ALL questions

1. One criterion for determining whether suspensions will be settling or non-settling is a particle Reynolds number of 2,0. For sand of relative density $S_s = 2,65$, indicate into which category "average" particles of sand, of mean particle diameter 38, 100, 250, 1000 and 2000 μm at concentrations of 0, 10, 20 and 30%, will fall. Tabulate your results and show how they can be presented graphically. Hence determine for each of the four concentrations, the particle size which designates the boundary between settling and non-settling suspensions.

   (a) Compare the above results with those obtained by two other methods.

   (b) Repeat the above procedure for coal of sphericity 0,7 and relative density as given by Fig. 3.11.

   (c) Repeat the above procedure for iron ore assuming spherical particles and a relative density of 4,0. In this case include particles of size d = 2,5 mm. Assume $\nu = 1,14\ mm^2/s$

2. Carry out a feasibility study for transporting 10 million metric tonnes (1 metric tonne = 10^3 kg) of iron ore of relative density 4,0, a distance of 600 km in a horizontal pipeline with a load factor of 95%.

   Assume the pipe roughness is constant at k = 0,06 mm and the kinematic viscosity of water is $\nu = 1,14\ mm^2/s$.

   In order to carry out the feasibility study, consider five alternative proposals.

   (i) Assume that the ore is crushed to an average particle size of d = 2,5 mm and the mean drag coefficient can be taken as $C_D = 0,44$.

      (a) Which flow regime would you consider as being feasible for transportation of this material and why?

      (b) Assume that the delivered volumetric concentration is $C_{vd} = 20\%$. Determine the limit deposit velocity according to Durand and show that the pipe diameter required to operate at the minimum energy loss is approximately 300 mm.

      (c) What is the total power required per km? Compute this value as the average obtained by four methods.

      (d) Compare the pipe diameter obtained above with that obtained by another method for determining the value of the limit deposit velocity.

/(ii) .....

2. (Continued)

(ii) In order to transport the material in the pseudo homogeneous regime at the same rate and volumetric concentration in a 300 mm diameter pipe it is possible to grind the material finer.

(a) Determine the drag coefficient of the finer material if it is just transported as a pseudo homogeneous mixture at the same rate (i.e. same mixture velocity).

(b) What is the mean particle size of this finer material ? Assume that the analysis for spherical particles applies. Compare this result with the results obtained in (i)(c) above.

(c) What is the total power requirement in this case?

(iii) The finer material can also be transported at a lower mean mixture velocity as a heterogeneous suspension in the 300 mm diameter pipe.

(a) What is the power requirement in this case? Assume that the heterogeneous mixture is transported at the minimum deposit velocity as determined from the Durand equation with the coefficient $F_L = 0{,}95$. Note that the delivered volumetric concentration will be greater than 20% in this case.

(iv) The material is ground further to give a non-Newtonian suspension at 20% volumetric concentration.

(a) What would the average size of particle have to be in this case?

(b) The rheological properties as determined by means of a capillary tube viscometer, 3 mm in diameter and 3 m long, are as follows:-

Mass Flow (g/s)	0,848	1,69	2,54	4,24	8,48
Pressure Drop (kN/m^2)	4,0	7,2	10,8	16,8	36,0

Determine the power requirement for the same flow rate as in schemes (i) and (ii)

(v) Consider a pipe diameter of 500 mm with the average roughness size of 0,06 mm and for the same mixture flow rate and material concentration as in scheme (iv), determine the power requirement.

Summarise the power requirements, in tabular form, for the five schemes considered above and comment briefly on the feasibility of scheme (v) as compared with the other schemes.

3. Coal of size d_{50} = 225 μm was tested in pipeline test loops of 100 mm and 200 mm diameters at a concentration by weight of C_w = 53%. The relative density of the coal is 1,5 and the kinematic viscosity of water $\nu = 1{,}14\ mm^2/s$. The following test results were obtained at $V_m = 1{,}75$ m/s:-

D(mm)	100	200
i_m	0,0457	0,0224

/The pipes ....

3. (Continued)

The pipes were found to be hydraulically smooth.

Determine the head loss in a 3000 mm diameter pipe at a mean mixture velocity of 1,75 m/s. Use three different methods of scaling and compare them.

4. Calculate the mixture head loss in units of clear fluid (water) for the coal described above, assuming a heterogeneous flow regime in a pseudo homogeneous mixture (i.e. the method of Wasp et al) in a 300 mm diameter pipe. Compare with the Durand equation.

Assume that the Weltman Green equation $\mu = (\mu_o + A)\, e^{\beta v_r}$ applies

with $u_o = 1{,}14 \times 10^{-3}$ kg/ms

$A = 0{,}000064$ kg/ms

$\beta = 4{,}29.$

Ignore the effect of hindered settling of the particles.

UNIVERSITY OF CAPE TOWN

DEPARTMENT OF CIVIL ENGINEERING

M.Sc. IN CIVIL ENGINEERING

UNIVERSITY EXAMINATION : JULY 1977

CE 525 : Coastal Hydraulics

All Questions may be attempted | Time : 3 hours

Constants

Sea water density = 1025 kg/m^3
Sea water weight = 10 kN/m^3

1. A beach site has an average underwater slope of 1 in 50, and the beach material is a coarse quartz sand of relative density 2,65 and average size 1,35 mm, the shoreline being essentially straight.

   Two conditions of wave attack are being considered :-

   (A) swell of 10 second period with a deep water wave height of 1,6 m approaching the beach with wave crests parallel to the shore line.

   (B) as in (A) above, but with a deep water wave incidence of 35°, (angle between wave crest and contour)

   For case (A) make the following calculations :-

   (a) the wave length and wave celerity in deep water.
   (b) the water depth at which the wave begins to be affected by the presence of the sea bed.
   (c) the wavelength, celerity and height for water depths at 10 m intervals between d=80 m and d=10 m, and at 1 m intervals between d= 10 m and d=1 m.
   (d) the water depth in which the wave breaks, the breaker type, and the wave height at breaking. Ignore the effect of wave set up or down.
   (e) the deep water energy flow.
   (f) the wave height and energy flow in a water depth of 1 m.
   (g) the water depth in which the sand is on the point of moving.
   (h) the water depth in the which the sand is in motion but has no net drift.

For case (B) make the following calculations :-

(i) the water depths in which the angle of incidence becomes 30°, 20° 10° and 5°, and the wave heights at these depths.

(j) the water depth and wave height under breaking conditions. (assume the depth at breaking is 80 per cent of the value obtained for parallel waves)

(k) the thrust on the mass of water in the surf zone, per metre length along the shore.(N)

(l) an estimate of the bulk sand volume flow rate in m^3/s in the alongshore direction.

2. A cylindrical pipe is laid on the sea bed across a harbour entrance in 10 m of water, the pipe diameter being 0,3 m, and the axis of the pipe is parallel to the local wave crests. If the local wave length is 50 m, estimate the wave period, and find the peak magnitudes of the velocity and acceleration force components per metre length of pipe. Estimate the peak resultant force in the inshore direction, and the timing of this in relation to the passage of the wave crest. The wave height is 2 m, take C_D = 1,2 and C_M = 2,16

3. (a) A steady wind of speed 15 m/s blows over a fetch for a period of 8 hours, producing a significant wave height of 1,8 m at the downwind end of the fetch. Estimate the fetch length in km and the wave period. Check whether the wind duration is sufficient for this condition to be stable and also check whether this is the fully arisen sea for this wind speed.

(b) In a zero damage design calculation for the armour protection of a rubble mound breakwater, 3 tonne and 5 tonne dolosse are specified for the trunk and head respectively, the slope of the breakwater face being $\cot\theta = 2$. Estimate the block masses and block heights if tetrapods had been used in the same design. If the design wave height was 3 m, and a storm causes damage of the order 20-30 per cent to the tetrapod scheme, estimate the storm wave height.(concrete density = 2245 kg/m^3)

(c) An incoming swell has crests parallel to a straight beach with a deep water wave height of 2 m. Estimate the horizontal force (per metre along the beach) acting on the beach inside the refraction zone, due to the dynamic action of the waves.

(d) In an area where the sea bed is horizontal, and the water depth is 3 m, a wave has a period of 7 s, a wavelength of 38 m, and a wave height of 1,5 m. Estimate the drift velocity at bed level, and indicate the direction. Compare this velocity with the maximum orbital velocity at the same level, and indicate the influence on bed drift of a strong onshore wind.

(e) A storm at sea generates waves with a period range of 8 to 16 seconds. The resulting swell travels towards a harbour 500 km away. Estimate the time interval between the arrival of the shortest and longest waves, assuming deep water throughout.

UNIVERSITY OF CAPE TOWN

DEPARTMENT OF CIVIL ENGINEERING

UNIVERSITY EXAMINATION NOVEMBER 1977

CE 526 COASTAL ENGINEERING PRACTICE

Time allowed: 2 hours

Answer ALL questions

OPEN BOOK

There is a potential of 142 marks
120 marks will be regarded as 100%

Section 1 is to be handed in at the end of the first hour

1. Answer all questions on the attached sheets, in the space provided. If additional space is required the answer is to be completed in an Examination Answer Book where the answer must be clearly numbered.

[64]

2. The attached plan shows the bathymetry of False Bay to M.S.L. Using this plan and annotating it if necessary, answer the following questions, stating all assumptions and sources of information.

If the wind were to blow from the North at an average speed of 100 km/hr estimate for a point in the vicinity of Whittle Rock:

i) The time taken to develop a fully arisen sea (2)

ii) The significant wave height: H_s (2)

iii) The significant wave period: T_s (2)

iv) The depth at which this wave would break (2)

[8]

3. If a wave recorder of the 'Wave Rider' type were to generate a record with the following characteristics:
Record length = 340 seconds
Number of 'zero-upcrossings' = 43
Number of crests = 104

i) Calculate the zero crossing period (1)
ii) Calculate the mean crest period (1)
iii) Calculate the spectral width parameter (1)
iv) What type of waves are these (i.e. swell, sea, mixed etc)
Give your reason (1)
v) If the height of the highest crest in the record is 2,1 m * and the depth of the lowest trough is 1,9 m* calculate the value of H_s (significant wave height) (2)
and H_{max}^{s} (the 6 hour maximum) (2)
Use the method proposed by L. Draper 1967 in his paper 'The Analysis and Presentation of Wave Data - A Plea for Uniformity'.

* *dimensioned from the zero crossing line*

[8]

4. A lake of area 4×10^6 m^2 is to be joined to the sea by a navigation channel with sides formed by vertical sheet piles driven into the sand bed. The tidal range is 1,8 m.

a) What dimension would you recommend for the width of the channel assuming a bed depth of 2 m below M.S.L. ? (4)

b) Estimate the average outflow velocity (2)

c) If the size and grading of the sand is typical of the Cape Flats at what velocity would you anticipate scour would commence ? (1)

[7]

5. Two vertical aerial photographs of the coast taken at 12 seconds apart are mounted in a viewer. Two adjacent wave crests (A and B) approaching a shallow shoreline are examined. In the first photograph the distacce between A and B is 127 m apart. In the second photograph the distance between A and B is 117 m apart. The second position of A is 84 m ahead of its position in the first photograph.

a) Estimate the average wave celerity of crest A and of crest B during the twelve second interval (2)

b) Assuming the water is effectively shallow, estimate the average water depth under each crest, and check that the assumption is valid. (3)

c) Calculate the wave period for each crest (2)

d) To what do you attribute the difference in period (2)

e) Have these waves been generated locally, or at a considerable distance (1)

[10]

6. a) Explain the term 'spectral window' as applied to electromagnetic radiation in the region 0,2 to 20 micrometres (3)

b) Explain why colour-false infrared film is particularly suitable for demarcating the tide line in an estuary (3)

c) Explain what is meant by the term 'spectral signature' of a ground material such as sand or grass; and hence explain how a 'classification' of a set of multi-spectral images of a ground scene can be achieved (7)

[13]

7. The attached plan shows contours of the sea bed at the Strand, near Gordons Bay. It will be seen that rocks outcrop in many places and provide a relatively calm area which is considered to have some potential for a small craft harbour and in particular a boat ramp.

a) Outline briefly the investigations and work you would recommend to establish the feasibility of constructing a small craft harbour in this location (7)

b) Identify the personnel and equipment required to undertake each of the investigations outlined above in (a). Estimate the time, rates and hence the cost of undertaking this work. (7)

c) Draw on the plan provided the main features of a proposal to provide a small craft harbour at this location (10)

d) Identify the number of boats at moorings and in dryboat storage that can be accommodated (3)

e) Give a rough estimate of quantities for any harbour protection works (e.g. breakwaters) proposed. State any assumptions. (5)

[32]

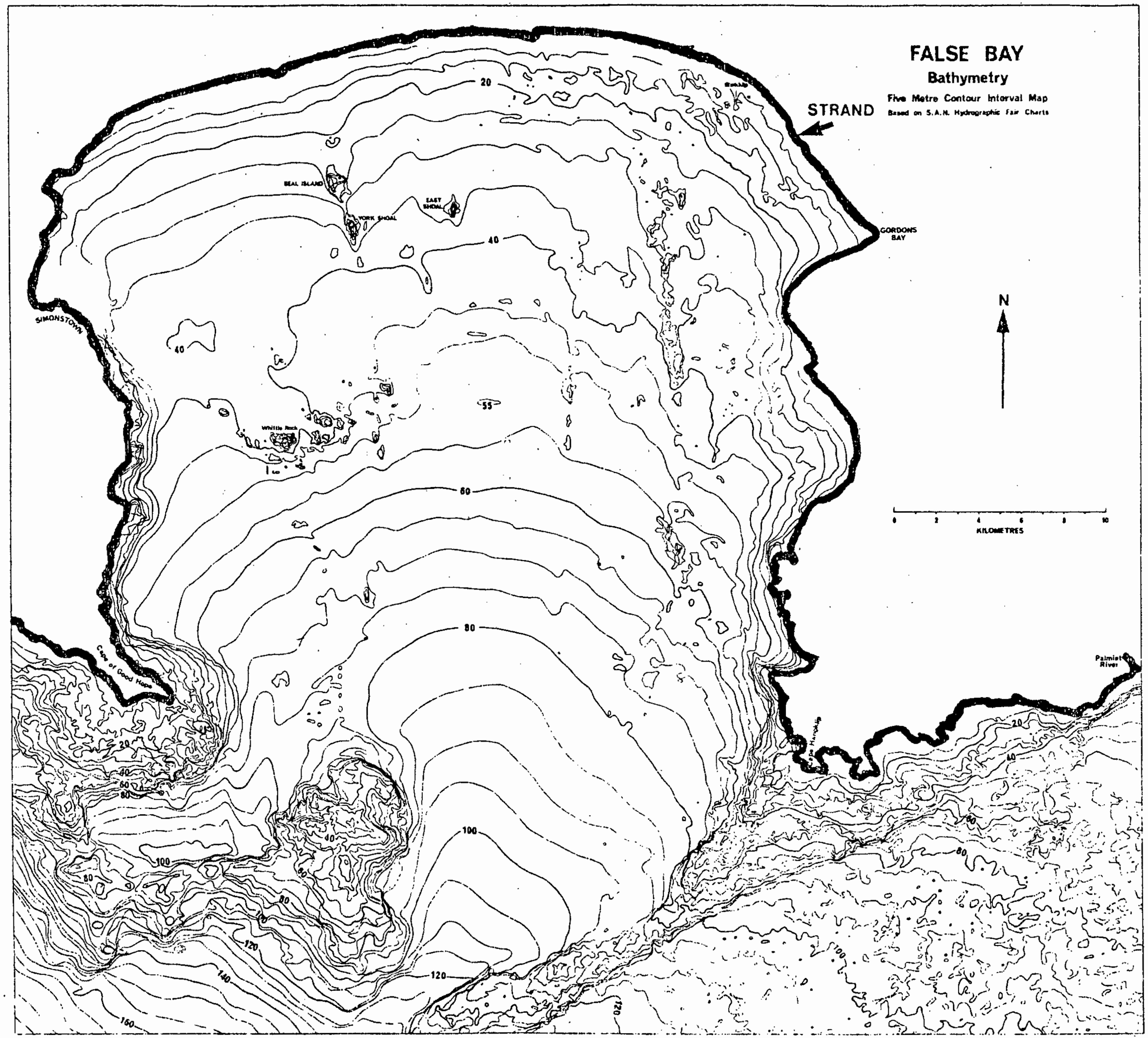
FALSE BAY
Bathymetry
Five Metre Contour Interval Map
Based on S.A.N. Hydrographic Fair Charts
STRAND
GORDONS BAY
SEAL ISLAND
YORK SHOAL
EAST SHOAL
SIMONSTOWN
Whittle Rock
Cape of Good Hope
Palmiet River
N
KILOMETRES
0
2
4
6
8
10
20
40
55
60
80
100
120
140
160

QUESTION 1 Name ....

1.1 The optimum orientation for the mooring of sailing craft is

-- (1)

1.2 The economic advantage in providing locks in a tidal harbour is in respect of --

-- (1)

1.3 The optimum location for waterside fuelling facilities is

----

because -- (2)

1.4 Minimum dredged depths in a small craft harbour are the sum of individual depths allowed for the following

--------------------	typically	-------------------------	m
--------------------		-------------------------	m
--------------------		-------------------------	m
--------------------		-------------------------	m
--------------------		-------------------------	m
--------------------		-------------------------	m
--------------------		-------------------------	m
--------------------		-------------------------	m
--------------------		-------------------------	m (3)

USE ADDITIONAL LINES IF REQUIRED

1.5 Detail in plan and dimension typical floating berthing to provide double occupancy for boats of length 8 m. Show the system of mooring proposed.

(3)

Assuming an average overall cost of R100/m^2 of floating berth deck area, estimate the cost of providing this berthing <u>per boat</u>

--------------------- m^2 @ R100/m = ----------------------

(2)

1.6 Give a local example of a leeshore anchorage ----------------------

-- (1)

1.7 Why is a leeshore disadvantageous to a harbour --------------------

-- (1)

1.8 Explain the significance of providing a turning basin in the harbour on the Buffalo River at East London ------------------------------

----

-- (2)

1.9 Explain briefly how the position of a dredger may be ascertained by using a sextant

(3)

1.10 Explain what is meant by the term 'controlling depth' of a harbour

----

-- (2)

1.11 Sketch the main elements of a float type tide recorder such as is installed at Hout Bay

(3)

1.12 Explain how a 'clinometer' is used for wave recording. Identify the main elements of the system ______________________________

____

____

____

____ (3)

1.13 Tabulate the advantages and disadvantages of a 'clinometer' system as compared with a 'wave rider' system of wave measurement

Clinometer		Wave Rider	
Advantages	Disadvantages	Advantages	Disadvantages

(5)

1.14 Draw the approximate form of the wave orthogonals to reach A, B, C and D as they approach the coastline drawn in plan below. (Assume refraction without diffraction).

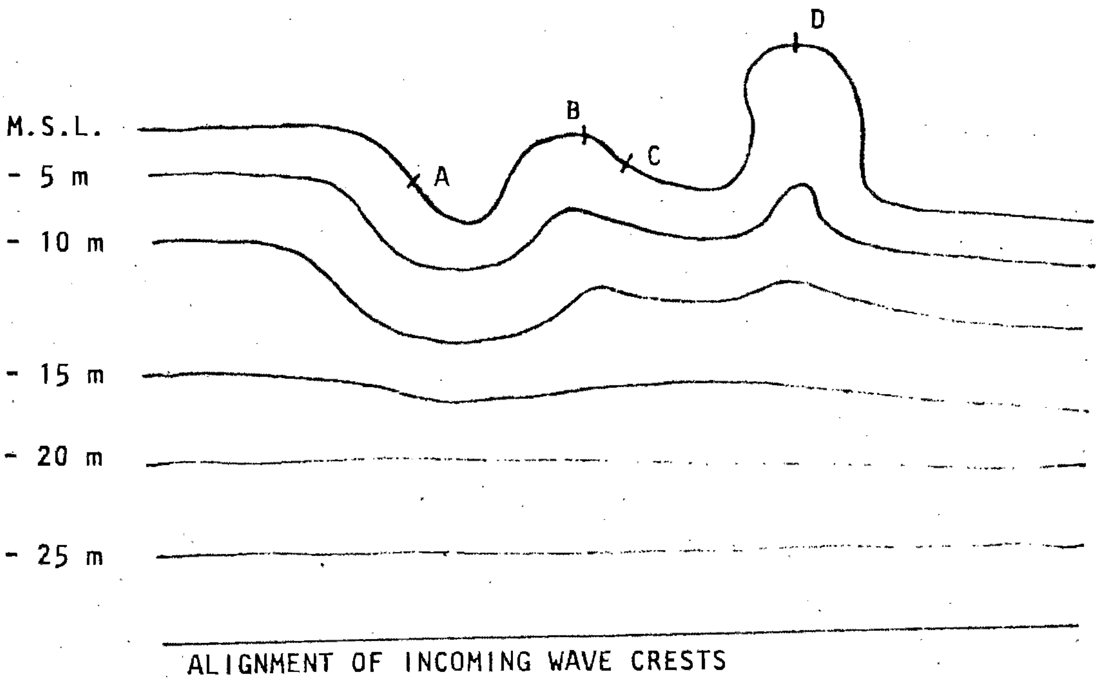

(4)

1.15 For the harbour entrance detailed below sketch

a) the approximate form of 4 wave orthogonals as they enter the harbour (2)

b) 3 wave crests (1)

c) If the gap width is equal to 1 wave length draw in a dotted line the location of diffracted wave heights of one half the incident wave height. (Refer to Fig. 2-44 in CERC Shore Protection Manual) (2)

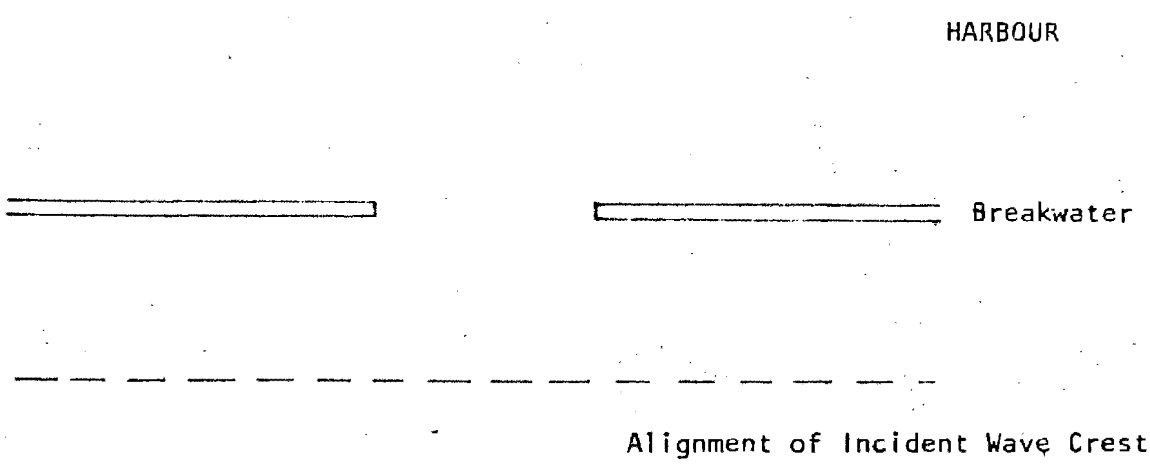

1.16 a) What is the significance of waves entering a harbour with a period equal to the fundamental period of oscillation of one of the basins ?

--- (1)

b) Name two design features that may be incorporated in a harbour design to reduce reflection ? __(1)______________________________

____________________(2)____ (2)

c) Sketch where you would site the two features described above in 16b) in the basin shown below

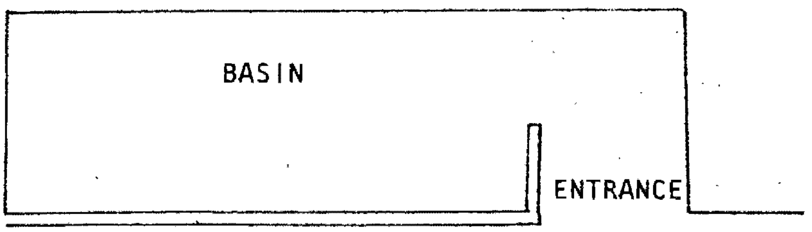

(2)

d) Sketch sectional elevations of the two features described above

(2)

1.17 Give an example of a situation in which it would be appropriate to commission:

a) A 3-dimensional hydraulic model ___________________________________

____

b) A 2-dimensional hydraulic model ___________________________________

____

c) A mathematical model ____

____ (3)

1.18 Explain briefly the function of coastal sanddunes in maintaining the stability of a sandy coastline ______________________________

____

____

____

____

____

____ (3)

1.19 Identify by means of annotated sketches the procedures involved in implementing the following stages which might occur in the construction of a jetty on a rock bed covered in a thin layer of sand.

a) Temporary staging (2)

b) Airlift (2)

c) Placement of precast bases (2)

d) Placement of bearer piles (2)

e) Placement of concrete underwater (2)